Volume: 5 : 2022 ISSN: 2220-7643

Ethiopian Journal of Water Science and Technology (EJWST)

Ethiopian Journal of Water Science and Technology (EJWST) Volume: 5 : 2022 ISSN: 2220-7643

Ethiopian Journal of Water Science and Technology (EJWST)

Volume: 5 : 2022 **ISSN: 2220-7643**

Ethiopian Journal of Water Science and Technology (EJWST)

AIM & SCOPE: The Ethiopian Journal of Water Science and Technology (EJWST) is an open-access journal hosted by Arba Minch University, Water Technology Institute. EJWST is a multidisciplinary double-blind peer-reviewed journal that publishes original research papers, critical reviews, and technical notes which are of regional and international significance on all aspects of the water science, technology, policy, regulation, social, economic aspects, management and applications of sustainable use of water resources to cope-up with water scarcity. The journal includes, but is not limited to, the following topics:

Hydrology & integrated water resources management

- Water resources Potential Assessment; Integrated Watershed Management; Optimal Allocation of Water Resources;
- Hydraulic modeling; Eco-hydrology and River Basin Governance and water Institutions

Irrigation and Drainage

- Irrigation Potential Assessment;
- Irrigation Scheme Performance Improvements;
- Agriculture Water Management;
- Conjunctive Use of Surface and Groundwater Irrigation;
- Rain water Harvesting and spate Irrigation.

Water Supply and Sanitation

- Rural and Rural Water Supply and Sanitation;
- Water Quality Modeling;
- Wastewater Treatment and Re-use; Solid Waste Management;
- Ecological Sanitation and Sustainability of Water supply Services.

Renewable Energy

- Assessment of hydropower Potential and development;
- Small scale Hydropower and alternative energy sources;
- Dam and Reservoirs; Wind Energy for Water Pumping and;

Solar Energy for Water pumping

Climate Variability, change, and impacts

- Impacts of climate change on water resources
- Climate Changes Impacts, Vulnerability,
- Adaptation options; Climate Forcing & Dynamics and Predictability of weather and climate extremes.

Emerging Challenges

- Hydro politics and conflict Resolution; Equitable Resources and Benefit-sharing; Gender and Water Resources Management and Cross-cutting Issues

Editorial Board:

The journal editorial board is comprised of multiple disciplines in the areas of Water Resources Engineering, development, and management. The editorial board welcomes all interested authors to join the review and advisory board of EJWST.

Advisory Board:

Ethiopian Journal of Water Science and Technology (EJWST)

DOI: https://doi.org/10.59122/15519g6

Vol. 5 , 2022, pages: 1~23 ISSN(Print): 2220-7643

Hydraulic and Utility Performance Evaluation of Ataye Town Water Distribution Network, Ethiopia: case for small towns in developing countries.

Zewdu Shewafera[a] and Kinfe Kassa[b]

[a]*Department of Water Supply and Sanitary Engineering, Bahir Dar University, Bahir Dar, Ethiopia*
[b] *Faculty of Water Supply and Environmental Engineering, Arba Minch University, Arba Minch, Ethiopia*
Corresponding author email address: zshewafera@gmail.com

ABSTRACT

Evaluating hydraulic and utility performance of water distribution network is a way to check the functionality degree of a system. Water CAD software was used in developing a model and evaluating the hydraulic performance of water distribution system of Ataye Town, Amhara Region, Ethiopia. Both steady state and extended period simulation analysis were carried out to determine hydraulic parameters (pressure and velocity). The model was calibrated using Darwin Calibrator and validity was checked by both correlation coefficient and scatter plot. The utility performance was also evaluated using international water association performance indicators. The simulated result for steady state analysis showed that 68.7% of the nodes operated within optimum adopted pressure (15-60 meter) and 93% of the distribution pipes had a velocity of <0.6 m/s which was a minimum adopted velocity. For extended period simulation 34.3% during maximum demand time and 16.8% during minimum consumption hours had pressure <15meters. 10.8% had negative pressure during maximum demand hours located at Sudan, Selama, and Zigba sefer and 14 nodes (8.4%) during low consumption time had a pressure greater than 60meter, which was a maximum adopted pressure. The areas of high pressure were located at around mosque, Worku Hotel and Hamus Gebaya. The distribution system performs within the adopted pressure at minimum demand time (74.7%) and maximum consumption hours (65.1%). 23.5% of the systems had a velocity of 0.6-2 m/s and the rest had a velocity less than 0.6m/s during high demand time. During low consumption hours, 100% of the system velocity was estimated to be <0.6m/s. Based on the IWA performance indicators, water utility of Ataye Town was evaluated and had low, technical, financial, personnel, and environmental performances. Finally, the distribution system was modified and optimized by providing alternative connections with pressure reducing valves and changing pipe diameter to improve the hydraulic performance and reduce system disruption of the Town.

Keywords: Extended period simulation; Hydraulic performance; IWA Utility performance; Steady state analysis; Water CAD

Received: 29 Apr 2022; received in revised form 15 May 2022; accepted 20 May 2022

1. INTRODUCTION

Availability of potable drinking water and provision of safe sanitation facilities are the basic and minimum requirements for healthy living (Trifunovic N., 2006). Water distribution systems are designed to adequately satisfy the water demand for domestic, commercial, industrial, and firefighting purposes at all times and at satisfactory hydraulic performance (Terlumun U.and Robert E.,2019). Most water utilities fail to deliver water because of poor distribution system and the efficiency of the water utility is very low. In Southern Ethiopia customer satisfaction is below 50 percent (Kassa, k., et al., 2017).

The utilities' performance efficiency has a direct effect on the performance of the distribution systems (Van den Berg and Danilenko A., 2017). The performance efficiency of utilities is responsible for the proper functioning of the systems and the efficiency is seriously very poor in developing countries, like Ethiopia. The reason behind the low services of the utilities is that they are provided in a monopolistic environment mostly by government. In the absence of market forces, it is hard to find motivation for efficiency. For instance, in the case of Ethiopian water utilities that sell water at a subsidized rate to help the poor and therefore utility personnel payments are also low, as a contributing factor. All the stakeholders in the water supply business have realized that, , utilities can be forced to continually improve their performance by assessing the performance of the services in a systematic way, with the consequential benefits for all those involved (Alegre, H. et al, 2009).

The distribution network is responsible for delivering water from the source to consumers at serviceable pressure (Zyoud S., 2003) which is the main contributor for technical aspect of the utilities performance. Because of failure of system components and variation of demand, occasional disruptions may occur over the service life of the system. Some of the factors which affect the performance of a distribution system are incorrect design, population increase, increase service connections than estimated, expansion of service areas, failure of distribution network components, and increase roughness of pipe surface as a result of ageing (Terlumun U. and Robert E.,2019). The rapid growth of population and expansion of service connection in Ataye increase

water demand which exerts extra load on existing water supply system. As a result, some consumers are left with little or no water supply.

The aim of this study was to evaluate the Ataye Town water supply system by International water association (IWA) utility performance indicators and by water CAD based hydraulic analysis in order to identify the problems to provide technical suggestions.

2. MATERIALS AND METHODS

2.1. Study Area

The study was carried out at Ataye Town located in North Showa, Amhara Regional State, Ethiopia. The Town is located at latitude between 10° 19' and 10° 22' North and Longitude between 39° 56'and 39° 58'East, 280 km away from Addis Ababa. It belongs to Awash Basin which is located at an average elevation of 1450m. It belongs to semi-desert climatic zone with two main seasons (rainy and dry seasons).

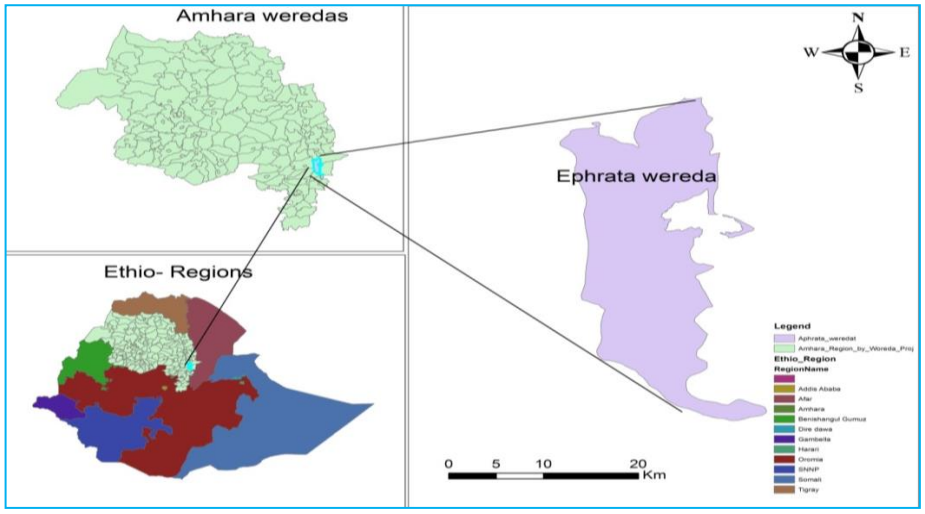

Figure 1 Location of Ataye Town in Ethiopia

Existing water supply system of Ataye town was constructed in 2014/2015 and designed for 30 years. The source of water is from three well fields of deep boreholes. The Town water utility had average daily production capacity of 24.8 l/s (2142.72m^3/d) (ATWSS, 2020).

2.2 Data Collection

To build the model of the distribution network and to evaluate hydraulic & utility performance, the required data of the distribution system parameters were gathered. Pressure, tank water level, location, and elevation of points were collected by field surveying and direct measurement. Daily water production and consumption, pipe, tank and pump, financial and water tariff, staff and customer, and well history were collected through Key Informant Interview annual report and design document, and as built or completion report document review.

2.3 Allocating Demand

For population forecasting the geometric increase method is mostly applicable for growing towns and cities having vast scope of expansion (CSA, 2007). The population projection of Ataye Town was calculated using equation (1):

$$Pn=P_o(1+r)^n \qquad (1)$$

Where, P_o= base population, P_n = population at n decades or year, n = decade or year, r = rate (percent increase).Three modes of services are given in the Town: house connection (35%), yard connection (48%), public fountain (15%) and unprotected water source users 2% (ATWSS, 2020). The per capita demand of the town was projected and allocated to each node by mode of services. The annual growth rate was 2 % for public fountain users and 3% for yard and house connection (Mamush, 2016).

For preliminary calculation of the nodal demands, a simple method was applied using water consumption rate per linear meter of distribution pipe. Once the total demand on each pipe was determined, the pipes were separated between two corresponding nodes. This method was based on the assumption that service connections were evenly distributed. To assign base demand to each nearest supply node, the houses around each supply nodes were identified with direct count. The demand of each node depends on the population around the node (along half of pipe length connecting two nodes) multiplied by base demand. Unit consumption per meter of the pipe length for each loop was estimated by

$$ql = \frac{Ql}{\sum_{j=1}^{m} Lj,l} \quad \text{.....(2)}$$

Where, Ql. is the average demand within loop l (along a pipe), and Lj is the length of pipe j forming the loop and ql is unit per meter flow.

2.4 Water CAD model preprocessing

Distribution layout survey data from Auto CAD civil-3D was imported into Bentley Water CAD v8i using model builder. The imported distribution layout was edited using property dialog box by entering the following: nodes elevation, base demands, pipe diameter, pipe length, pipe material, friction factors, tank base, minimum and maximum level, tank diameter, reservoir elevation and pumps input data. In order to build and analyze the distribution network 38,950 m pipes with internal diameter of 50-200mm, 3 tanks, 4 boreholes with submersible pump, and 166 junctions were used.

2.5 Model Calibration and Validation

After the first run, the model was calibrated using Darwin calibrator by adjusting sensitive parameters related with flow like pipe roughness coefficient and water demand until it becomes within the acceptable limit. Therefore, for this study the model data quality was analyzed by comparing and calibrating the computed pressure data with the actually measured ones. Pressure readings were taken at specific time using pressure gauge at 10 sample points for calibration and 10 samples for validation.

Finally validation was done with equation (3) using the correlation coefficient equation (R^2) method using Microsoft Excel.

$$R^2 = \frac{\Sigma(X - \bar{X})(Y - \bar{Y})}{\sqrt{\Sigma(X - \bar{X})^2} * \sqrt{\Sigma(Y - \bar{Y})^2}} \quad \text{.....(3)}$$

Where: R^2 = coefficient of determination, X and Y are the computed and observed pressure values, and $\bar{X}$ and $\bar{Y}$ are mean value of computed and observed pressure, respectively.

For the calibration, the head loss between sample (main nodes and the site) where pressure was measured has been considered which include only the elevation head. Pipe friction loss was ignored since the distance between the points was 10-20 m, assuming friction losses were insignificant.

2.6 Model Simulation and Analysis

The distribution network analysis was conducted using Water CAD software by building distribution system model. Hazen–Williams equation was used to compute pressure and velocity at both steady state and extended period simulation of the water supply system. The hydraulic performance of the distribution network was identified and evaluated by comparing these hydraulic parameters with design criteria of the distribution network and areas of high or low pressure zone. The static pressure in the distribution system is the pressure head in the network is equal to the height to which the column of liquid could be raised (Swamee and Sharma, 2008). The adopted design criteria for the evaluation that is 15- 60 meter of water (mw) and flow velocity 0.6- 2 m/s was according to MoWR (2014).

2.7 Utility Performance Evaluation

To evaluate the utility performance, a set of IWA key performance indicators (KPIs) were used as the basis for the performance evaluation. The KPIs used were selected and adopted based on the availability of data. Under the IWA system, performance indicators (PIs) were classified into 5 groups: personnel, technical, environmental, quality of service and economic and financial Alegre et al. (2017). PIs could be different for developing and developed countries owing to the availability of data (IWA, 2006). The methods of calculation for performance indicators are shown in Table 1. Finally, the analyzed results were discussed by comparing them with benchmark target, which was obtained from IWA standard and MWIE (2014) guideline for GTP II.

Table 1 Key performance indicators and their calculation methods

No.	KPIs	Method of calculation	Unit
1	Average daily per capita water consumption	Total billed water (m^3) during the assessment period x 1000/ (365x total number of served population)	l/c/d
2	Average selling price per m^3 of water	Total billed water sales (Birr)/ Total domestic, institutional, and commercial water sales (m^3)	Birr
3	Operating costs per m^3 of water sold	Operation & Maintenance (O&M) and administrative costs/ Net water sales (m^3)	Birr
4	Working ratio (Efficiency Ratio) for water service	Operation & Maintenance (O&M) and administrative costs / Operating revenues from water	number
5	Collection efficiency	Water fees collection during the year / total annual water billed sales (Birr)×100%	%
6	Non-Revenue Water (NRW)	Total billed quantity (m^3) during the assessment period/ (Total supplied water during assessment period ± difference in stored quantities in utility reservoirs) x 100%)	%
7	Staff productivity index (SPI) per1000 customers	Total number of working staff/ (number of active water subscribers)/ 1000 customers	Number
8	Water losses in (m^3) per km in the distribution per year	Total water losses during the year (m^3)/ Total Network length (km)	m^3
9	Water samples taken from distribution network containing free chlorine residual (RC)	Number of Samples taken from network containing free chlorine residual/ Total number of tested samples for RC x100%	%
10	Water samples (taken at distribution) free from total coliform contamination	Number of tested water samples (taken at distribution) free from total coliform contamination/ Total number of tested samples for this purpose x 100%	%
11	Samples (taken in distribution) free from fecal coliform contamination	Number of tested water samples (taken at distribution) free from fecal coli form contamination/ Total number of tested samples for this purpose x 100%	%
12	Microbiological tests	Number of microbiological tests carried out during the assessment period/ number of microbiological tests required by applicable standards during the assessment periodx100%	%

2.8 Optimization of the distribution network

After analyzing and identifying the distribution network problems, the distribution system was modified by different mechanisms. Nine pressure reducing valves (PRVs) were provided at P-69, P-70, P-72, P-79, P-81, P-83, P-86, P-191, and P-193 to reduce excess pressure in the distribution system. Alternative connection was another way to increase pressure and flow velocity. T-1 was connected with J-98 and T-2 with J-41. The pipe diameters of P-140, P-141, P-142, P-144, P-145, P-147, P-148, P-150, P-151 and P-152 were resized and the pump operation time changed. Thus, the distribution system was improved. Besides, injecting additional water into the system was another way of improving the system.

3. RESULTS AND DISCUSSION

3.1 Population and Demand projection

The population of the town at 2020 was 31,600. According to the Ministry of Water guideline (MoWR, 2014), the percentage of population served by house connection (HC), yard connection (YC), and public fountain (PF) were estimated for 2021, 2025 and 2030. Water consumption varies with mode of services. Customers with house connection use more water than customers with yard or public tap connection. Table 2 shows Ataye Town population and water demand projection up to 2030. The total domestic demand can be worked out by multiplying the per capita per day demand with population served by each mode of service.

Table 2 Population and demand projection by mode of service

Description	**Years**			
Population/Service Levels	2020	2021	2025	2030
Population	31600	32709	37549	44596
Percentage (%) of Population Served by:-				
House connection	35	36	40	44
Yard connection	48	49	53	56
Public Fountain	15	14	7	0

Description	**Years**			
Per Capita Demand (Lpcd)				
House connection	70	71	75	80
Yard connection	30	31	35	40
Public Fountain	25	26	30	35
Demand by Service Standard (m^3/d)				
House connection	774.2	836.39	1128.72	1575.7
Yard connection	455.04	507..48	699.52	1006.4
Public Fountain	118.5	119.15	79.22	0
Average domestic water demand (m^3/d)	1347.74	1463.03	1907.46	2582.11
Commercial & institutional demand (10 %)	134.77	146.3	190.75	258.21
Unaccounted water demand (25 %)	336.93	365.8	476.86	645.52
Projected average water demand (m^3/d)	**1819.44**	**1975**	**2575.1**	**3485.8**
Maximum day factor	1.2	1.2	1.2	1.2
Maximum daily water demand (m^3/d)	2183.34	2370	3090.09	4183
Peak hour factor	1.7	1.7	1.7	1.7
Peak hour water demand (m^3/d)	3093	3358	4377.63	5925.9

The average water demand of Ataye town in 2025 will be **2575.1** m^3/d. The town water utility has four boreholes with total average daily production capacity of 24.8 l/s (2142.72 m^3/d) (ATWSS, 2020) which cannot meet the water demand after 2022. So, there should be additional source after 2022. Base or average water demand for each node was computed and assigned based on population, types of demand, and mode of service around the node. Public fountain may not be used after 2030. House connection will be more than yard connection after 2021 as the income of the population increases.

3.2 Model Creation, Calibration, and Validation

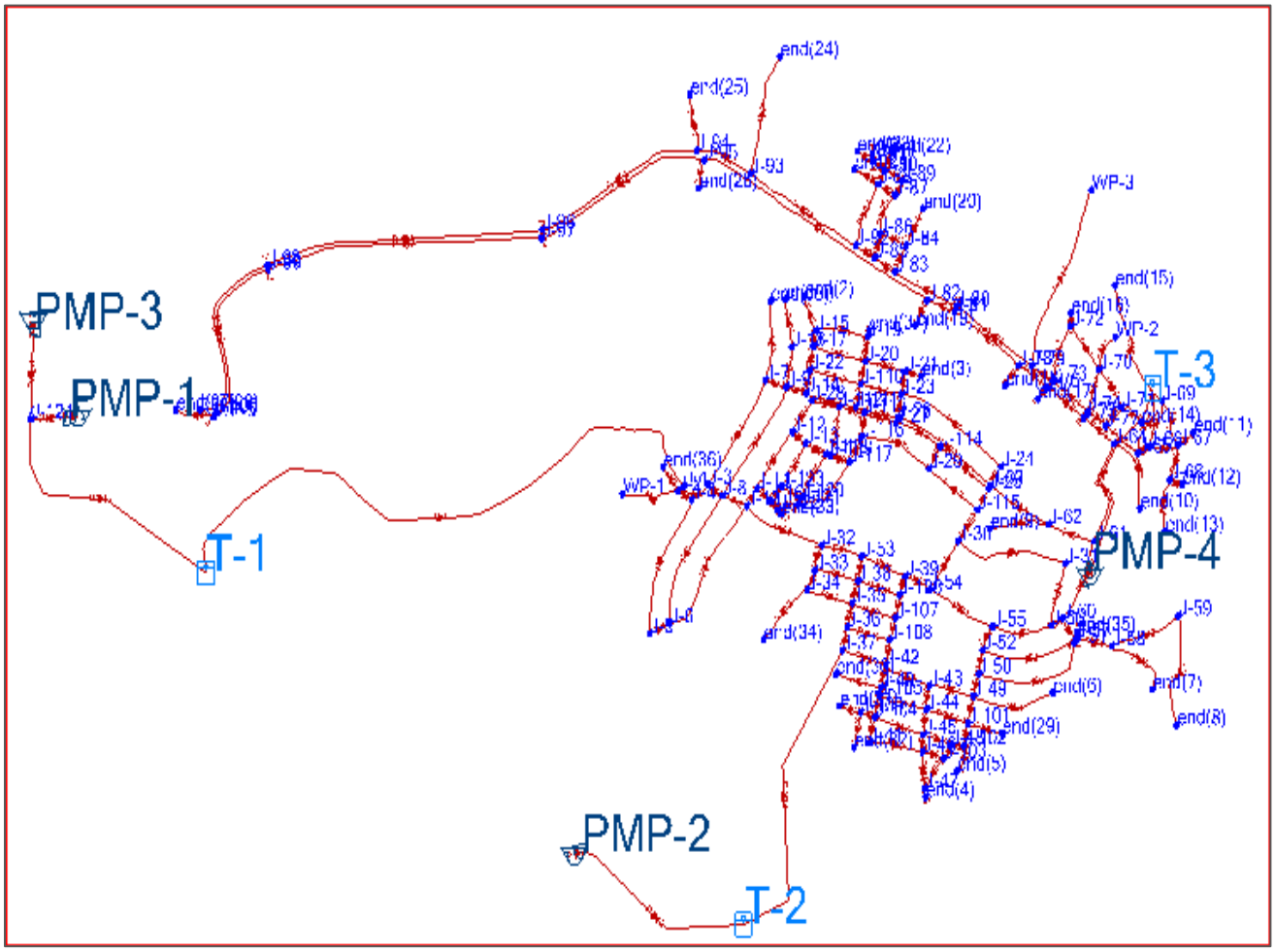

Figure 2 Ataye Town Distribution network layout

Figure 2 shows the water distribution network of Ataye town designed with water CAD. The model has 166 nodes, 222 pipes (links), 3 tanks, 4 reservoirs (boreholes) and 3 pumps. Table 3 shows measured and simulated pressure at different time and sample nodes. Head losses between the two points were added to measured pressure at customer tap to get measured pressure at sample node.

Table 3 Simulated and observed pressure at specific time after the first run

C	Nodes	Measurement time	Simulated model pressure (mw)	Measured pressure at costumer tap (mw)	Head losses b/n nodes and customer tap (mw)	Likely measured pressure at sample Node (mw)	Error(m)
1	J-63	7:00	26	22.07	0.58	22.65	-3.35
2	J-32	17:30	29	25.48	0.7	24.78	-4.22
3	J-10	18:00	24	21.40	0.83	20.57	-3.43
4	wp-1	11:00	0	0.00	0	0.00	0
5	J-8	17:00	20	18.54	0.41	18.13	-2.87
6	J-9	18:30	20	18.34	0.85	17.49	-2.51
7	J-62	8:25	55	49.55	1.05	48.50	-6.50
8	J-6	16:35	10	7.63	0.53	7.10	-3.90
9	J-73	17:50	30	26.70	0.11	26.81	-3.19
10	J-76	15:00	52	49.65	0.03	49.62	-2.38
11	J-78	18:30	28	24.97	1.46	23.51	-4.49
12	J-81	7:30	27	18.33	0.59	17.74	-9.26
13	J-75	19:30	56	52.10	1.02	51.08	-4.92
14	J-71	8:00	30	26.09	0.92	25.17	-4.83
15	WP-3	11:20	2	0	0	0	-2.00
16	end(32)	6:00	4	0	0	0	-4.00
17	J-101	23:00	13	8.67	0.36	9.03	-3.97
18	end(3)	13:00	52	48.76	0	48.76	-4.24
19	J-117	21:00	53	42.94	0.66	42.28	-10.72
20	end(21)	5:00	18	12.75	0	12.75	-5.25

Note: mw= meter of water

The error was the calculated difference between measured and simulated pressure. The negative values for error showed that simulated pressures were greater than the measured pressured. At all junctions except wp-1, the simulated and the measured pressure values had differences in relationship. The model was over estimated at those junctions. So, model calibration using Darwin calibrator was done. In Table 3, nil values for pressure indicated that there was no pressure at the junction during the measurement time and the nil head loss values showed that there was no head difference between sample nodes at customer taps.

The measurements were taken at 20 junctions at different location in the town. Nil pressure was recorded at WP1 in Selama, at WP3 in Zigba Sefer and at the end (32) in Sudan Sefer.

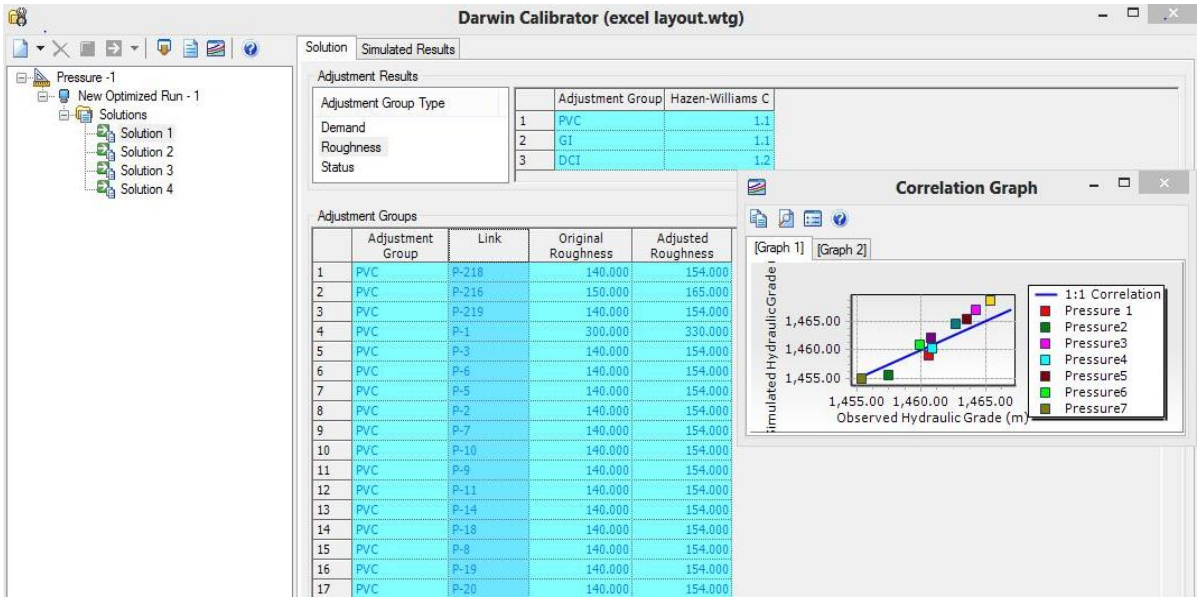

Figure 3 Original and adjusted pipe roughness values and correlation graph after model calibration

Figure 3 shows Darwin's calibration result of original and adjusted pipe roughness and correlation graph. The correlation graph showed the relationship between measured and simulated pressures.

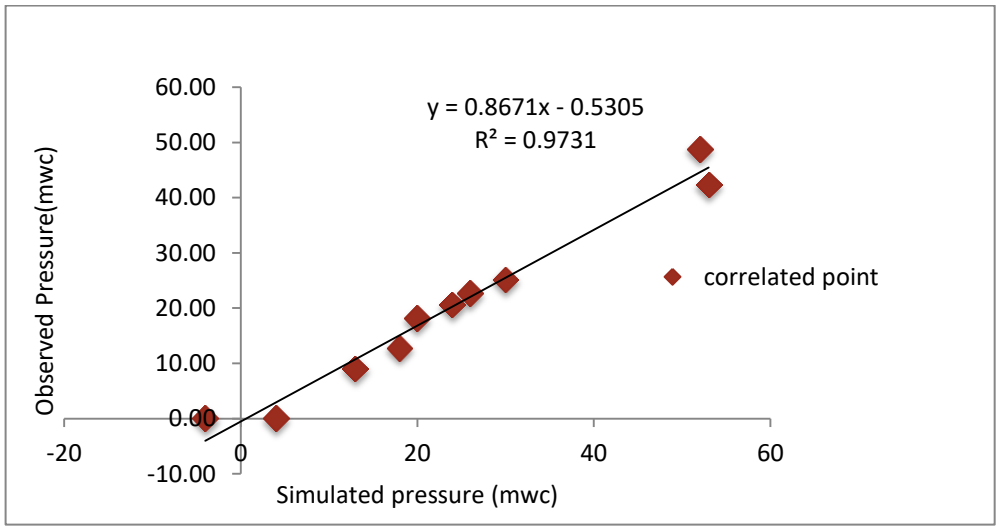

Figure 4 Scatter plot of simulated versus observed pressure for validation

In Figure 4, x-axis refers to simulated pressure while y- axis indicates observed pressure for 10 sample points which were used for model validation. After calibration, the model was validated using correlation coefficient equation (R^2) for scatter plot of observed versus simulated pressure. The more the correlated points approached the line the more the data had linear relationship. For both methods the correlation coefficient (R^2) value was 0.97 (97%) which implied strong linear relationship between observed and simulated pressure. Thus, the simulated was in agreement with the real one.

3.3 Pressure and velocity analysis

3.3.1 Pressure for steady state analysis

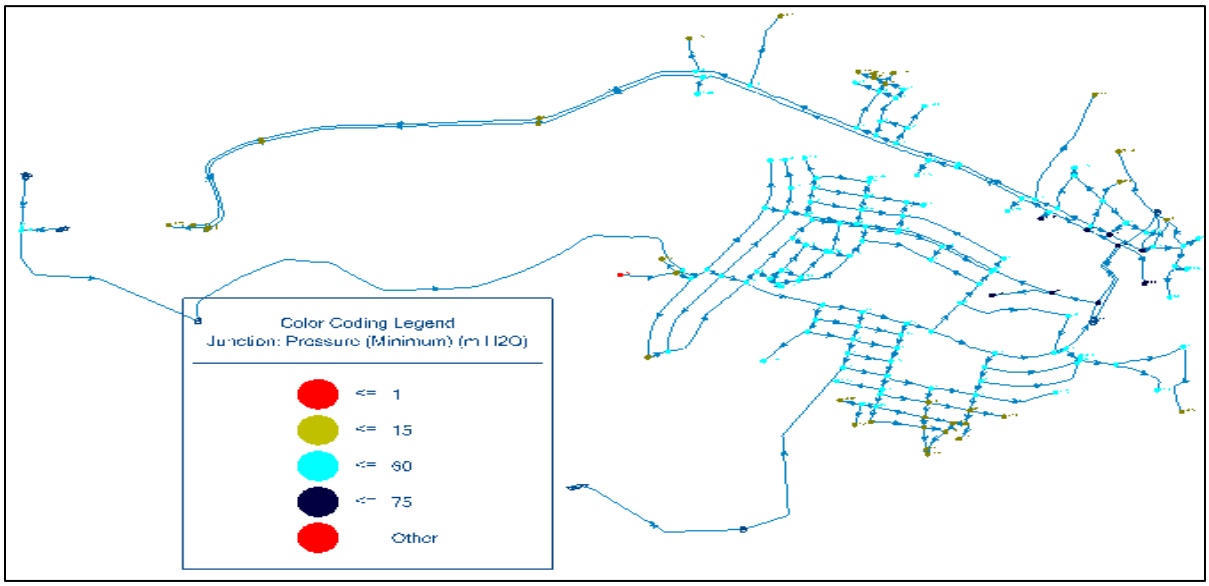

Figure 5 Pressure values for steady state analysis from Water CAD.

Figure 5 shows the model result analyzed at steady state run for the average daily demand, which does not change at every node 24 hours of a day. The nodes with red color represent negative pressure (<=1m), nodes with yellow color show pressure in the range **1- 15 m**, nodes with aqua color represent pressure **15-60 m** and those with blue color show pressure greater than **60 m**. From simulated result for steady state analysis, one junction (**WP-1**) located at Selama Sefer had negative pressure, 37 nodes (**22.29%)** had pressure below minimum adopted pressure (15m), **9** junctions (**end (9**), J-61, J-62, J-64, J-65, J-75, J-77, end (10), and end (17) or (**5.4%)** had pressure

greater than maximum adopted pressure (60m). The remaining **119** nodes (**71.68%)** had pressure in the range **15-60 m** which was optimum adopted pressure range (MWIE 2014). For steady state analysis only **15** pipes in Zigba, Slama and Sudan Sefer or **7%** of the distribution system performed with optimum velocity of (0.6m/s to 2 m/s). The rest was operated under optimum velocity.

3.3.2 Extended Period Simulation (EPS) Result

Extended period simulation showed more detailed variation of hydraulic parameters, demand, supply, and tank level fluctuation in 24 hours of a day.

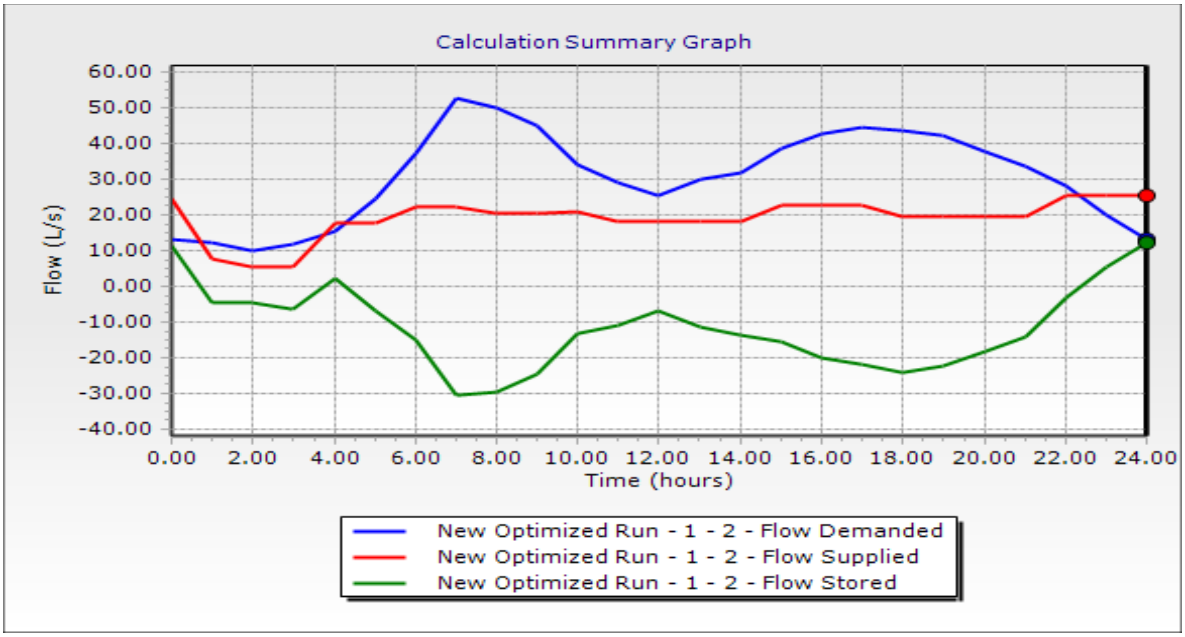

Figure 6 demand, supply and tank storage fluctuation summary graph

Figure 6 shows that base flow demand reached a peak of 7:00 (52 l/s) and flow supply was 22 l/s. So, tank storage was -30 l/s. The negative sign indicated that the tank was at full status. The flow stored from 0:00 to 1:00 and 22:00 to 24:00 was taken as positive, which means the tank was draining/ overflowing.

It was difficult to discuss all 166 nodes in 24 hours. The low and high pressure occurs at low and high demand time, respectively. High daily demand for this study occurred from7:00 to 9:00 and 17:00 to 19:00. Low daily demand happened within 0:00 to 3:00 and 22:00 to 24:00 hours. The maximum pressure was **70** m at end (10) and minimum pressure was **-14**m at wp-1.

In Figure 7, areas or nodes with red color represent less pressure of 1 meter water column (mwc), pink color shows area with pressure **1- 15**m, blue color represents **15-60** m pressure, and aqua color represents areas with **60 to 70**m pressure at peak demand time. **18** Nodes (wp-1, J-47, end(4), J-69, end(15), wp-3, wp-5, end (24), end (25), J-98,J-99, J-100, end(27), end(28), end(5), WP-4, end (22) and end (32)) with red color had negative pressure at maximum demand time. **39** nodes had pressure **1-15 m** at maximum demand time. End (10) had greater than 60m pressure even at maximum demand time. The remaining **108** nodes with green color had pressure **15-60m** (**65.06**%) which adopted optimum design pressure.

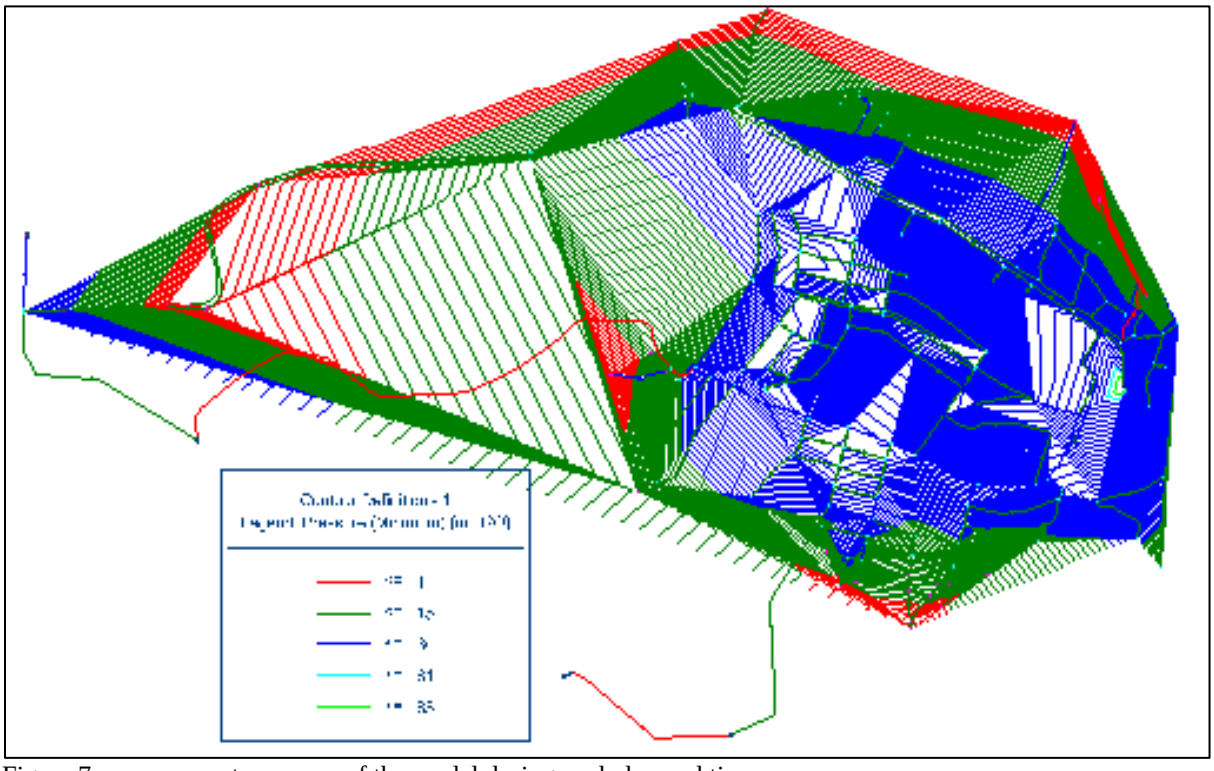

Figure 7 pressure contours map of the model during peak demand time

Figure 8 shows pressure contour map of distribution during minimum demand time. During minimum demand times, **28** nodes or **16.86%** were operating under the minimum adopted pressure (1- 15m). Areas with aqua color and located at 02, Laygnaw Ataye, Sudan Sefer and Zigba showed less pressure of 15mwc. **14**nodes (J-30, J-31, J-61, J-62, J-115, end (9), J-64, J-65, J-74, J-75, J-77, end (10), end (17), and end (18)) or **8.4%** areas shown with red color and located around Worku Hotel, Roman Hotel and Mosque, had pressure greater than **60m** during low demand times. **124** nodes (**74.7%)** were operating within optimum adopted pressure (15-60m). This was represented by blue color. **57** nodes (**34.34%)** during maximum demand times and 28 nodes (**16.86%)** during minimum demand time had pressure less than 15m H_2O in the distribution system, which was not sufficient for effective system performance. **18** nodes had negative pressure during maximum demand time. That means **4500** people around these nodes could not get water during maximum daily water consumption hours. **14** nodes during minimum demand time and **1** node during maximum demand time had pressure greater than 60mwc which was a maximum adopted pressure. These pressures had adverse effect on the performance of the distribution system. Pipes and valves around these nodes burst; thus, causing high water loss in the system. Only **74.71%** during minimum demand time and **65.06%** during maximum demand time of the distribution system were performing within the optimum adopted pressure.

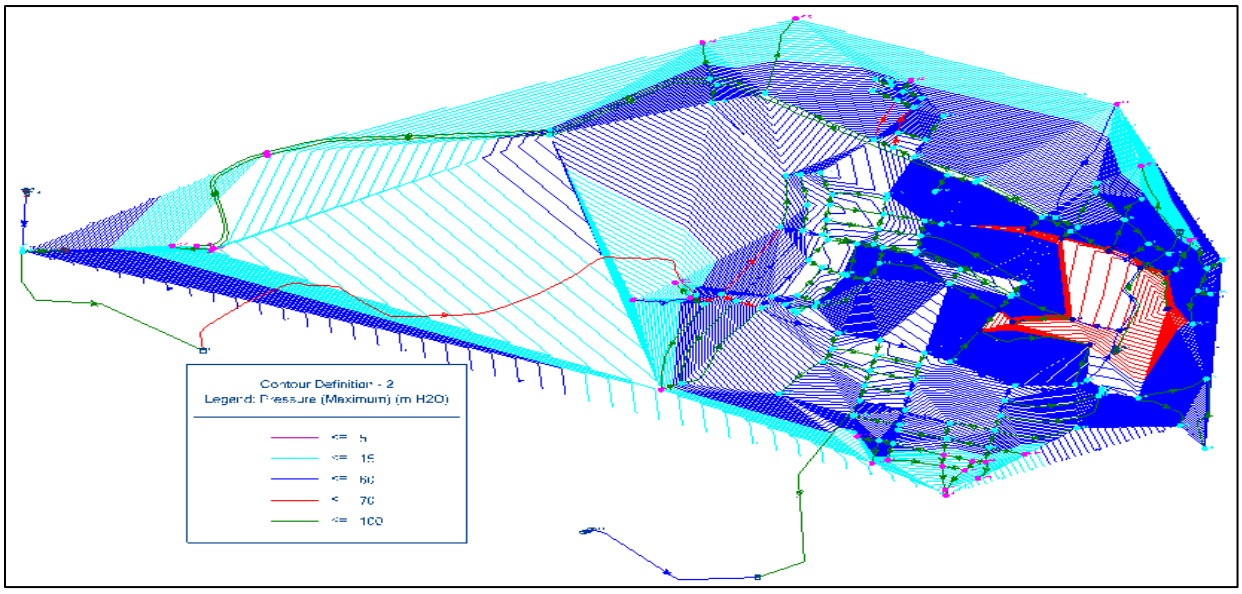

Figure 8 pressure contour map of Ataye Town distribution during minimum demand time

3.3.3 Flow Velocity for extended period simulation

Figure 9 shows the flow velocity for extended period simulation at maximum demand time. The maximum velocity was 1.61 m/s in P-1 at high demand hours and the minimum velocity was 0.0 m/s. **8** pipes (p-1, p-5, p-10, p-11, p-18, p-124, p-124, and p-137) with red color in Figure 9 had velocity of **1.08-2 m/s** at high demand hours**. 42** pipes with blue color represent a velocity of 0.55m/s to 1.08m/sand. The green color shows a less velocity of 0.55m/s at peak demand hours. All pipe flows had a velocity less than 0.60 m/s at low demand hours in the distribution system. At high demand hours, **50** pipes **(23.47%)** had a velocity of 0.6m/s to 2m/s which were believed to be optimum adopted velocity. The remaining had a velocity of less than 0.6m/s. There was not a pipe with a velocity greater than 2m/s in the distribution system.

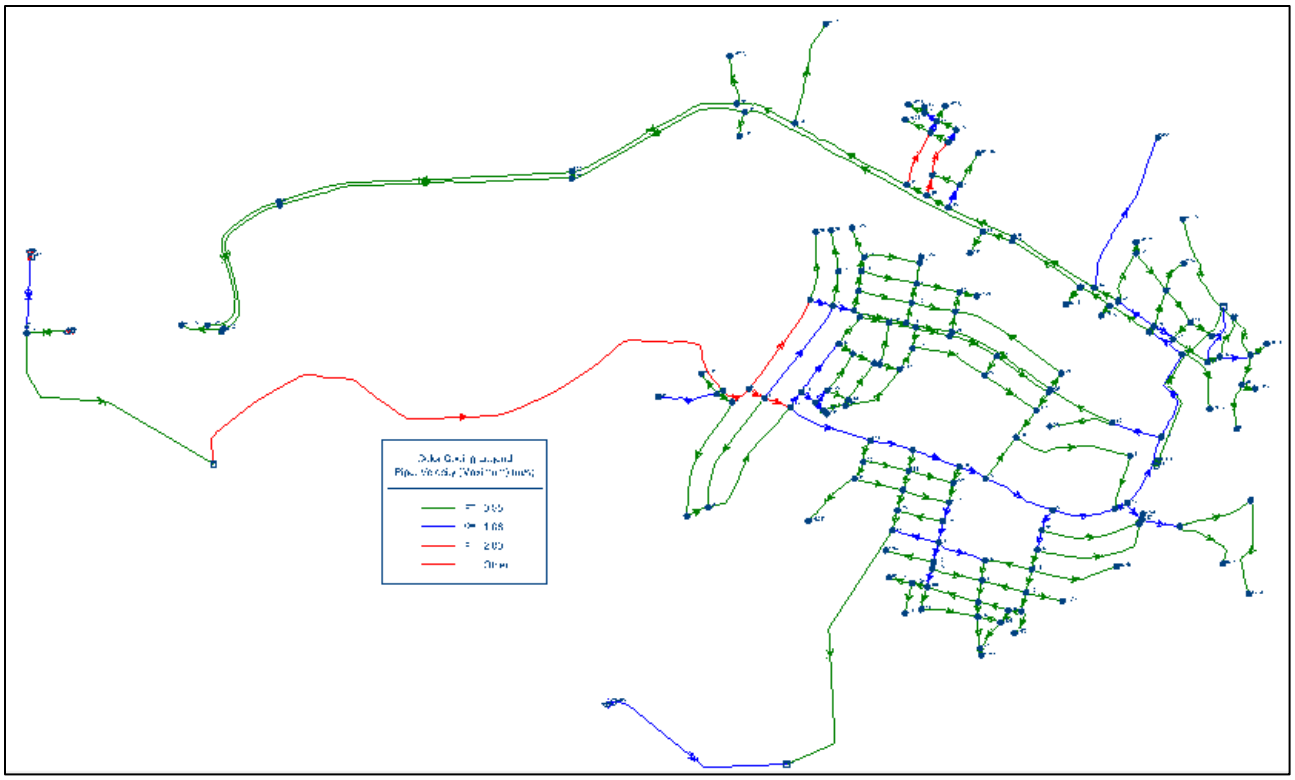

Figure 9 Result flow velocity for extended period simulation at maximum demand time

3.4 Mitigation by modifying the distribution network

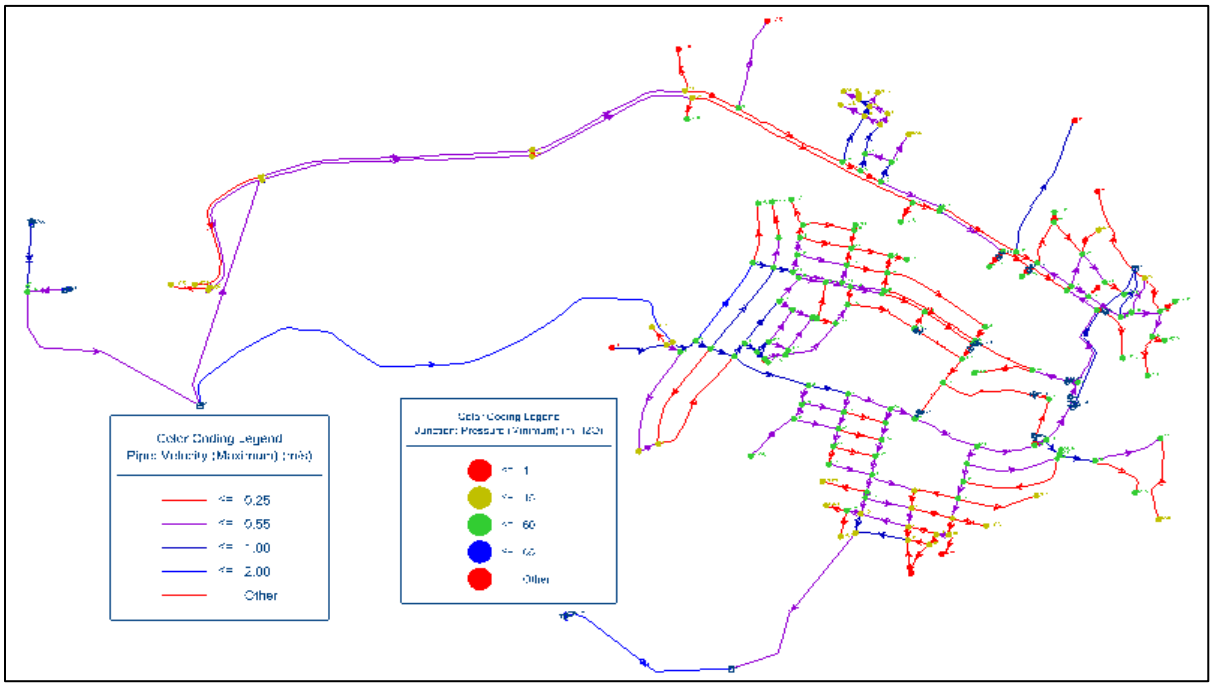

Figure 10 Modified and Optimized Networks by adjusting pipe diameter and connection points

Figure 10 shows the modified pressure in the accepted range of the distribution system by adding, or replacing pipes or elements. Based on the results of the model simulation, the distribution system was modified to reduce observed high pressure and increase low pressure and velocity. Nine pressure reducing valves (PRV) were added at P-69, P-70, P-72, P-79,P-81,P-83,P-86,P-191,P-193 to adjust the pressure. Alternative connection is another way to increase pressure and flow velocity. T-1 was connected with J-98 and T-2 with J-41 as shown in Figure 10. The diameters of P-140, P-141, P-142, P-144, P-145, P-147, P-148, P-150, P-151 and P-152 were resized (increased or reduced). After modifying the model, numbers of nodes with negative pressure were reduced from 18 to 8 and junctions with high pressure were reduced from 14 to 3 nodes. So, by applying the above mechanisms the distribution system was improved. Besides, additional water should be injected into the system by placing a storage tank at appropriate location. The utility may improve the distribution system based on these findings.

3.5 Utility Performance Evaluation

Table 4 shows the utility performance of Ataye town against International Water Association (IWA) performance indicators. For urban water supply, average per capital water consumption was 50 l/c/d for category-4 towns/cities (with a population range of 20,000-50,000) (MWIE), 2015). But average per capital water consumption of Ataye town in 2020 as shown in Table 4 was 23.18 l/c/d which was much lower than 50 l/c/d. Water supply coverage of the town was 83%.

In Table 4, the working ratio or efficiency ratio of the study area was **0.75** which showed that the utility was generating surplus income and could cover its operating, maintenance, and administrative costs. According to GTP-2 national plan, the utilities should 100% recover their operation and maintenance costs. So, the utility had good performance in this condition. Revenue collection efficiency of the utility was **95**%. There was 5% (103, 636.1 ETB) outstanding balance collected from the previous year. This ratio reflected the efficiency of the staff in performing their duties and consumers' willingness to pay. The IWA benchmark target was 100%. Therefore, the utility had less performance in collecting arrears from customers. Non-revenue water of the study area was 18.15%. Based on the national plan for Water Supply and Sanitation Sub-sector (2015/16- 2019/20), urban Non-Revenue Water (NRW) was planned to decrease from 39% to 20% by 2020 for urban water supply utilities. According to the national plan, there would be 59,318.52m^3(18.15%) of annual NRW in the distribution system.

Table 4 Ataye Town utility performance indicators by IWA utility performance indicators

Category	Performance indicators	Computed value	Benchmark target
Technical performance	Water supply coverage (%)	83	100
	water production (liters/person/day)	28.32	variable
	Water consumption (liters/person/day)	23.18	50
	Non-revenue water (NRW) (%)	18.15	<20

Category	Performance indicators	Computed value	Benchmark target
Financial performance	Average water revenue (Birr/m^3) annual water sold	1,958,631.5	
	unit operation cost of water (Birr/m^3 produced)	8.78	
	Operating Ratio (Efficiency Ratio)	0.75	<1
	Revenue collection efficiency (%)	95.00	100
	Average water selling price(Birr/m^3)	7.32	variable
Quality of service	Continuity of service (hours/day) and /week	24	24
		7	7
	No. of complaints/1000 connections	1025	variable
Human resource utilization and management	Staff productivity index (SPI) per1000 customers	7.44	7
	Staff training participation (%)	16.67	30
	Labor cost versus operational cost (%)	4.61	20
water Quality/ Health or environmental	Water samples taken from distribution network containing free chlorine residual (RC) (%)	25	100
	Water samples (taken at distribution) free from total coli form contamination (%)	58.33	100
	Samples (taken in distribution) free from fecal coli form contamination (%)	50	100
	Microbiological tests (%)	16.67	100

Staff productivity index (SPI) per 1000 customers was the other personnel performance indicator that considered the efficiency of managing human resources of the utility. For this study, staff

productivity index per 1000 customers was **7.4.** But the benchmark for African water utilities was **5** (Van den Berg and Danilenko, 2017) and IWA benchmark was 7. The staff productivity index was more than the benchmarks and this could incur additional cost on the utility. All the performance indicators related to water quality/ health was under the benchmarks which showed less performance of the utility in water quality control activities.

4. CONCLUSIONS

The study was focused on evaluating Ataye town hydraulic performance by water CAD, and the utility performance by IWA performance indicators. The population and water demand of the town was projected until 2030 and the projected demand exceeded the current water production capacity of the town, which suggested the need for additional water sources. In some areas, there were insufficient pressures to satisfy the required demand at all times. The lowest pressure (<15m) was identified during maximum demand (**34.34%)** and during minimum consumption (**16.86%). 10.84%** of consumption nodes had negative pressure during maximum demand hours meaning; around 4,500 people were not getting water during this time. The distribution system performed within the optimum adopted pressure only **74.71%** during minimum demand time and **65.06%** during maximum demand hours. **14** nodes (8.43%) had pressure >60m which was maximum adopted pressure and this caused water losses in the system. **23.47%** of the system pipes had optimum adopted velocity of (0.6 -2m/s) and the remaining had a velocity less than 0.6 m/s during high demand time. Hence, the distribution system had limitations hydraulically. Based on the results, the network was modified by providing pressure reducing valve, resizing pipes diameter and alternative connection of pipes and junctions to reduce observed problems.

The town water utility performance was also evaluated by IWA performance indicators. The performance indicators showed that the utility had low technical, personnel, and environmental performance. Thus, to the researchers recommend that the distribution network should be modified by providing pressure reducing valve, resizing pipes diameter, alternative connection of pipes, and junctions. Additional water wells should be added into the system besides improving the utility performance.

REFERENCES

Alegre, H., Cabrera Jr., E., Merkel, W. (2009). Performance assessment of urban utilities: the case of water supply, wastewater and solid waste. Journal of Water Supply: Research and Technology – AQUA, 58, 5, 305-315.

ATWSS (2020) Ataye Town Water supply and Sewerage office Report documents. Report.

CSA (2007) Centeral Statistic Agency: Population and Housing Census of Ethiopia, Addis Ababa.

Alegre, H., Batista, J.M., Cabrera Jr, E., Cubillo, F., Duarte, P., Hirner, W. Merkel, W, Parena, R. (2017) Performance indicators for water supply services, 3rd edition, IWA publishing, London SW1H 0QS, UK.

Kassa, k., Chernet, M., Kelemework, G., Zewde, B., Woldemedhin, A. (2017) Customer satisfaction survey: the case of urban water supply services in Southern Ethiopia, Water Practice & Technology, 12. doi: 10.2166/wpt.

Tekle, M. (2016) Hydraulic modeling of water supply distribution nework. a case study on Debre Birhan town, Amhara regional state Ethiopia. Master Thesis, Jimma University, Ethiopia.

MoWR (2014) Federal Democratic Republic of Ethiopia: Ministry of Water Resource Urban Water Supply Design Criteria, Addis Ababa.

MWIE (2014) Federal Democratic Republic of Ethiopia Ministry of Water, Irrigation and Electricity Second Growth and Transformation National Plan for the Water Supply and Sanitation Sub-Sector (2015/16 – 2019/20), Addis Ababa.

Swamee, P.K. and Sharma, A. K. (2008) Design of Water supply pipe Networks. Hoboken, New Jersey: John Wiley & Sons, Inc.

Terlumun, U. J. and Ekwule, O.R. (2019) Evaluation of Municipal Water Distribution Network Using Watercard and Watergems, Journal of Engineering and sciences, 5(2), pp. 147–156.

Trifunovic, N. (2006) Introduction to Urban Water Distribution, London, UK: Taylor & Francis/ Balkema. Available at: www.balkema.nl.

Van den Berg, C. and Danilenko, A. (2017) Performance of Water Utilities in Africa. International Bank for Reconstruction and Development/ The World Bank 1818 H Street NW, Washington, DC 20433. Available at: www.worldbank.org/water.

Zyoud S.H.A.R. (2003) Hydraulic Performance of Palestinian Water Distribution Systems (Jenin Water Supply Network as a Case Study). MSc Thesis. Master Thesis, An-Najah National University, Nablus, Palestine.

Ethiopian Journal of Water Science and Technology (EJWST)

DOI: https://doi.org/10.59122/15519k7

Vol. 5 , 2022, pages: 24~50 ISSN(Print): 2220-7643

The Grand Ethiopian Renaissance Dam (GERD): Geopolitical Implications

Gashaw Ayferam Endaylalu

PhD Candidate, Department of Political Science and International Relations, Addis Ababa University, +251925697676, mugashawbzu@gmail.com

ABSTRACT

This study examined the geopolitical implications of the GERD project in light of the 'framework of benefit-sharing'. The study adopted a qualitative research approach in which data were gathered from multiple sources, such as key informant interviews, books, journal articles, policy briefs, commentary, and opinions; and documents such as declarations, agreements, letters, and statements, water policies, government communications, reports, and media sources. In light of this, the paper argues that GERD foreshadows a new emergent order based on principles of benefit-sharing capable of replacing the existing inequitable water-sharing regime. The GERD has the potential to create cooperation between the riparian countries because of its proven benefits to the region. The potential cost of non-cooperation may also push Egypt towards opting for cooperation. Furthermore, the GERD could shift the power dynamics by positioning Ethiopia as a regional anchor state, which could further enhance prospects for cooperation. The study also highlights that the conflict over the GERD extends beyond the physicality of the dam and is deeply rooted in the geopolitical rivalry between Ethiopia and Egypt. Egypt perceives the GERD as an existential threat to its existing water-sharing regime while Ethiopia regards it as a benefit-sharing project and an existential necessity. However, the study highlights the possibility that the GERD may transform the geopolitical rivalry between Ethiopia and Egypt from a water-based conflict into a power trade competition, implying that cooperation and conflict, competition and cooperation, may coexist in this complex geopolitical landscape. The study implies that understanding the geopolitical implications of the GERD is crucial for navigating the complexities of the issue and finding sustainable solutions.

Keywords: Geopolitics, GERD, Benefit-sharing, Water-sharing, Ethiopia, Egypt, Nile

Received: 11 May 2022; accepted 15 May 2022.

1.1. INTRODUCTION

The GERD is a hydropower project constructed on the Abbay River, which is one of the main tributaries of the Nile River, in Ethiopia. Construction of the dam began in 2011 amidst the Arab Spring and started generating 375 MW in February 2022 from one of its turbines (Ethiopian News Agency, 2014). It is expected to become fully operational shortly. The primary objective of the dam is to generate electricity to meet the growing energy demands both at home and in the region, which in turn will drive economic development, achieve self-sufficiency, and overcome poverty and underdevelopment. The project is also seen as an emblematic initiative (Dejen, 2021) symbolizing Ethiopia's national independence, pride, identity, and resilience, being built by the "blood, tears, and sweat" (Seleshi, 2021) of all Ethiopians. It is also a project reclaiming Ethiopia's past, with parallels drawn to the historic Adwa victory against the Italian invasion (Yalemzewd, 2020). Furthermore, GERD is viewed as a present-day battle against abject poverty (Yalemzewd, 2020) and a vision for projecting power in the future.

However, the development of GERD remains controversial. It has been a source of conflict and geopolitical tension between Ethiopia, Sudan, and Egypt since its inauguration in 2011 (Mbaku, 2020; De Falco and Giulia, 2022, Al-Anani, 2020; Miehe *et al.*, 2020). In addition, non-riparian countries and multilateral institutions have been involved in the GERD dispute, playing roles ranging from negotiation facilitation (Africa Union) to self-appointed mediation (U.S.) and interference (the Arab League). The tension and disputes surrounding GERD primarily stem from the differing perspectives and concerns of Ethiopia, Sudan, and Egypt. Ethiopia presented GERD as a benefit-sharing project and an existential necessity (FDRE, 2020a). In contrast, Egypt views it as an existential threat to its existing water-sharing regime, closely tied to its national security and identity (State Information Service, 2021; Embassy of Egypt Washington D.C, n.d; Al-Anani, 2022). Sudan finds itself in a hydro-political dilemma, swinging like a pendulum. It sometimes aligns with Egypt and other times with Ethiopia or remains in the middle (Otinov, 2022; BBC, 2021).

The controversy surrounding the GERD also extends beyond the three riparian states and has ignited intense academic debates. Existing literature on GERD has primarily focused on the potential downstream impacts of the dam including its benefits and costs (Basheer *et al.*, 2020; Asegdew and

Semu, 2014; He *et al.,* 2022; Abdelkader and Mohamed, 2019; Bekhit *et al.,* 2019), filling and operations (Asegdew *et al*, 2014; Abdo *et al.*, 2016; Block *et al.*, 2016), as well as the transboundary cooperation implications of the dam (Cascão *et al.*, 2019; Jeuland *et al.*, 2014; Tawfik, 2016; 2015). Studies on the GERD also utilize various international relation theories, such as realism (Kaleb, 2022), constructivism (Adam *et al.* 2021; Lindqvist, 2021), securitization (Gienanth, 2020; Frida, 2021), ontological security (Fana and Dawit, 2021; Stenberg, 2021), geopolitics (Anwar, 2017; Goitom, 2014), and critical hydro politics (Rubin, 2019; Tayie, 2018; Tawfik, 2015; 2016). These analyses have generated a variety of predictions and different perspectives regarding the potential outcomes of the dam's construction. Some scholars view GERD as a potential source of conflict and regional instability (Gonzalez, 2020; Ayenat, 2020; Colton, 2021; International Institute for Middle-East and Balkan Studies, 2020; Ibrahim, 2021). Conversely, others such as Cascão and Alan (2016) view the GERD as a potential catalyst for regional cooperation.

Tawfik (2016) also analyzed the benefits and costs of GERD labeling it a "game-changer" but from a downstream perspective. From a geopolitical point of view, Goitom (2014) studied the potential of GERD to end the oldest geopolitical rivalry between Ethiopia and Egypt. However, current situations showed the beginning of new forms of geopolitical rivalry which required thorough investigation. Rubin (2019) and Tayie (2018), allegedly asserted that the construction of the GERD signified a move towards Ethiopian hydro-hegemony.

Despite the relevance of the studies reviewed, they are not without limitations. First, they tend to focus merely on the hydro-political, conflict, and cooperation aspects of GERD, disregarding its broader geopolitical context. Second, territorial states are often assumed to be the only actors in transboundary water management, overlooking the roles of non-state actors and the complexities of transnational water governance. Finally, previous research failed to consider the long-term geopolitical consequences of GERD, including its potential effects on regional power dynamics and the rise of new actors in the region. The varying narratives surrounding GERD may suggest that the conflict is not just about the physical dam and water but involves deeper geopolitical interests. This study, therefore, intends to examine the geopolitical implications of the GERD in light of benefit-sharing framework which in turn fills the gaps in the existing literature.

The research questions to be addressed in this study include:

1. What are the key geopolitical factors that have influenced the construction and recent development of the GERD project?
2. What are the geopolitical implications of the GERD for the region, its potential impact on regional power dynamics and the emergence of new actors?
3. What type of geopolitical order and rivalry, features, and contending actors are anticipated with respect to the GERD?
4. What are the push and pull factors that could contribute to the emergence of a post-GERD geopolitical order and rivalry?

By addressing these research questions, this study aims to provide a more comprehensive understanding of the geopolitical implications of GERD and thereby contributes to the existing literature on the subject.

1.2. THEORETICAL AND METHODOLOGICAL APPROACH

In the existing literature, GERD is approached mainly from mainstream international relations theories such as realism (Kaleb, 2022), constructivism (Adam *et al.* 2021; Lindqvist, 2021), securitization (Gienanth, 2020; Frida, 2021), ontological security (Fana and Dawit, 2021; Stenberg, 2021), geopolitics (Anwar, 2017; Goitom, 2014), and critical hydro politics (Rubin, 2019; Tayie, 2018; Tawfik, 2015; 2016). However, these approaches are conceptually 'territorial traps' (Agnew, 1994), which may contravene the transboundary nature of international rivers such as the Nile, where the GERD is being under construction on one of its tributaries, Abbay. Thus, it is an imperative to search for an alternative lens that goes beyond the state-centric approach of mainstream international relation theories. These theories often overlook the interests and influence of a multitude of actors involved in transboundary water resources development.They are believed to shape and complicate the geopolitical dynamics in the region.

Thus, the researcher first believes that addressing the problem of shared water resources requires a move beyond the 'territoriality of state' assumption. Second, there is a need to apply a three-level analysis (basin, sub-basin, and regional level). Finally, a sustainable water regime cannot be realized

without the deterritorialization of transboundary water resources. Thus, all countries equitably share the benefits. Accordingly, the researcher adopted the 'benefit-sharing framework' as a viable theoretical lens to examine the broader geopolitical implications of GERD in the region. The need for a new theoretical perspective beyond state-centric international relations theories is justified due to the complex nature of water resources development projects on transboundary rivers. These projects involve multiple actors with diverse interests: local communities, downstream riparian, geopolitical actors, global environmental regimes, intergovernmental organizations, international financial institutions, and others. Traditional state-centric approaches are insufficient in capturing the intricate geopolitical dynamics surrounding the GERD issue as they fail to consider the range of actors involved and their varying interests. A benefit-sharing framework provides a more comprehensive understanding of the geopolitical implications of the GERD, considering the diverse perspectives and power dynamics involved. This approach allows for a holistic examination of the geopolitical complexities surrounding the GERD issue, going beyond the limitations of state-centric theories.

Methodologically, this study also adopted a qualitative approach. The data were gathered from multiple sources. Primary data were gathered through interviews with water experts, diplomats, and researchers. Secondary sources of data included books, journal articles, and opinions. Documents such as letters and statements, water policies, agreements, declarations, and reports were also used.

1.3. DISCUSSION

The Nile River Basin has long been a source of geopolitical rivalry among countries that the Nile River traverses, specifically between Ethiopia and Egypt (Interview with Senior Diplomat, Ministry of Foreign Affairs, November 2021). They have conflicting interests and disagreements over water-sharing and benefit-sharing. The 1929 and 1959 bilateral agreements, along with the Cooperative Framework Agreement (CFA), can be seen as a water-sharing framework (Zerihun, 2011), whereas the Nile Basin Initiative (NBI) is a benefit-sharing arrangement (Zerihun, 2011; Council of Ministers of Water Affairs of the Nile Basin States, 2001; NBI, 2009). However, there are contradictory positions on water and benefit-sharing between upstream and downstream countries. Downstream countries view water sharing as the 1959 agreement (Daily News Egypt, 2014) which exclusively allocates Nile River water to themselves. They strongly believe that any modification of their share of

the river, as defined by the 1959 treaty and the established hydro-political order, poses an existential threat to their water security, which is closely tied to national security. An informant noted that

> *the Red Sea and the Nile determine the region's power configuration and have been a source of geopolitical rivalry between Egypt and Ethiopia for centuries. Regarding the Nile, Egypt's geopolitical strategy has been to control the Nile's water resources. Egypt has made agreements with Britain and Sudan that allow the water to flow downstream without restriction, and grant veto power to downstream countries to prevent the upper riparian countries from using the water without their consent* (Interview with Senior Diplomat, Ministry of Foreign Affairs, November 2021).

Even though upstream countries are not legally bound by the treaty due to its "legal defects" (Wuhibegezer and Sheferaw, 2014; Mohammed, 2004), they face challenges in accessing finance from international financial institutions owing to the precedent set by the 1959 treaty (Anonymous Interview, Ministry of Water and Energy, August 2023).

In contrast, Ethiopia offered a benefit-sharing framework through the construction of the GERD, signaling the rebirth of a new hydro-political order from which both Nile riparian and non-Nile riparian neighbors could benefit equitably. An informant argued that the philosophy behind the GERD represents a departure from the historical trend of malign hydro hegemony in the Nile River Basin where Egypt has historically sought to control the river (interview with a hydro-politics expert, Hawassa University, January 2023). Instead, the GERD embodies a "philosophy of cooperation and mutual benefit," and it is non-consumptive water (interview with a hydro-politics expert, Hawassa University, January 2023). However, critics may doubt the claim that GERD is a benefit-sharing project (Tawfik, 2015) because it is solely owned and financed by Ethiopia, but there are strong reasons why GERD can indeed be classified as a benefit-sharing hydraulic infrastructure.

First, Ethiopia has explicitly marketed GERD as a benefit-sharing project. This was evident in the inauguration speech delivered by late Prime Minister Meles Zenawi who emphasized the regional advantages that would arise from GERD. He stated that "the benefits that will accrue from the Dam will by no means be restricted to Ethiopia. They will clearly extend to all neighboring states, and particularly to the downstream Nile basin countries, to Sudan and Egypt"(Meles, 2011). The Prime Minister even invited downstream countries to participate in the project, suggesting a cost-benefit sharing formula where 50% of the project cost would be covered by downstream countries, with 30%

and 20% covered by Egypt and Sudan respectively, for the benefits they would gain from the GERD (Meles, 2011).

Furthermore, Ethiopia has taken diplomatic steps to make GERD a real benefit-sharing project, such as delaying the ratification of the CFA (Anonymous Interview, Ministry of Water and Energy, August 2023; MoWIE, 2013) and inviting downstream countries for joint consultations on the GERD project (International Panel of Experts, 2013). These diplomatic measures came as a response to the Egyptian accusation that the GERD is a strategic-political project (Tayie, 2018) that came to reality by exploiting and "take[ing] advantage of the turmoil" (Al-Masry, 2019) amid Egypt's 2011 January revolution (Interview with Senior Diplomat, Ministry of Foreign Affairs, June 2021). The former was a concession from Ethiopia that postponed the ratification of CFA, which is more consequential to the existing Nile water regime, assuring Egypt that the GERD is a developmental rather than a political project with benefits that go beyond Ethiopia. However, it should be noted that the Ethiopian People's Revolutionary Democratic Front (EPRDF) adopted a proactive media strategy to curb the spillover effect of the Arab Spring while exploiting the opportunities presented by it (Skjerdal, 2016). For a long time, there has also been a perception among elite circles that it would not be possible to dam the Abbay River until the right time came (Interview with Senior Diplomat, Ministry of Foreign Affairs, April 2022).

Both decisions which ultimately led to trilateral negotiation were intensely criticized by many Ethiopians including those involved in the GERD on three grounds. First, critics claim that the invitation for joint consultation over a project owned and financed by Ethiopia undermines Ethiopian sovereignty (Dejen, 2021). Second, postponed CFA ratification eroded the upstream alliance as shown during the CFA negotiation (Anonymous Interview, Ministry of Water and Energy, August 2023). It is also perceived as a unilateral move that can undermine the upstream coalition and spirit. Furthermore, it has made Ethiopia's Nile policy unclear as to whether an upstream alliance and a multilateral approach to Nile water governance are tactical or strategic priorities for Ethiopia. GERD may indicate Ethiopia's preference for basin-based, bilateral, and context-specific engagement rather than a multilateral basin-wide approach. However, while a basin and context-specific approach may be strategically significant, as seen in Ethiopia's reserved position on the IGAD transboundary water resources framework (Anonymous Interview, Ministry of Water and Energy, August 2023), it risks

ceding its long-term strategic interests in the Nile River. However, from a diplomatic perspective, it is argued that the decision to postpone ratification neither eroded the upstream coalition nor negatively impacted Ethiopia's interests (Interview with Senior Diplomat, Ministry of Foreign Affairs, June 2021). One piece of evidence cited is the ratification of the CFA by four countries which took place after the commencement of GERD.

Third, trilateral negotiations have further complicated the GERD project and increased Ethiopia's vulnerability to external diplomatic pressure through Egypt's securitization policy (Dejen, 2021). Despite these critics, the measures taken by Ethiopia may show Addis Ababa's effort to make the GERD project a benefit-sharing one to the extent of losing some of its key interests.

Moreover, in addition to inviting downstream countries for dialogue on GERD, Ethiopia has taken several steps to demonstrate its commitment to making the GERD a source of regional cooperation. These steps include the establishment of the International Panel of Experts (IPoEs) responsible for reviewing the dam design documents and assessing the benefits and costs of the dam to three riparian countries (IPoEs, 2013). According to Ambassador Alemayehu Tegenu, the former Minister of Water Resources of the Federal Democratic Republic of Ethiopia, the IPoEs were established as a confidence-building measure aimed at building trust and easing Egypt's concerns stemming from a lack of information about the dam (Ministry of Water, Irrigation and Energy, 2014). Ethiopia also provided 153 documents related to the GERD project for review by the IPoEs (IPoEs, 2013). A geotechnical expert group was also established to review the geotechnical documents of the project including dam site investigation (IPoEs, 2013) to study the rock foundation of the dam, a step taken in response to accusations from Egypt regarding potential foundation issues with the dam (Anonymous Interview, Ministry of Water and Energy, August 2023). Other steps included hiring consultants to implement the recommendations of the IPoEs, signing the Declaration of Principles (DoP), establishing the Tripartite National Committee, and establishing the National Independent Scientific Research Group. These measures collectively demonstrated Ethiopia's commitment to transparency, cooperation, and addressing concerns raised by downstream countries through the involvement of independent experts.

Second, the GERD project stands in opposition to the negative historical precedents that have led to its inception. In 2007, the three Eastern Nile countries (Egypt, Ethiopia, and Sudan) jointly conducted prefeasibility study of the GERD as a multipurpose project under the Eastern Nile Subsidiary Action Program of the NBI, with an Egyptian expert leading the study (FDRE, 2020b). However, when upstream countries signed the CFA in 2010 (Agreement on the Nile River Basin Cooperative Framework, 2010) downstream countries suspended their involvement in NBI activities and projects (Tadesse, 2017), thereby creating an impasse in the development of a benefit-sharing regime. This has also disrupted the Eastern Nile Council of Ministers' (ENCOM) annual meetings for four consecutive years (2010-2014), effectively holding the Eastern Nile Technical Regional Office (ENTRO) a geopolitical hostage (ENCOM, 30 January 2014). Moreover, the rejection of Ethiopia's proposal for multilateral projects by downstream countries hindered the potential for joint ownership and financial access from international institutions (Salman, 2016; Tawfik, 2015). For instance, World Bank turned down financing the joint proposed project (interview with senior expert, ENTRO, May 2022). These factors pushed Ethiopia, the only active member of the ENTRO, to construct the GERD unilaterally. Thus, Ethiopia's unilateral decision to construct the GERD can be attributed to the failure of regional cooperation under the auspices of the NBI.

Despite the downstream ego-centric approach to the Nile Water, Ethiopia initiated the GERD as a benefit-sharing project. An informant asserted that the philosophy of GERD is cooperation and mutual benefit, which contravenes Egypt's historical malign hegemonic approach in the Nile Basin (interview with a hydro-politics expert, Hawassa University, January 2023). Thus, GERD is a project that emerges as a result of cooperation failures but serves as a catalyst for regional cooperation through the implementation of benefit-sharing frameworks.

Third, the scientific community believes that the GERD benefits the riparian countries of the Eastern Nile and the region as a whole. This is supported by the 2013 reports of the IPoEs, the Amicus Brief by the International Non-partisan Eastern Nile Working Group in 2014, as well as studies conducted by Jeuland *et al.* (2014), Belachew (2013), Basheer *et al.* (2020), Asegdew *et al.* (2014), Asegdew and Semu (2014) and Getachew *et al.* (2020).

Fourth, GERD has also introduced a new legal norm that can supersede the norms of the existing inequitable water-sharing regime. The DoP serves as a case in point. Some of the norms included in the DoP can serve as a baseline for the evolving benefit-sharing regime. One of the principle is the commitment among the three countries to engage in cooperative efforts to understand the water needs of all riparian countries (DoP, 2015). This cooperation is guided by principles rooted in international law, mutual benefit, win-win approaches, good faith, and mutual understanding (DoP, 2015). Another principle is the principle of equitable and reasonable utilization of the shared Nile Water, which guides the water use of the three signatory countries (DoP, 2015). The DoP also includes principles aimed at enhancing cooperation, such as principles to cooperate on the first filling and operation of the GERD. It also incorporates principles related to dam safety and the peaceful settlement of disputes (DoP, 2015).

In article two, for instance, the three countries recognized the purpose of GERD as hydropower generation having an indispensable role in economic development, transboundary cooperation, and regional integration (DoP, 2015). Ethiopia also agreed to give priority to downstream countries to purchase power generated from the project, thinking as a confidence-building measure. In Article 10, the three countries also agreed to resolve disputes through peaceful means such as joint requests for reconciliation, mediation, and requests to their Heads of State and governments. This is a major shift in the Nile region.

Furthermore, the DoP also introduced new legal norms, such as the principle to consider "the contribution of each Basin State to the waters of the Nile River system" (Article 4(h), DoP, 2015). This might serve as a guide to countries in realizing the principle of equitable and reasonable utilization of the Nile water within their respective territories. However, this was not included in the 1997 convention of the Law of the Non-navigational Uses of International Watercourses. Rather, it was drawn from article 4(2)h of CFA (Agreement on the Nile River Basin Cooperative Framework, 2010) which was rejected by Egypt (Anonymous Interview, Ministry of Water and Energy, August 2023). A senior expert disclosed that Article 4(2)h of the CFA was not accepted by Egypt, but Egypt signed the same idea embodied in the DoP. This signing showed Egypt's recognition of Ethiopia's rights to the Nile water for the first time, which represented a new legal environment (Interview with Senior Diplomat, Ministry of Foreign Affairs, November 2021). Noting this change, scholars asserted

that the DoP enshrined a "fairness principle" for sharing the Nile waters (Zeray, 2017) and "a new legal order" (Salman, 2016) that superseded the old order. It might also foreshadow the end of the inequitable water-sharing regime, as Egypt recognized Ethiopia's right to the Nile water, which contradicted the 1959 agreement that Egypt insisted on.

Thus, the GERD could be considered a benefit-sharing project as theorized and outlined in the benefit-sharing framework by Grey and Claudia (2002). The first benefit, according to the benefit-sharing framework, was 'benefits to the river'-ecological benefit derived from an eco-friendly sustainable water management system (Alam *et al*., 2009). These benefits would improve water quality and flow, enhance management of the watershed, reduce sediment, and preserve biodiversity (Tawfik, 2016). Accordingly, the GERD would offer scientifically verified benefits to the river. These included flood reduction, controlled and uniform flow of water, drought mitigation, increased water as a result of constant flow, reduction of water losses by infiltration and evaporation, and sedimentation control (Ethiopian National Panel of Experts, 2013; Jeuland *et al.*, 2014; Khalil *et al.*, 2017; Belachew, 2013; Basheer *et al.*, 2020).

In comparison, the evaporation loss from the operation of GERD was estimated 0.4 BCM (Belachew, 2013; Tesfaye, 2015), while the evaporation from the Aswan High Dam in Egypt and Sudan dams was reported 14.3 BCM and 4.7 BCM, respectively (Tesfaye, 2015; Belachew, 2013). Even the evaporation rate, for instance, in Jebel Aulia was higher than the storage capacity of the dam (Ibid.). Owing to its topographical leverage, the full operation of the GERD project would be expected to reduce the average annual losses of the High Aswan Dam from 10.8 BCM/year to 9.5 BCM/year (Belachew, 2013).

In addition, the GERD was projected to decrease sedimentation by 86%, which in turn might increase the generation capacity of downstream countries' hydropower plants, reduce maintenance costs, and increase crop productivity by reducing floods (Belachew, 2013). Nevertheless, it might affect soil fertility in downstream countries because of reduced sedimentation. Moreover, the GERD reservoir would provide a consistent water flow to downstream countries when it would be fully operational (Tesfaye, 2015; Asegdew *et al.*, 2014). Therefore, the construction of more reservoirs in upstream Ethiopia would save more water, thereby preserving the river ecosystem from extinction resulting

from unilateralism and competition. This was supported by He *et al.* (2022:15) who argued that "the GERD could serve as a sediment trap and water storage for Sudan and Egypt, protecting them from flooding, pollution, and sedimentation."

The second category of benefit is 'benefit from the river' denoting economic benefits from hydraulic infrastructure (Alam *et al*., 2009). As a hydraulic infrastructure, GERD has socio-economic benefits for three riparians and the region at large. An informant emphasized that among the ten major benefits of the GERD seven go to downstream countries without paying to Ethiopia (Interview with Senior Diplomat, Ministry of Foreign Affairs, November 2021). For Ethiopia, the GERD would play an essential role in the realization of the country's vision of attaining a middle-income country, universal electricity access, and a regional energy hub by 2025 (FDRE, 2019; Ministry of Water and Energy, 2013). Currently, only 44% of the country's population has access to electricity (FDRE, 2019), and the majority of the population (87%) is in abject poverty (WFP, 2020). However, the number varies. According to the energy advisor to the Minister of Water and Energy, per capita electricity of Ethiopia (130 kWh) is the least in the world and electricity access is 51 percent (an interview with senior energy advisor, Ministry of Water and Energy, July 2023). Moreover, nearly 57 million people have no access to modern energy (interview with senior energy advisor, Ministry of Water and Energy, Addis Ababa, July 2023). Since 80% of the total economic benefit of the GERD is hydropower generation (Jeuland *et al.*, 2014), the GERD is key in realizing a universal electrification access program under the motto of 'Lighting to All' (FDRE, 2019) and bringing structural transformation in economic and social sectors.

In this regard, the full operation of the GERD is expected to double the current power generation (4818.2 MW) capacity of Ethiopia (Ethiopian Electric Power, n.d). This could bring structural transformation by reducing the power shortage problem of the economic and service sectors of the country. Getachew *et al.'s (*2020) study suggested that improved access to reliable and affordable energy will, thus, boost the Ethiopian economy by 1.5%. Increased access to energy could also enhance productivity in manufacturing, industry, the service sector, and other energy-dependent sectors.

Furthermore, the completion of the GERD will dramatically increase Ethiopia's power export. An increase in power trade potentially contributes to the economic growth of the country and enhances regional integration through power and infrastructure connectivity. Currently, Ethiopia exports power (532 GWh) to Djibouti (Africa Development Bank Group, 2023). At the same time, Samuel (2022) reported that Ethiopia sells 100 MW to Sudan, and 200 MW to Kenya, creating an energy-interdependent region. Thus, Ethiopia generates more than $50 million annual revenue from power exports to Sudan and Djibouti with plans to increase it to $400 million by 2032 (Ethiopia News Agency, 2022). In the 2020/21 fiscal year, revenue from power exports brought about a significant growth of 36.2% (Ashenafi, 2022). By then, the country earned $95.4 million by exporting 1,700 GW (gigawatts) to Djibouti and Sudan (Samuel, 2020).

However, Ethiopia has not yet met the growing energy demand of its neighboring countries. Sudan, for example, has requested 1000 MW (Africa Business Networking, 2021) while Djibouti, which relies on imports for over 80% of its total power, will request 314 MW by 2037 (Red Sea Power, n.d.). An informant noted that Sudan has high electricity demand of 500 kV interconnection line currently under construction to increase exports to 3000 MW, financed by the World Bank (interview with senior expert, Planning and Investment Department, Ethiopian Electric Power, May 2022). In Djibouti, the second Ethio-Djibouti power connectivity infrastructure construction is underway, financed by Africa Development Bank (interview with senior expert, Planning and Investment Department, Ethiopian Electric Power, May 2022). This will increase power export to Djibouti by 30% (Africa Development Bank Group, 2023). Moreover, Ethiopian Electric Power plans to expand power exports to eight destinations following the completion of GERD. Memorandums of Understanding have been signed for power purchase agreements, including a deal with Tanzania to export 400 MW (Tesfa-Alem, 2016). Moreover, agreements have been reached with South Sudan to initially supply 100 MW, with plans to increase it to 400 MW (Ethiopia News Agency, 2022), as well as with Yemen (100 MW) (Tigrai Onlne, 2014). Ethio-South Sudan interconnection project feasibility study is at the preparation stage (interview with senior expert, Planning and Investment Department, Ethiopian Electric Power, May 2022). Somalia and Somaliland have also requested power purchase from Ethiopia (interview with senior expert, Research and Development Department, Ethiopian Electric Power, May 2022). In the former case, a feasibility study of 500MW Ethio-

Somalia interconnection line is currently undertaken, financed by the World Bank (interview with senior expert, Planning and Investment Department, Ethiopian Electric Power, May 2022). An informant from Ethiopia Electric Power has stated that a project is underway to extend the Ethio-Kenya transmission line to Tanzania and South Africa, including Burundi and Rwanda (interview with senior expert, Planning and Investment Department, Ethiopian Electric Power, May 2022). The Ethio-Eritrea interconnection is also being discussed at a higher level (interview with senior expert, Planning and Investment Department, Ethiopian Electric Power, May 2022). These power export plans are expected to be implemented once the GERD is fully operational, positioning Ethiopia as an emerging hydropower state and a regional energy hub. The GERD not only increases Ethiopia's power exports and foreign currency earnings but also supports the region's transition to energy economy free from carbon. Furthermore, power exports may contribute to the creation of an interdependent grid community around the GERD.

The remaining 20% of the benefits resulting from GERD encompass various aspects like fishery development (5,000 to 10,000 tons of fish annually), mitigation of CO2 emissions, tourism, job creation, investment, and knowledge transfer (Office of National Council, 2017a: 8; 2017c: 2; Interview with an expert at Office of National Council for the Coordination of Public Participation on the Construction of GERD, April 2022). During the construction phase, approximately 15,000 Ethiopians were employed, and further job opportunities would be expected upon the project's completion (Ethiopian Electric Power Corporation, as quoted in Tawfik, 2016).

Beyond its economic benefits, the GERD project has also political and symbolic significance. An informant recalled that the GERD is an emancipatory project as it has transformed the spirit of "impossible" into the spirit of "possible," both in idealistic and practical terms (interview with a researcher at the Institute of Foreign Affairs, November 2021). It is also seen as a symbol of revivalism, self-reliance, and self-esteem, and a sign of modernity (Yalemzewd, 2020; Khalil *et al.*, 2017; Zeray, 2017). It has revived the spirit and values of the Battle of Adwa (Interview with Senior Transboundary Resources Affairs expert at the Ministry of Water and Energy, July 2023), a historic event that transcended provincialism, ethnicity, gender, religion, and other social classes (Maimire, 2005). The dam has connected all sections of the society as inseparable and revived the values of the

victory of Adwa such as fraternity, togetherness, oneness, courage, magnanimity, victoriousness, and heroism (Maimire, 2005). Like Adwa, the GERD is framed as a fight against injustice in the utilization of Nile Water, rooted in the colonial legacy.

Next to Ethiopia, Sudan is indeed an immediate beneficiary of the GERD project. However, Sudan's position on the GERD project lacks clarity, consistency, and persistence (BBC, 2021), as it has been swinging like a pendulum. There are instances where Sudan aligns with Egypt to the extent of being an instrument for the latter, as seen in the AU-led negotiation under the Chairmanship of Félix Tshisekedi (EIU, 2021). In the 2021 Kinshasa Tripartite Negotiation, Sudan has presented a proposal that undermines the AU-led negotiation, which is in the best interest of Egypt (Interview with Senior Diplomat, Ministry of Foreign Affairs, November 2021). Supporting this assertion, an informant strongly argued that,

> *Sudan is an unfinished state and a political marketplace with the involvement of several regional actors, including Egypt. Egypt has consistently maintained a close watch on Sudan's internal political developments, sometimes utilizing it as a tool against Ethiopia in their dispute over the GERD* (interview with a researcher at the Institute of Foreign Affairs, November 2021).

However, on other occasions, Sudan supports Ethiopia. Sometimes, Sudan has also played a bridging role between Ethiopia and Egypt (Otinov, 2022; Al Masry, 2017). Despite this, Sudan's occasional support for the GERD does not appear to be driven by political or geopolitical motives. An informant also noted that

> *Sudan recognizes the benefits of hydropower dams in Ethiopia, as they have experienced the advantages of the Tekeze Dam. They acknowledge that for every dollar Ethiopia earns from the dams, Sudan gains three dollars. However, the challenge they face is external pressure that affects their stance on the issue. Since its independence, Sudan has been marked by a series of crises and coups. Historically, the security sector in Sudan has maintained strong ties with Egypt, indicating that they are not entirely free from Egyptian influence* (Interview with Senior Diplomat, Ministry of Foreign Affairs, November 2021).

Instead, Sudan's support to the GERD stems from the recognition and acknowledgment of the benefits that the GERD can bring to Sudan. Sudan has not yet fully utilized its hydropower and irrigation potential owing to seasonal fluctuations in the Nile Water, the absence of mega-water storage infrastructure, and the devastating impact of seasonal floods and sedimentation (Basheer *et*

al., 2020). For instance, the Sennar and Roseires dams have experienced a reduction of 71% and 36% respectively in their initial capacity because of sediment deposited in the reservoir (Belachew, 2013). This sedimentation has decreased the lifespan, water storage capacity, and hydropower generation capabilities of these dams while also increasing maintenance and sediment removal costs (Belachew, 2013). The GERD, however, offers an opportunity for Sudan to overcome these challenges and realize its potential.

Some of the benefits to Sudan include an increase in hydropower generation capacity for its seasonal storage dams, reduction of damages caused by seasonal flood, enhanced potential for irrigated agriculture, water conservation, reduced evaporation, sediment control, navigation opportunities, and the option to purchase power from the GERD project (Office of National Council, 2017a:9; Jeuland *et al.*, 2014; Khalil *et al.*, 2017; Belachew, 2013; Basheer *et al*., 2020; He *et al*., 2022; Getachew *et al.*, 2020).

Empirical studies show that the GERD has the potential to reduce alluvial sediment in Sudan by 100 million cubic meters, reduce approximately 40 km of flooding, and irrigate 500,000 ha of new agricultural land (Khalil *et al.*, 2015). This can enhance the energy production capacity of the Roseires, Sennar, and Merowe hydropower plants (Jeuland *et al.*, 2014). In addition, it can increase agricultural production by providing regulated clean water throughout the year, reduce harvest losses caused by floods and water shortages. However, the decrease in flood may have long-term negative impact on soil fertility. Alongside these benefits, Sudan can also save the cost it allocates for sediment removal, dam maintenance, and settlement of flood-induced migrants. According to Belachew (2013:10), "Sudan alone could save approximately USD 50 million per year by reducing costs associated with canal dredging". Hence, the benefits that the GERD offers to Sudan in terms of energy, food, and navigation has a positive impact on the Sudanese economy. Studies reveal that the associated benefits of GERD will contribute US$ 27-29 billion to Sudan's GDP between 2020 and 2060 (Basheer *et al.*, 2020). Getachew *et al.* (2020) reported that Sudan is the second largest beneficiary of the GERD. Thus, Sudan can be considered fortunate as an immediate downstream riparian because it receives these benefits without having to share the associated costs, which goes against the principle of equitable benefit-sharing.

The benefits of the GERD to Egypt are "an increase in irrigated area, a decrease in sedimentation in Lake Nasser, and a reduction in flooding" (IPoE, 2013:41), reduction of evaporation loss to 9.5 BCM/year from 10.8 BCM/year at High Aswan Dam (Belachew, 2013:10). Furthermore, the GERD extends the life of High Aswan Dam, enhances navigation as a result of regulated and increased water flows, and mitigates drought (Ethiopian National Panel of Expert, 2013). Getachew *et al*. (2020) argue that Egypt will gain 0.17 billion in additional real GDP each year starting in 2024 once the GERD becomes operational, compared to Egypt's GDP in 2020.

The third benefit is 'the reduction of costs because of the river', which refers to the mitigation of political tensions arising from competition over water resources (Grey and Claudia, 2002; Alam *et al.*, 2009). In this regard, the GERD has revealed the coexistence of conflict and cooperation, and competition and cooperation. Despite Egypt's and Ethiopia's securitizing of the GERD as an existential threat (State Information Service, 2021; Embassy of Egypt Washington D.C, n.d; Al-Anani, 2022) and necessity (FDRE, 2020a) respectively, the absence of overt conflict contradicts prediction of a water war (The International Institute for Middle-East and Balkan Studies, 2020; Ibrahim, 2021). Instead, conflict and cooperation over GERD occur simultaneously.

In terms of cooperation, there are evolving norms emerging from the trilateral negotiation that have significant implications to the existing inequitable treaty regime. The DoP is an illustrative example. First, the DoP incorporates principles of international water law enshrined in the CFA. Second, the DoP recognizes the issue of property rights associated with the Nile by recognizing the GERD as a hydropower generation project with a role in economic development, hydro cooperation, and regional integration (DoP, 2015). Third, an agreement has been reached to prioritize power purchases and promote energy-based integration as a confidence-building measure for downstream countries (DoP, 2015). Thus, the signing of the DoP can serve as a foundation and cornerstone for future cooperation. Salman (2016:14) reports that the GERD shows the changing power relations and emergence of a "new legal order" so as to replace the 1902 and 1959 agreements.

In addition, three factors may stimulate cooperation in the Nile region. First, the GERD creates an opportunity to foster cooperation based on a benefit-sharing framework. Second, the costs of non-cooperation may push Egypt towards opting for cooperation. Third, the GERD could potentially

change the power dynamics of the region by positioning Ethiopia as a regional anchor state. As discussed earlier, the GERD has the potential to reconfigure the regional power balance. It may strengthen Ethiopia's material power (economic power) as well as non-material power, specifically bargaining and ideational power. In terms of the latter, various water-based institutions have emerged because of the GERD. These includes the National Panel of Experts, Water, Hydro-Diplomacy and Communication Forum; Hydro Politics and Diplomacy Desk within the Ministry of Water and Energy's Transboundary Resources Affairs Directorate, and Public Diplomacy Centers at universities and research institutes. This demonstrates how the physical dam is evolving into an intellectual GERD, potentially increasing Ethiopia's ideational power and breeding a water-conscious society. In addition, the project may serve as an emancipatory force for Ethiopia and other African countries by emphasizing the feasibility of constructing large-scale hydraulic infrastructure for development without having to rely on external financial sources (Interview with Senior Researcher at the Institute of Foreign Affairs, November 2021). The success of the GERD may inspire other countries to pursue similar projects, leading to a shift in the regional dynamics of power and development. Thus, the GERD may inspire self-reliance and catalyzes regional transformation and empowerment toward justice and equitable order. These developments could have long-term implications for the geopolitics of the Nile Region and may make Egypt accept cooperation.

Contrary to Goitom's (2014) claim, the GERD may not end the geopolitical rivalry between Ethiopia and Egypt but it rather may change the playing field from water to power trade. Both countries are now engaged in a power trade rivalry. Ethiopia aims to become a clean energy hub in the region, which will fundamentally alter the regional balance of power while Egypt seeks to block Ethiopia's power agreements (Mikhail, 2021). Egypt's opposition to the GERD is to maintain its geopolitical superiority by portraying Ethiopia as a rising hydropower state. Thus, the future may entail a coexistence of conflict and cooperation, and competition and cooperation within the power trade field.

The last category is 'benefits beyond the river'. This may suggest cooperation in regional integration, trade agreements, labor movements, hydropower interconnections, and investments. In this respect, the realization of cooperation makes the GERD a catalyst to draw extra benefits 'beyond the river'

(Cascão *et al.*, 2016). Such benefits include market integration, trade agreement, power trade and interconnectivity, and investment. Nevertheless, an inclusive agreement among the three countries is a prerequisite to realize such benefits.

1.4. CONCLUSION

This paper has examined the broader geopolitical implications of the GERD in light of the benefit-sharing framework and the conflict between Ethiopia and Egypt. It is evident that the conflict over the GERD extends beyond the physicality of the dam and is deeply rooted in the geopolitical rivalry between the two countries. Egypt perceives the GERD as an existential threat to its existing water-sharing regime while Ethiopia markets it as a benefit-sharing project and an existential necessity.

The conflict surrounding the GERD is not solely about competing water regimes, but rather about the potential geopolitical implications it holds. The GERD has the power to reposition Ethiopia as a rising clean energy hub, leveraging its economic, ideational, and bargaining power in the region. This reconfiguration of power has the potential to redraw the existing geopolitical map and alter the regional balance of power in favor of a benefit-sharing regime, which Egypt sees as a threat to its water-sharing regime.

Furthermore, the GERD has the potential to induce cooperation between riparian countries for several reasons. First, it offers proven benefits to the region, serving as an incentive for cooperation. Second, the cost of non-cooperation may push countries to engage in dialogue. Third, the GERD can enhance Ethiopia's power matrix by repositioning it as a rising clean energy hub, increasing its economic, ideational, and bargaining power.

However, the study also highlights the possibility that the GERD may also transform the geopolitical rivalry between Ethiopia and Egypt from a water-based conflict into a power trade competition. This implies that cooperation and conflict, competition and cooperation may coexist in this complex geopolitical landscape. Understanding these geopolitical implications is thus crucial for navigating the complexities of the issue and finding sustainable solutions.

REFERENCES

Abdelkader, T. A. & Mohamed, H.E. (2019). Impacts of Constructing the Grand Ethiopian Renaissance Dam on the Nile River. GERD Failure Analysis and the Impacts on Downstream Countries. In A.F. Sommer & A.M. Negm (Eds.), *Grand Ethiopian Renaissance Dam Versus Aswan High Dam: A View from Egypt* (pp. 149–172). Springer International Publishing AG.

Abdo, G. M., Kevin, G. W., Mohammed, B., Zelalem, T. M., Sami, O.E., Azeb, M., Edith, A. Z., Jim, W. H. & Simon, J. D. (2016). Cooperative filling approaches for the Grand Ethiopian Renaissance Dam. *Water International*, *41:4*, 611-634, DOI: 10.1080/02508060.2016.1177698

Adam, B., Raimund, B. & Sabrina, K. (2021). Implications of the Resource Nexus on International Relations: The Case of the Grand Ethiopian Renaissance Dam. *Z Außen Sicherheitspolit, 14,* 397–409. https://doi.org/10.1007/s12399-021-00878-1

Africa Development Bank Group (2023). Multinational - Ethiopia Djibouti Second Power Interconnection Project, Phase II - Ethiopia part. Retrieved from https://projectsportal.afdb.org/dataportal/VProject/show/P-Z1-FA0-179

Africa Business Networking (2021, August 6). Sudan requests purchase of 1,000 MW electric power. Retrieved From https://africabusinessnetworking.com/sudan-requests-purchase-of-1000-mw-electric-power/

Agnew, J. (1994). The Territorial Trap: The Geographical Assumptions of International Relations Theory. *Review of International Political Economy*, 1(1), 53-80.

Agreement on Declaration of Principles between the Arab Republic of Egypt, the Federal Democratic Republic of Ethiopia and the Republic of the Sudan on the Grand Ethiopian Renaissance Dam (GERDP), 23rd March 2015, Khartoum, Sudan.

Agreement on the Nile River Basin Cooperative Framework. Retrieved from https://nilebasin.org/images/docs/CFA%20-%20English%20%20FrenchVersion.pdf

Alam, U., Ousmane, D. & Paul, J. (2009). The benefit-sharing principle: Implementing sovereignty bargains on water. *Political Geography 28*,90–100.

Al-Anani, K. (2022). The Grand Ethiopian Renaissance Dam: Limited Options for a Resolution. Arab Center, Washington. D.C.

Al-Masry, A. (2019, October 9). Ethiopia took advantage of 2011 turmoil in Egypt to build GERD: PM. Retrieved from https://egyptindependent.com/ethiopia-took-advantage-of-2011-turmoil-in-egypt-to-build-gerd-pm/

Al Masry, A. (2017, Novemebr 29). Sudan initiates effort to bridge gap between Egypt,

Ethiopia over GERD. Retrieved From https://www.egyptindependent.com/sudan-initiates-effort-to-bridge-gap-between-egypt-ethiopia-over-gerd/

Anwar. H.T. (2017). The Geopolitics of Water Negotiations Succeeding The GERD Project in the Nile River Basin: The Case of Ethiopia, Egypt, and Sudan. Insamer.

Asegdew, G. M. & Semu. A. M. (2014). Assessment of the Impact of the Grand Ethiopian Renaissance Dam on the Performance of the High Aswan Dam. *Journal of Water Resource and Protection*, *6*, 583-598. http://dx.doi.org/10.4236/jwarp.2014.66057

Asegdew, G. M. & Semu. A. M. & Yosif, I. (2014). Impact and Benefit Study of Grand Ethiopian Renaissance Dam (GERD) During Impounding and Operation Phases on Downstream Structures in the Eastern Nile. In A. M. Melesse, W. Abtew & S. G. Setegn (Eds.) *Nile River Basin: Ecohydrological Challenges, Climate Change and Hydropolitics* (pp.543-564). Springer International Publishing, Switzerland

Ashenafi, E. (2022, May 7). Ethiopia opts to export electricity to five additional African states. The Reproter, Retrieved From https://www.thereporterethiopia.com/23595/

Ayenat, M. (2020). The Ethiopian-Egyptian Water War Has Begun. Foreign Policy. Retrieved from https://foreignpolicy.com/2020/09/22/the-ethiopian-egyptian-water-war-has-begun/

Basheer, M., Khalid, S. & Jonas, L. (2020). Long-Term Economy-Wide Impacts of The Grand Ethiopian Renaissance Dam on Sudan. *Economic Research Forum Working paper series No 1427.*

BBC (2021, April 22). GERD: Sudan talks tough with Ethiopia over River Nile dam. *BBC News*. Retrieved From https://www.bbc.com/news/world-africa-56799672

Bekhit, H., Ahmed, H. S. & Alaa E.Z. (2019). In A.F. Sommer & A.M. Negm (eds.), *Grand Ethiopian Renaissance Dam Versus Aswan High Dam: A View from Egypt* (pp. 149–172). Springer International Publishing AG.

Belachew, T. (2013).Benefit of Grand Ethiopian Renaissance Dam Project (GERDP) for Sudanand Egypt. Discussion Paper. EIPSA Communicating Article: Energy, Water, Environment & Economic, http://eprints.hud.ac.uk/19305/

Block, P., YinG, Z. & Solomon, T.E. (2016). Filling the GERD: evaluating hydroclimatic variability and impoundment strategies for Blue Nile riparian countries. *Water International, 41(4),* 593-610. DOI: 10.1080/02508060.2016.1178467

Cascão, A.E., Zeray, Y. & Alistair, R. C. (2019). *The Grand Ethiopian Renaissance Dam andthe Nile Basin: implications for transboundary water cooperation.* Routledge

Cascão, A.E., Zeray, Y. & Alistair, R.K. (2016). How has the Grand Ethiopian Renaissance Dam

Changed the legal, political, economic and scientific dynamics in the Nile Basin? *Water International, 41(4),* 503-511.

Cascão, A.E. & Alan, N. (2016). GERD: new norms of cooperation in the Nile Basin? *Water International, 41(4),* 550-573.

Colton, R. (2021, January 24). Water Security and the GERD: Is Conflict Brewing on the Nile*? Global risk Insights*. https://globalriskinsights.com/2021/01/water-security-and-the-gerd-is-conflict-brewing-on-the-nile/

Council of Ministers of Water Affairs of the Nile Basin States (2001). Nile Basin Initiative Shared Vision Program: Socio-Economic Development And Benefit-Sharing. Project Document

Daily News Egypt (2014, February 21). We are committed to 1959 Nile water sharing agreement: Egyptian and Sudanese officials. Retrieved from https://www.dailynewsegypt.com/2014/02/21/committed-1959-nile-water-sharing-agreement-egyptian-sudanese-officials/

De Falco, S. and Giulia, F. (2022). The GERD dam in the water dispute between Ethiopia, Sudan and Egypt. A scenario analysis in an ecosystem approach between physical and geopolitical geography. *AIMS Geosciences, 8(2),* 233–253

Dejen, Y.M. (2021). Mystery of the GERD Negotiations: From Coercion to Obligation of Treaty Conclusion. *Mizan Law Review, 15(2),* 523-542. 10.4314/mlr.v15i2.7

Eastern Nile Council of Ministers (2014, 30 January). Eastern Nile Council of Ministers 26th Meeting [Press Release]. http://entro.nilebasin.org/61e7-331-1e7-3990-e7x7/

EIU (2021, February 25). Egypt, Ethiopia and Sudan seek renewed GERD mediation. https://country.eiu.com/article.aspx?articleid=1320755315

Embassy of Egypt Washington, D.C (n.d). Grand Ethiopian Renaissance Dam: An Existential Threat. https://egyptembassy.net/media/02-Egypt_Fact_Sheet_GERD-1.pdf

Ethiopian Electric Power (n.d). Power Generation. Retrieved From https://www.eep.com.et/en/power-generation/

Ethiopian National Panel of Experts (2013). The Grand Ethiopian Renaissance Dam (GERD) and some Egyptian experts' hyperbole. https://waltainfo.com/50198/

Ethiopia News Agency (2022, May 5). Ethiopia Plans to Export 100 MW Electric Power to South Sudan in Three Years. Retrieved From https://www.ena.et/web/eng/w/en_35457

Ethiopia News Agency (2022, May 5). Ethiopia Plans to Export 100 MW Electric Power to South Sudan in Three Years. Retrieved From https://www.ena.et/web/eng/w/en_35457

Ethiopian News Agency (2014, August 5). የታላቁ የኢትዮጵያ ህዳሴ ግድብ ሁለተኛው ተርባይን ሃይል ማመንጨት ጀመረ . Retrieved From https://www.ena.et/web/amh/w/am_181088

Fana, G. & Dawit, Y.W. (2021). New Dimensions in the Grand Ethiopian Renaissance Dam Negotiations: Ontological Security in Egypt and Ethiopia, *African Security*, *14, (1),* 80–106. DOI: 10.1080/19392206.2021.1905921

FDRE (2020a). Ethiopia's statement at the UN Security Council on the Grand Ethiopian Renaissance Dam, Delivered by H.E. Ambassador Taye Atske-Selassie, Permanent Representative of the Federal Democratic Republic of Ethiopia to the United Nations, at the Security Council open VTC on Peace and Security in Africa 29 June 2020, New York. Retrieved from https://www.ethioembassy.org.uk/ethiopias-statement-at-the-united-nations-security-council-on-grand-ethiopian-renaissance-dam/

FDRE (2020b). Letter from the Permanent Representative of Ethiopia to the United Nations . Addressed to the President of the Security Council, 14 May 2020, UNSC, S/2020/409, UNSC.

FDRE (2019). National Electrification Program 2.0: Integrated Planning for Universal Access. Addis Ababa, Ethiopia.

Frida, M. (2022). "*We are dealing here with a hydroelectric dam, we are not building a nuclear plant" : A case study of securitization processes in water cooperation contexts*. [Unpublished Master Thesis]. Lund University.

Getachew, D., Tewodros, N. & Tadele, F. (2020). The economic significance of the Grand Ethiopian Renaissance Dam (GERD) to the Eastern Nile Economies: A CGE modeling approach. Policy Working Paper 05/2020

Gienanth, E.V. (2020). *"#Itsmydam": An analysis of Ethiopian and Egyptian discourses surrounding the Grand Ethiopian Renaissance Dam*. [Unpublished Master Thesis]. Universiteit van Amsterdam.

Goitom, G. (2014). Ethiopia's Grand Renaissance Dam: Ending Africa's Oldest Geopolitical Rivalry? *The Washington Quarterly, 37(2),* 25-37.

Gonzalez, R. (2020). Countdown to a Bitter Battle Over the Water of the Nile? http://www.ipsnews.net/2020/07/countdown-bitter-battle-water-nile/

Grey, D. & Claudia. W. S. (2002). Beyond the river: the benefits of cooperation on international Rivers. *Water Policy*, *4*, 389–403.

He, Z., Jianwu, Z. , Jing, Z., Marye, B., Jinsong, D. & Shizong, W. (2022). Identify the Impacts

of the Grand Ethiopian Renaissance Dam on Watershed Sediment and Water Yields Dynamics. *Sustainability*, 14, 1-16. https://doi.org/10.3390/su14137590

Ibrahim, S. (2021). Egypt may be looking for a military solution to Ethiopia dam dispute. Middle East Eye.https://www.middleeasteye.net/opinion/egypt-ethiopia-military-solution-gerd-dispute

International Institute for Middle-East and Balkan Studies (2020). Egypt-Ethiopia 2020: Will the grand GERD dam trigger a war between Egypt and Ethiopia? https://www.ifimes.org/en/researches/egypt-ethiopia-2020-will-the-grand-gerd-dam-trigger-a-war-between-egypt-and-ethiopia/4600

International Non-partisan Eastern Nile Working Group(2014). The Grand Ethiopian Renaissance Dam:An Opportunity for Collaboration and Shared Benefits in the Eastern Nile Basin. An Amicus Brief.

International Panel of Experts (2013). Grand Ethiopian Renaissance Dam Project. Final report.

Jeuland, M., Dale, W. & John Waterbury (2014). The Grand Renaissance Dam and prospects for cooperation on the Eastern Nile. *Water Policy, 16*, pp. 595–608. 10.2166/wp.2014.011

Kaleb, D. (2022). Realist Perspectives on Nile Politics: Conflict and Cooperation between Ethiopia and Egypt. *African Security, 15 (3),* 213-236. https://doi.org/10.1080/19392206.2022.2081763

Khalil, A., Yohannes, Y. & Hilmi, S. S. (2017). Nile River's Basin Dispute: Perspectives of the Grand Ethiopian Renaissance Dam (GERD). *Global Journal of Human-Social Science, 17(2),* 1-21

Lindqvist, J. (2021). *Lord of the Nile: Explaining how the Grand Ethiopian Renaissance Dam has affected Ethiopian Foreign Relations*. [Unpublished Master Thesis]. Linnéuniversitetet.

Maimire, M. (2005). Ethiopian history and critical theory: The case of Adwa. In Getachew, M. & Paulos, M. *The Battle of Adwa: Reflections On Ethiopia's historic victory Against European Colonialism (pp.*253 300). New York: Algora Publishing.

Mbaku, J.M. (2020). The controversy over the Grand Ethiopian Renaissance Dam. Commentary, Brookings

Meles, Z. (2011). The speech delivered by H.E. Prime Minister Meles Zenawi to mark the official commencement of the Millennium Dam project, April 02/2011, Guba, Beneshangul Gumuz. Retrieved from https://www.yumpu.com/en/document/read/39834129/speech-delivered-by-he-prime-minister-meles-zenawi-to-mark-the-

Miehe, L., Tobias, V.L. and Stephan, R. (2020). Nile Conflict: Compensation Rather Than

Mediation: How Europeans Can Lead an Alternative Way Forward. *SWP Comment 11*

Mikhail, G. (2021, 20 July). Egypt, Ethiopia compete to export power to Africa. Retrieved From https://www.al-monitor.com/originals/2021/07/egypt-ethiopia-compete-export-power-africa

Ministry of Water, Irrigation and Energy (2014). World Water Day.

Ministry of Water and Energy (2013). Ethiopian National Energy Policy (2nd DRAFT). Addis Ababa, Ethiopia.

Ministry of Water, Irrigation and Energy (2013). Water Resources of Ethiopia: The National and International Perspectives [Paper Presentation]. Awareness Creation Program Prepared for Public Relation Officials, August 2013, Addis Ababa, Ethiopia.

Mohammed, A. (2004). The Nile Question: The Accords on the Water of the Nile and Their Implications on Cooperative Schemes in the Basin. *Perceptions*, 45-57.

NBI (2009). Nile Basintransboundary Benefit Sharing Framework

Otinov, D. (2022). Wavering Sudan as Key to Resolving the Grand Ethiopian Renaissance Dam Conflict. *Journal of Asian and African Studies,* 1–15. org/10.1177/00219096221084256

Rubin, M. (2020). Ethiopia's Hydro-hegemony has Arrived. The National Interest, American Enterprise Institute

Red Sea Power (n.d.) Djibouti's Power Sector Outlook. Retrieved From https://redseapower.dj/djiboutis-power-sector-outlook/

Salman, S. M. A. (2016). The Grand Ethiopian Renaissance Dam: the road to the declaration of principles and the Khartoum document. *Water International.*

Samuel, B. (2022). With surplus power, Ethiopia exports more electricity to neighbours. The Reporter, Retrieved From https://www.thereporterethiopia.com/25841/

Samson, B. (2023). Sudan Backs Ethiopia's Dam. Retrieved From https://allafrica.com/stories/202301280002.html

Skjerdal, T. (2016). Why the Arab Spring Never Came to Ethiopia. In Mutsvairo, B. (Ed.) *Participatory Politics and Citizen Journalism in a Networked Africa: A Connected Continent* (77-89). New York: Palgrave Macmillan.

Seleshi, B.A. (2021). Statement by Seleshi Bekele Awulachew, Minister of Water, Irrigation and Energy of Ethiopia, at the UNSC, 8 July 2021, S/PV.8816

State Information Service (2021, 9 July). Egypt facing 'existential threat' due to Ethiopia's GERD on Nile.

https://www.sis.gov.eg/Story/157165/Egypt-facing-%27existential-threat%27-due-to-Ethiopia%27s-GERD-on-Nile?lang=en-us

Stenberg, L. (2021).*The Great Ethiopian Renaissance Dam - A study of its ontological importance and impact on Ethiopia*. [Unpublished Thesis]. Försvarshögskolan.

Tadesse, K.W. (2017). The Nile Basin Initiative and the Cooperative Framework Agreement: Failing Institutional Enterprises? A Script in Legal History of the Diplomatic Confront (1993–2016). *Mizan Law Review, 11(1),* 228- 197. http://dx.doi.org/10.4314/mlr.v11i1.7

Tawfik, R. (2016). The Grand Ethiopian Renaissance Dam: a benefit-sharing project in the Eastern Nile? *Water International*, 41, NO. 4, 574–592 http://dx.doi.org/10.1080/02508060.2016.1170397

Tawfik, R. (2015). Revisiting hydro-hegemony from a benefit-sharing perspective: the case of the Grand Ethiopian Renaissance Dam. Discussion Paper 5/2015/, Deutsches Institut für Entwicklungspolitik

Tayie, M.S. (2019). The Grand Ethiopian Renaissance Dam and the Ethiopian Challenge of Hydropolitical Hegemony on the Nile Basin. In A.F. Sommer & A.M. Negm (eds.), *Grand Ethiopian Renaissance Dam Versus Aswan High Dam: A View from Egypt* (pp. 485–518). Springer International Publishing AG.

Tesfaye A. (2015). *Eastern Nile River Basin Simulation with Grand Ethiopian Renaissance Dam / GERD: Application of distributed hydrological modeling with Mike Hydro modeling and Nile DSS.* [Unpublished Master Thesis]. Addis Ababa University.

Tesfa-Alem T. (2016, 28 August). Ethiopia and Tanzania agree on power export deal. *Sudan Tribune*. Retrieved From https://sudantribune.com/article58341/

Tigrai Onlne (2014, February 6). Yemen wants to buy electricity from Ethiopia. Retrieved from https://www.tigraionline.com/articles/yemen-to-buy-power.html

World Food Programme (2020). Ethiopia country strategic plan (2020–2025). WFP/EB.A/2020/8-A/1

Wuhibegezer, F. & Sheferawu, A. (2014).The Efficacy of Water Treaties in the Eastern Nile Basin. *Africa Spectrum*, *49*(1), 55–67. https://doi.org/10.1177/000203971404900103

Yalemzewd, N. (2020). The Great Ethiopian Renaissance Dam (GERD): A Quest for Surviving Abject Poverty. *Agrilinks*. https://agrilinks.org/post/great-ethiopian-renaissance-dam-gerd-quest-surviving-abject-poverty

Zeray, Y. (2017). The Fairness 'Dilemma' in Sharing the Nile Waters: What Lessons from the

Grand Ethiopian Renaissance Dam for International Law? *International Water Law, 2(2)*, pp. 1–80.

Zerihun, A. (2011). *Eastern Nile Basin: The Nexus Between Water Sharing and Benefit Sharing Arrangements*. [Unpublished Master Thesis dissertation]. Addis Ababa Univeristy.

Ethiopian Journal of Water Science and Technology (EJWST)

DOI: https://doi.org/10.59122/15519k8

Vol. 5 , 2022 , pages: 51~73 ISSN(Print): 2220-7643

Roadside PM2.5 concentrations measured with low-cost sensors and student science in Arba Minch, Ethiopia

Johannes Dirk Dingemanse, Mekdes Dawit Tadele, Tewodros Zerihun Tadesse

Faculty of Water Supply and Environmental Engineering, Water Technology Institute, Arba Minch University, Ethiopia. Email: johannesdirk.dingemanse@amu.edu.et

ABSTRACT

Exposure to PM2.5 poses one of the biggest health threats, with traffic and biomass burning as dominant sources in urban areas of low-income countries. In Ethiopia, the combination of these two sources suggests a high roadside exposure. Because of a lack of resources for data collection, only few studies were conducted on roadside exposure in Ethiopia. Using low-cost sensors and student science could partially remedy this lack of resources. Students collected PM2.5 data in Arba Minch at four stationary locations and inside two public transport tricycles during a period of six weeks with self-made low-cost sensors. Data was analyzed to gain insight into concentration levels, temporal variation, spatial variation, and difference between next to the road and on-road concentrations. Average concentrations ranged from 13-36 µg/m^3. Concentrations were highest during morning hours (42 ±12 for hours 6:00-10:00, versus 20 ± 1 and 32 ± 4 for 10:00-17:00 and 17:00-21:00, respectively), and concentrations were highest at the local bus station (36.2 µg/m^3). On-road concentrations showed the highest variation and were on average higher than concentrations next to the road (33 ± 25 and 30 ± 22 µg/m^3 versus 23.3 ± 18 and 22.6 ± 18 µg/m^3). On a daily average level, concentrations at different locations showed a high correlation (R^2 0.8-0.95) amongst each other. This suggests the possibility to interpolate concentrations from one location to other locations. Moreover, the PM2.5 concentrations exceeded air quality guidelines. In Ethiopia, more than ten cities have higher populations and traffic flows than Arba Minch. In those cities, similar or higher exceedances are expected. With this study as an example, other universities could likewise conduct research with low-cost sensors and student science in their cities. Cooperation across course instructors and universities in applying these methods will increase the insight in PM2.5 exposure in Ethiopian cities.

Keywords: ambient air pollution; traffic; Sensirion SPS30; student measurements; Particulate Matter

Received: 08 Oct 2022; accepted 06 December.2022

1. INTRODUCTION

Air pollution poses one of the biggest threats to health worldwide (Babatola, 2018; Gakidou et al., 2017; Shaddick et al., 2018). Ambient (outdoor) air pollution is estimated to cause 4.2 million premature deaths worldwide each year, especially owing to exposure to particles with a diameter smaller than 2.5 µm ($PM_{2.5}$) (World Health Organization [WHO], 2021b). Exposure to PM2.5 tends to be higher in low-income countries (Institute for Health Metrics and Evaluation, 2020). Dingemanse et al. (2022) found the bus station in Arba Minch, southern Ethiopia, exposed to high concentrations of PM2.5. This suggests that exposure related to motorized traffic is an important aspect of total exposure. Indeed, for urban areas in low-income countries, traffic is a major source of air pollution (Kim Oanh et al., 2013). Tefera et al. (2021) apportioned 31% of PM2.5 to traffic at one location in Addis Ababa. Furthermore, locations in low-income countries have the added burden of PM2.5 originating from biomass burning. Biomass is a common source for cooking, and open waste burning is a widespread practice as well. 18.3% of PM2.5 originated from biomass burning in the case of Addis Ababa (Tefera et al., 2021). Roadside exposure is potentially an important study area. However, to our knowledge in Ethiopia there are only three published studies on ambient or traffic related PM2.5 exposure. Two of these are conference abstracts which are not publicly available. These studies reveal that traffic-related concentrations in Addis Ababa and Adama exceed WHO air quality guidelines (Isaxon et al., 2019; Kumie, 2020; Tefera et al., 2020). They also reveal that the concentrations vary over time within days, between days and over seasons (Kumie, 2020; Tefera et al., 2020). Furthermore, they reveal that concentrations vary across different locations within the same city (Isaxon et al., 2019). Additionally, studies in other countries show variations in exposure between neighborhoods (next to the road) versus traffic participants (on-road) (Al-sareji et al., 2022; Jinsart et al., 2012; Kim Oanh et al., 2013). This aspect is not yet studied in Ethiopia. Arba Minch is smaller than Addis Ababa, with less vehicles and related traffic jams. Addis Ababa, Adama and Arba Minch were placed 1, 4 and 14 respectively based on the latest census and projections (Central Statistics Agency (Ethiopia) [CSA], 2013; Population Census Commission, 2007). The single measurement at the bus station in Arba Minch suggests high concentrations nearby traffic. It is unknown whether this is the case for other roadside (next to the road or on the

road) locations as well. If this would be the case, this would have ramifications for more cities in Ethiopia. The possibility of high roadside concentrations with variation over time and space in potentially more than ten cities suggests a high need for research. However, a lack of resources has resulted in low research undertaking. This can be partially remedied with low cost sensors (Dingemanse, 2022a; Isaxon et al., 2019) and student science (Dingemanse & Dingemanse-de Wit, 2022). This study has applied both methods. Undergraduate students of Arba Minch University measured PM2.5 at the bus station, next to traffic hot spots in town, and inside the most common public transport mode (Bajaj: public transport tricycle). They conducted measurements with a self-built set-up including a Sensirion SPS30. With the use of these methods, this study contributes to knowledge on roadside PM2.5 concentrations. The objectives of our study are to compare Arba Minch roadside concentration levels to guideline values, to distinguish temporal patterns on an hourly and daily level, to find whether concentrations vary significantly across distinct locations, and to evaluate the difference between on-road and next to the road concentrations.

2. MATERIALS AND METHODS

2.1 Study area

2.1.1 Characteristics

Arba Minch town is the administrative center of Gamo Zone in the Southern Nations, Nationalities and People's Regional State (SNNPR) of Ethiopia. It is situated between 1,200 and 1,400 meters above sea level, surrounded by mountains to the west and lakes (Abaya and Chamo) to the east. This topography causes wind flows towards the mountains during daytime and towards the lakes during nighttime (Minda, 2014). On a wider scale, the topography of the Grand Rift Valley also determines the wind direction, which results in a variety of wind directions. Local fishermen from the nearby lake identify four winds (Weiß et al., 2022). Arba Minch is mostly dominated by low-rise buildings. The natural wind movement from various directions and the presence of few high-rise buildings cause the dispersion of air pollutants. This decreases air pollution concentrations in comparison to a situation where there would not be such wind circulation. The annual rainfall is between 800 and 1,000 mm. 70-90% of this is accounted

for by two seasonal rainfall periods: September-November and March-May (Shalishe et al., 2022).

According to the latest projection, the population of Arba Minch town is 210,255 (CSA, 2023). Sources for PM2.5 are household cooking, traffic, and open waste burning. According to the census in 2007, 0.2% of the households used electricity for cooking, while 90% of the households used firewood (Population Census Commission, 2007). We do not have access to more recent figures. While electricity use has increased since 2007, use of biomass for cooking is still a common practice in Ethiopian cities (Dingemanse et al., 2022; Tefera et al., 2021). Minda (2014) hypothesized that for the town as a whole household biomass burning is the largest air pollution source. This will however be different at locations close to roads. Regular cooking hours are 05:30 – 9:00 and 17:00 – 21:00. These are also busy traffic hours. Arba Minch Town Road Transport Service has estimated the number of vehicles to be 9,356 of which 77.8% constitute motorcycles, 17.1% Bajajs (public transport tricycles), and only 5% cars and buses. In reality, these numbers will be different. We have witnessed that most cars and buses have an Addis Ababa license plate. Hence, the percentage of cars and buses might be higher than the locally registered 5%. However, the high skew of Bajaj and motorcycles is supported by their biggest share in road traffic accidents (33 and 40%) (Misker et al., 2017).

2.1.2 Measurement locations

Students conducted measurements at locations next to or on the road. They installed four instruments at fixed locations (A1-A4), and two instruments inside a Bajaj (B1-B2). Figure 1 shows the measurement locations.

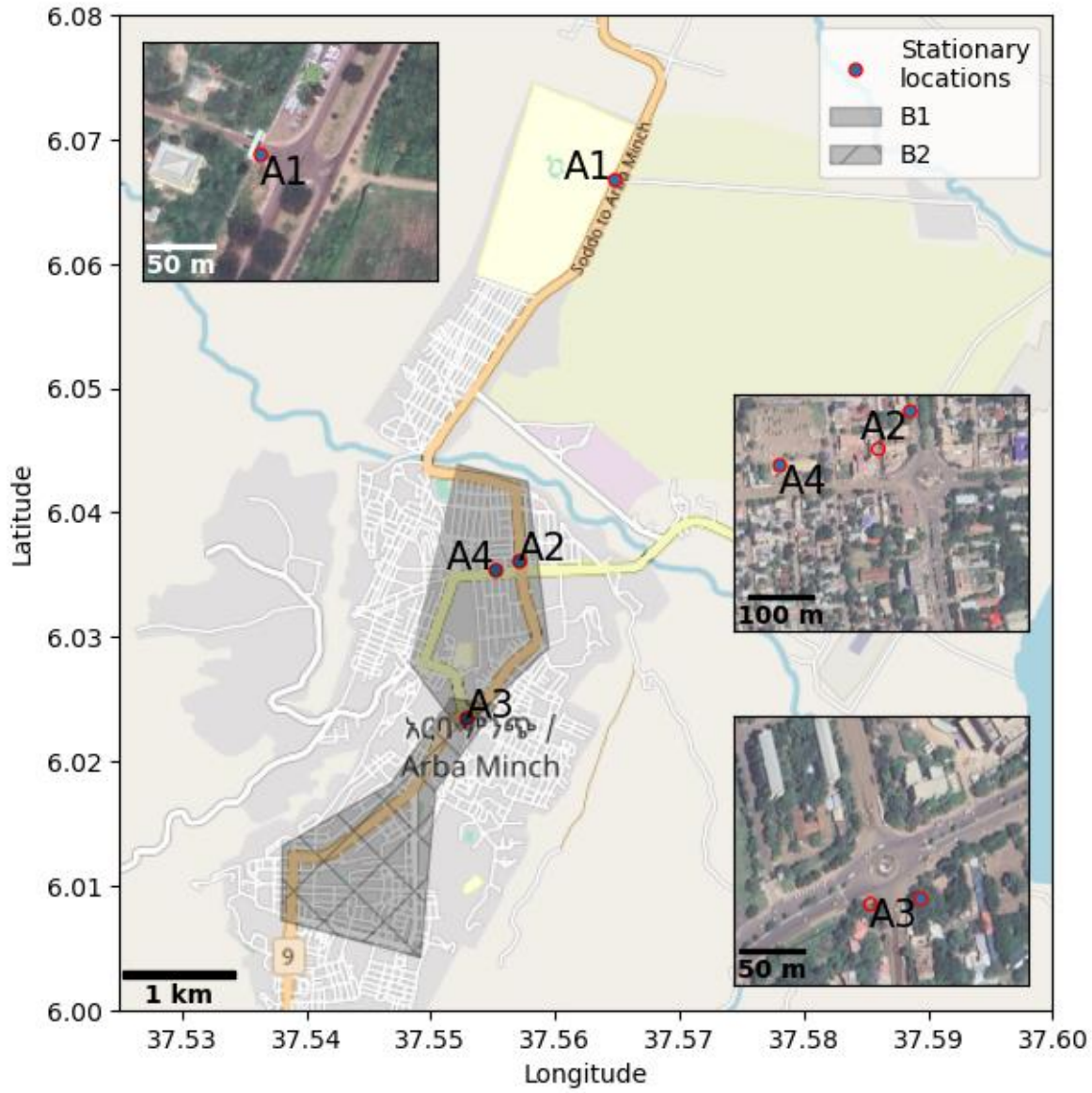

Figure 1. Locations of stationary measurements (A1-A4) and the normal working area for Bajaj with mobile measurements (B1, B2).

Locations A1-A3 were all 10-20 meters from the road, while location A4 was at an office with a window facing the bus waiting area of the bus station. Locations A2 and A3 were both near a traffic square. At both locations the instruments shifted to another orientation of the square during the measurement period. The waiting position for Bajaj B1 was close to location A2, while that of B2 was close to location A3. Table 1 shows an overview of the six locations.

Table 1. Measurement locations. Measurements took place between 8 April and 15 May 2022. See Section 2.3 for more information.

ID	Location	Measurement type	Description
A1	University Student Gate	Stationary	Main road for inter-city travel, Bajaj waiting for student customers
A2	Sikela Gamo Square	Stationary	Main road, business center, starting- and stopping travel for shops
A3	Nech Sar Square	Stationary	Main road, starting- and stopping travel for shops
A4	Bus station	Stationary	Short- and long distances buses arrival and departure
B1	Bajaj Sikela	Mobile	Driving with customers, standing idle when there are no customers
B2	Bajaj Nech Sar	Mobile	Driving with customers, standing idle when there are no customers

2.2 Measurement instrument

The instrument to collect data for this study is a self-built PM2.5 low-cost sensor, based on the Sensirion SPS30. The Sensirion SPS30 measures the PM2.5 concentration based on scattered IR light (Sousan et al., 2021). The SPS30 is a particle sensor that needs to be connected to either a computer or a microprocessor together with other components for data storage and access. For this study, the SPS30 was connected to an Arduino Mega microprocessor, together with a micro-SD module, a DS3231 real-time clock and a power bank. We refer to this full set-up as SPSA. The SPSA is low-cost because of its measurement principle and being self-built. The price of all components combined was approximately $50.00. The data quality of the SPSA was evaluated in Arba Minch at different ambient and high-exposure (kitchen) locations. Amongst itself, variation at ambient locations was small (coefficient of variation 4-6%, R^2 = 0.98-1). Based on comparison with a reference instrument, a calibration factor of 2 for ambient concentrations was found (Dingemanse, 2022a).

2.3 Data collection

Data was collected with the student science method: letting students conduct research as part of their curriculum (Dingemanse & Dingemanse-de Wit, 2022). As part of a course, students in groups of 5-6 studied traffic air pollution. They produced a measurement plan, collected and analyzed data, and wrote a measurement report. Seven student groups selected six locations and

got an instrument for 6 weeks. The instruments were set at either 10-second or 1-minute measuring frequency. Students took the instruments once a week to the lecturer to retrieve data from the SD card. At that moment, the lecturer performed quality checks such as the time setting, availability of data, and students having noted start and end times.

At location A1, the students placed the instrument in the morning and collected it in the evening. At locations A2 and A3, the instrument was placed inside for safety and charging during nighttime and placed outside during daytime. Students only discontinued measurements when they took the instrument for data retrieval. At locations A2 and A3, after two weeks the specific location changed to another place: at the same distance but another orientation relative to the nearby traffic square. We treated two locations at the same square as one location. At location A4, the instrument was placed in an office whose windows were open windows during daytime. At this location, less data was collected as the office holders were less dependable in connecting the instrument to a power source. For this location, we used only data between 6:00 and 21:00. Outside these times the power supply was irregular. For locations B1 and B2, the drivers placed the instrument in their Bajaj during their working hours.

Table 2 gives an overview of the amount of collected data per station.

Table 2. Available data.

Location	Days with data	Hours of data	Remark
A1	28	321	Only daytime
A2	35	643	Day and night (night inside)
A3	32	687	Day and night (night inside)
A4	20	258	Only daytime
B1	28	265	Only daytime
B2	23	259	Only daytime

Figure 2 visualizes the data collection times.

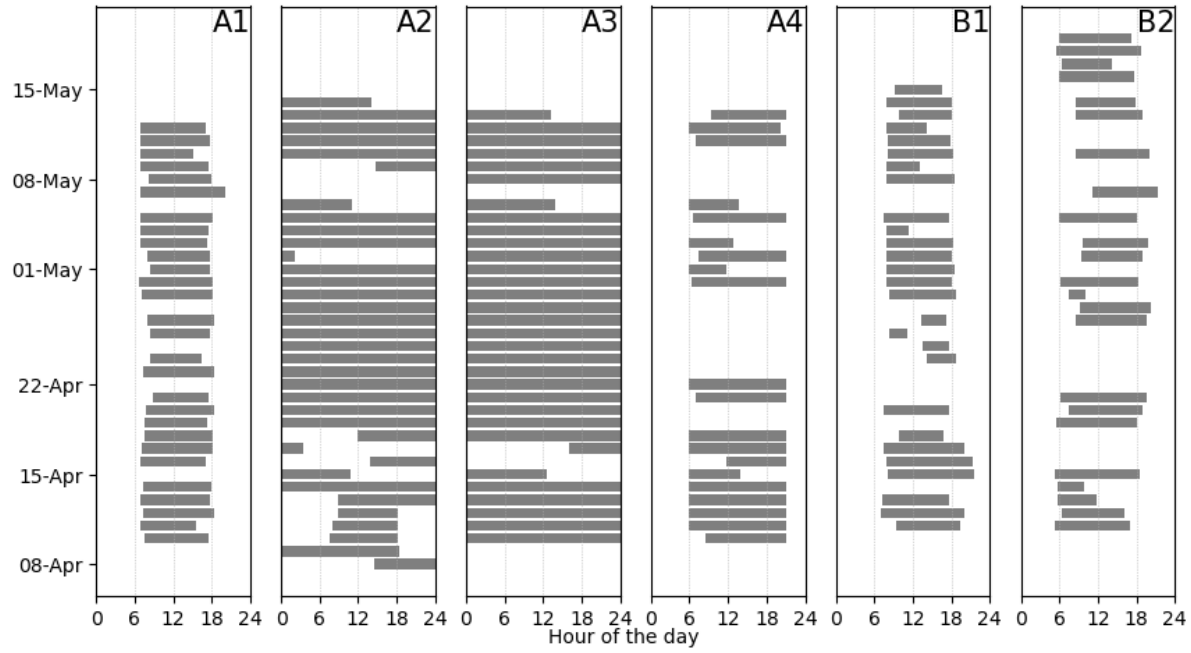

Figure 2. Data collection times for all measurement locations.

2.4 Data corrections

The real time clock of the SPSA failed in five occasions. Three times there was a full reset (two times at location B1, one time at location A4). Twice there was a 2-to-3-hour lag (location A2). In all incidents, we corrected the time during data retrieval, based on the time difference witnessed at that moment. A calibration factor of 2 is used based on comparisons of the SPSA with a reference method at an ambient location in Arba Minch (Dingemanse, 2022a). Grubb's Test was used to remove outliers at 99% level. This led to the removal of 2, 0.9, 2.3, 2.1, 4.4 and 3.5% of the data for locations A1, A2, A3, A4, B1 and B2, respectively.

2.5 Data analysis

The data analysis was based on 5-minute averaged data. All hour- and daily averages presented in this study are based on this 5-minute averaged data. Data is analyzed with respect to four topics: the concentration levels measured at the different locations, the temporal variation (hourly and daily), the spatial variation (difference amongst locations, whether those differences were significant, can be attributed to specific times, and have a correlation), and the difference between on-road and roadside concentrations.

3. RESULTS

3.1 General concentration levels

Figure 3 shows the daily averaged concentrations for all measurements combined (with hourly 5-95 percentile), and bar charts for the mean concentrations over time by location. Besides, the figure shows the 24-hour average guideline value of the WHO (15 µg/m^3).

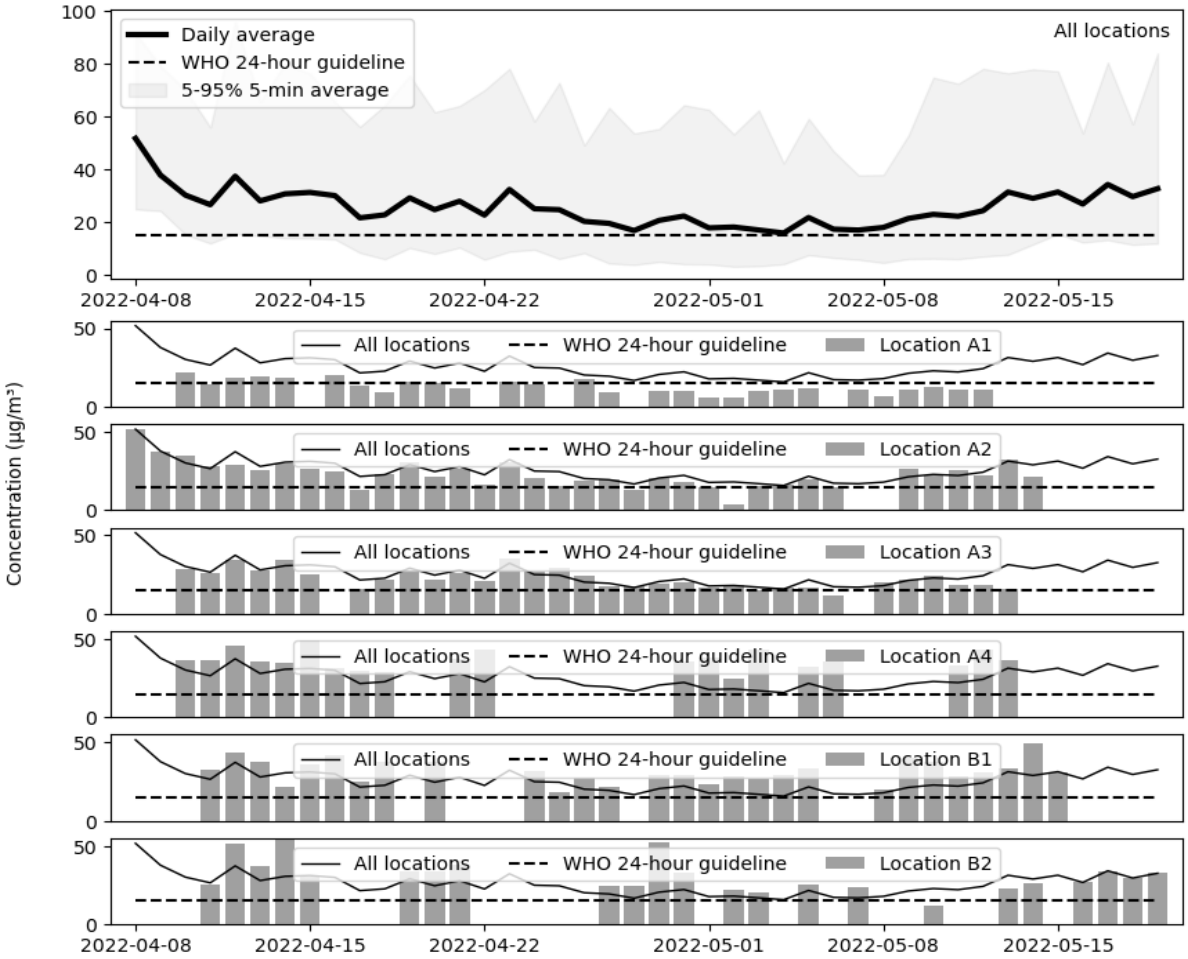

Figure 3. Daily averaged concentrations for all locations combined and individually. The shaded area shows 5-95% of five-minute averaged data for the corresponding day.

Concentrations varied between 10-50 µg/m^3 on a daily level, and between 5 and 100 µg/m^3 on 5-minute level. Averages for locations A1 through B2 were 13.0 ± 9.6, 23.3 ± 18.0, 22.6 ± 18.1, 36.2 ± 25.9, 32.6 ± 24.5 and 29.8 ± 22.3 µg/m^3, respectively. Night-time measurements were only

available for locations A2 and A3. Concentrations between 6:00-21:00 at those locations were on average 25.9 ± 19.1 and 26.9 ± 19.5 µg/m^3. Daily average concentrations for days with at least 20 hours of measurements ranged from 14.4 to 35.6 µg/m^3. These concentrations were close to up to well over the WHO 24-hour guideline of 15 µg/m^3.

3.2 Temporal analysis

Figure 4 shows the average concentration per hour of the day.

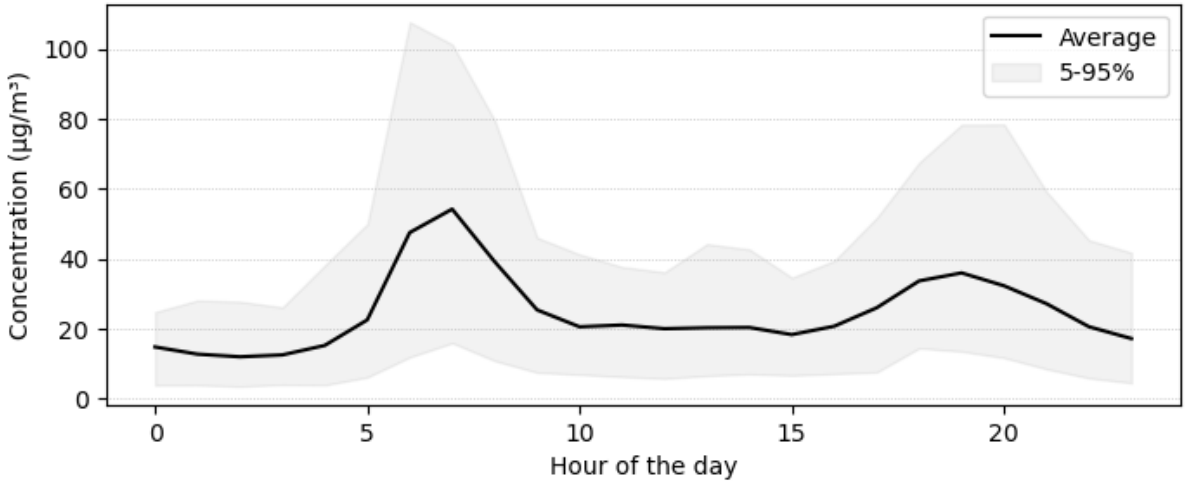

Figure 4. Concentrations averaged per hour of the day for all locations combined. Concentrations shown at hour x are those measured between hour x and x+1.

Based on figure 4, the day is split up in four distinct concentration periods. Concentrations peak in the morning and evening (6:00-10:00 and 17:00-21:00), and lowest concentrations are witnessed between those peaks (10:00-17:00 and 21:00-6:00). We call these two periods of lowest concentrations 'afternoon' and 'night'. The periods morning, afternoon, evening, and night had average concentrations of 42 ± 12, 20 ± 1, 32 ± 4, and 17 ± 5 µg/m^3, respectively. On average the morning and evening peaks reached up to 50 and 35 µg/m^3, with the top 5% of the data ranging up to 100 and 80 µg/m^3, respectively. The morning and evening peaks matched with times of higher traffic intensity (people leaving or coming back home) and morning and evening food preparation times. During daytime, solar energy heating results in vertical transport of air (convective mixing). Convective mixing disperses available air pollution. The pollutants are dispersed over a larger volume of air, which results in lower concentrations. The evening peak was lower than the morning peak because there was more convective mixing owing to the

preceding hours of solar energy heating. The afternoon and night periods showed similar concentrations with their average mostly around 20 µg/m^3. Emission of PM2.5 is lower during nighttime than during the afternoon. However, there is more convective mixing in the afternoon than during nighttime. These effects balance each other: despite lower emissions, during nighttime concentrations are not much lower.

Figure 5 shows the average daytime concentration for different days of the week (6:00-21:00) and the three distinct daytime periods. We excluded nighttime hours because there were nighttime measurements only at two locations.

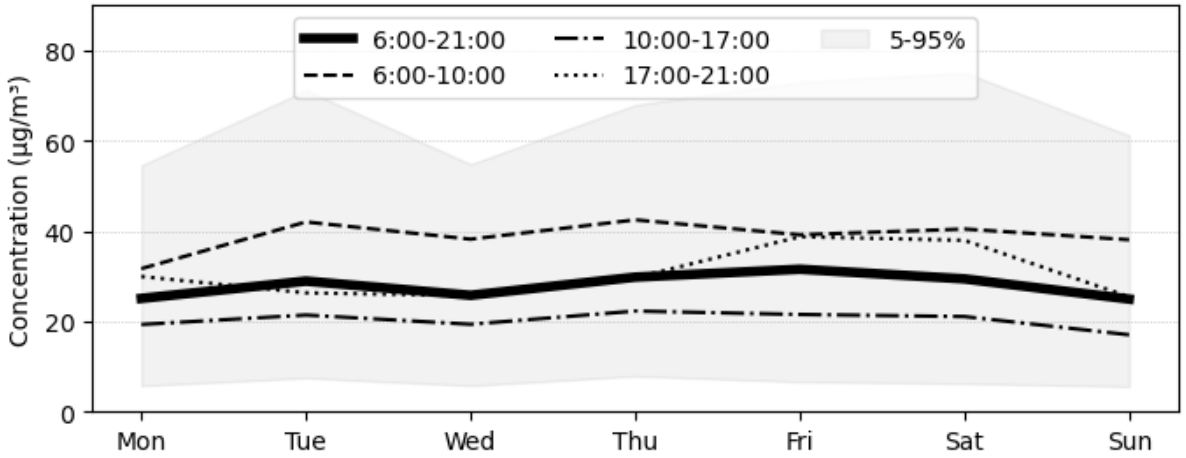

Figure 5. Concentrations averaged per day of the week for different time periods, for all locations combined.

The average day concentrations (from 6:00-21:00) did not vary significantly per day of the week. The evening peak was highest on Friday and Saturday (35 µg/m^3), while it was lowest on Sunday and Tuesday (20-25 µg/m^3). Highest concentrations were noted in the evenings of Friday and Saturday because of high traffic activities during weekends. The morning peak was lowest on Monday. On a Monday morning, many shops open late. Therefore, there is less traffic and a lower PM2.5 concentration. In between peak times (10:00-17:00), there is no significant variation across days of the week.

3.3 Spatial analysis

Figure 6 shows a boxplot of 5-minute averaged data for the six measurement locations. Only data measured between 6:00-21:00 is included. Nighttime hours were excluded as there were only nighttime measurements at two locations.

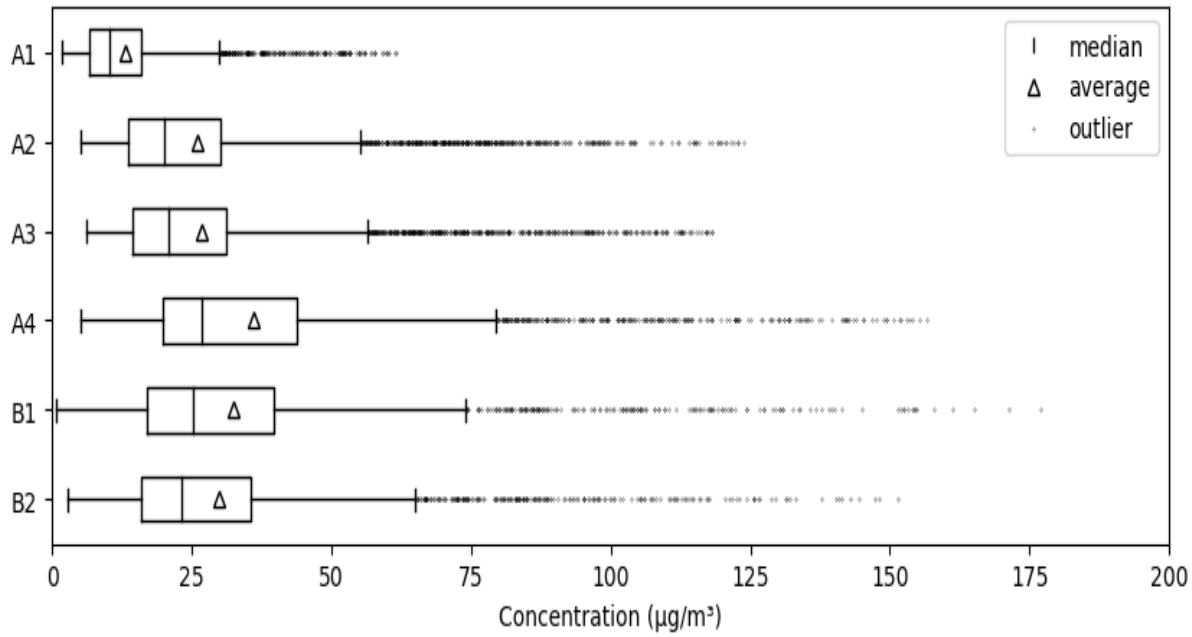

Figure 6. Boxplot of 5-minute average concentrations for all locations from 6:00-21:00. Outliers are all values outside the range of 1.5*(Q75-Q25) separated from the Q25 to Q75 box.

The variation was high at all locations. A high variation implies that concentrations were largely affected by nearby sources and dispersed soon after the moment of emission. If concentrations primarily originated from sources far away, the concentration would be more stable. Also, if concentrations would not disperse soon, the concentration would be more stable. A relatively fast dispersion of emitted PM2.5 results from the natural ventilation because of the surrounding topography of Arba Minch.

Location A1 had the lowest concentration. This location is in the periphery of Arba Minch. The traffic at this location has a steady flow, with fewer instances of starting and stopping. Also, there are not many houses near this location. The highest average concentrations were noted at location A4 (bus station). The locations with the highest variation were the mobile locations (B1, B2): they had the most outliers. Table 3 compares concentrations at hourly and daily averaged level with an independent samples t-test to evaluate whether differences are significant.

Table 3. Independent samples t-test between all locations for hourly averaged data and daily averaged data. Cells with insignificant results (p≥0.1) are shaded.

	Daily average concentration comparison ---->					
Hourly average concentration <- comparison ---	**A1**	t = -8.24 p<0.001	t = -9.69 p<0.001	t = -11.56 p<0.001	t = -10.47 p<0.001	t = -5.88 p<0.001
	t = -7.46 p<0.001	**A2**	t = -1.16 p=0.25	t = -4.97 p<0.001	t = -2.41 p=0.02	t = -1.47 p=0.23
	t = -10.88 p<0.001	t = -2.35 P=0.02	**A3**	t = -5.03 p<0.001	t = -1.64 p=0.11	t = -1.22 p=0.23
	t = -10.67 p<0.001	t = -5.35 p<0.001	t = -4.26 p<0.001	**A4**	t = 3.13 p=0.004	t = 1.37 p=0.19
	t = -13.62 p<0.001	t = -7.65 p<0.001	t = -3.66 p<0.001	t = -0.5 p=0.62	**B1**	t = 0.28 p=0.78
	t=-9.37 p<0.001	t=-2.03 p=0.04	t=-1.63 p=0.10	t=1.78 p=0.08	t=4.2 p<0.001	**B2**

Concentrations at hourly and daily averaged levels were significantly different (p<0.1) for most locations, except for location B2. At daily level, variation at location B2 was too big, relative to its average, to significantly distinguish it from concentrations at locations A2-A4 and B1. Interestingly, at an hourly averaged level, there was a significant difference. In other words, the hourly pattern over the day at location B2 was significantly different while overall (on a daily average) difference was insignificant.

A significant difference between the locations underlines the need for measurements at separate locations. Possibly, however, concentrations at one location can be estimated based on the concentrations at another location. Figure 7 shows the correlation coefficient (R^2) for ordinary least square regression without intercept between all stations on a daily and hourly averaged level.

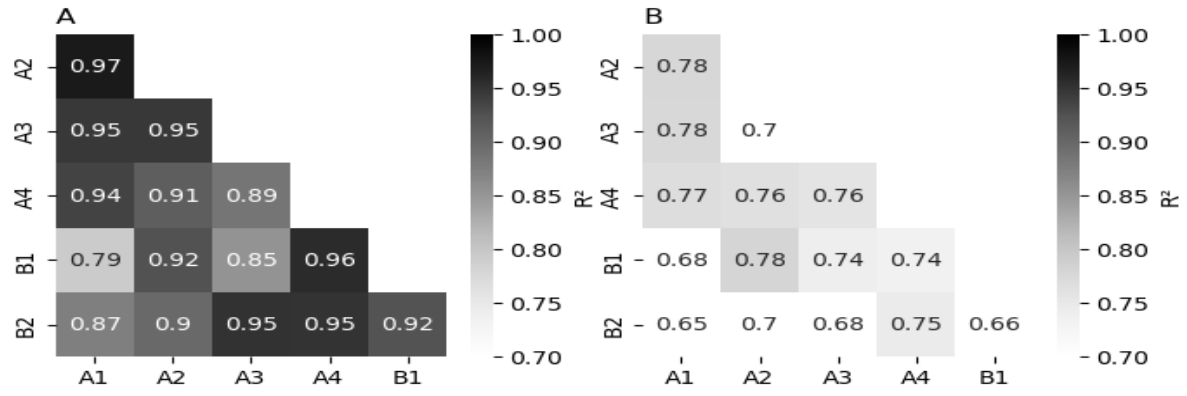

Figure 7. R^2 of data between all locations for daily averaged (A) and hourly averaged (B) concentrations. We used only the data for hours between 6:00-21:00.

On a daily level, strong correlations were noted between some of the measurement locations. Interestingly, location A4 strongly correlated with the mobile measurement locations ($R^2 \geq 0.94$). The stationary city locations A2 and A3 showed strong correlation with each other and with the out-of-town location (A1). In other words, concentrations could be predicted on a daily level for other locations based on one location. Concentration differences between locations were linear as differences in sources are linear as well. On an hourly level, however, correlations were much lower (R^2 = 0.66-0.79). To evaluate the difference between locations across hours of the day, figure 8 shows the hourly average concentration for all locations individually.

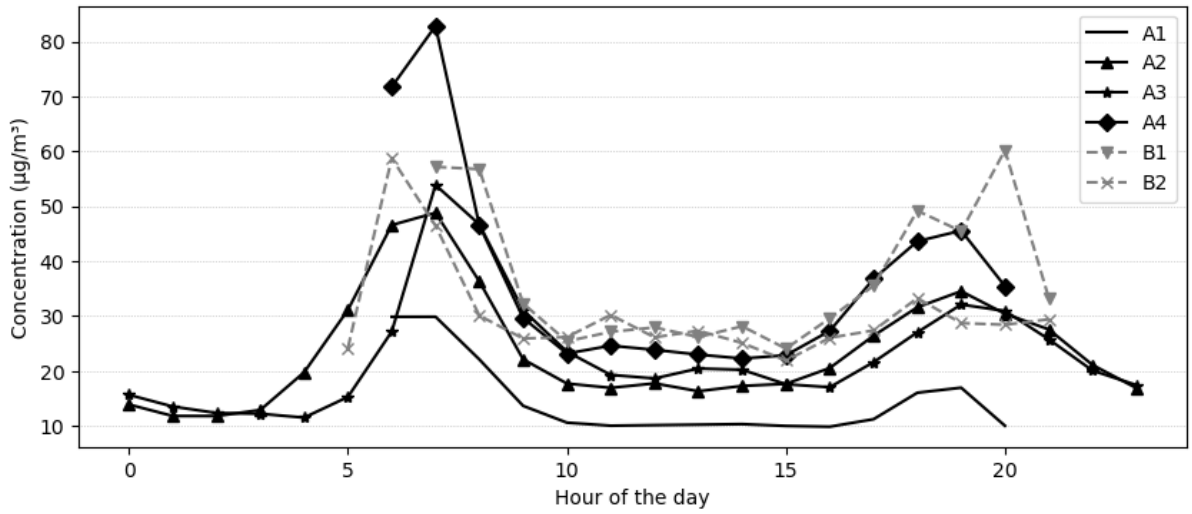

Figure 8. Concentrations averaged per hour of the day for all locations.

Figure 8 shows that concentration differences between locations were not the same across the day. This explains why the correlations at an hourly level were weaker. On a daily level, a linear difference in concentrations was observed between locations. However, this difference varied at hourly level. The highest average concentration at location A4 was due to concentrations during the morning period. The morning peak was distinctly highest at location A4 (bus station) while at other hours the concentration was the same to other locations. In the morning, long distance buses wait for passengers, running the motor. For the mobile stations, B1 concentrations were higher than B2 concentrations throughout most of the day. The work area of B1 was closer to the city center than B2. Hence, B1 was exposed to higher sources.

3.4 Next to the road versus on-road concentrations

Concentrations inside the Bajaj experienced the highest variation. On the road, variable concentrations are experienced due to nearby sources. At 10-20 meters from these sources, the concentrations become more diffuse, resulting in lower variability. Average on-road concentrations between 6:00-21:00 (33 and 30 µg/m^3 for B1 and B2) were lower than bus station concentrations (36 µg/m^3), but higher than the concentrations at the two locations next to the road (26 and 27 µg/m^3 for A2 and A3). The morning peak concentrations were in the same order of magnitude (38, 40, 45 and 38 µg/m^3 for locations A2, A3, B1 and B2, respectively). However, the concentrations on-road between 10:00-17:00 were higher than those next to the road (18, 19 µg/m^3 at A2, A3 versus 26, 27 µg/m^3 at B1, B2). Higher on-road concentrations imply traffic is a dominant source of roadside concentrations. If biomass burning was instead the main source for roadside locations, on-road concentrations would be lower than concentrations next to the road.

4. DISCUSSION

4.1 General concentration levels

Concentration levels ranged from 13.0 to 36.2 µg/m^3, and averages for days with at least 20 hours of measurements ranged from 14.4 to 35.6 µg/m^3. In Addis Ababa, average concentrations of 43.3 and 53.8 µg/m^3 were found at two locations (Kumie, 2020; Tefera et al., 2020). Daily averages ranged from 19.1 to 127.0 µg/m^3 (Tefera et al., 2020). Concentrations in Arba Minch are lower than those in Addis Ababa because Arba Minch is significantly smaller than Addis Ababa and has lower traffic flows and less household cooking. Still, multiple daily averages in Arba Minch exceeded the WHO guideline of 15 µg/m^3 as 24-hour average. With cities having higher populations than Arba Minch, we expect these cities to exceed the WHO guidelines. Even more, the topography around Arba Minch results in a natural ventilation. Cities with the same level of emission, but not a topography promoting ventilation, will experience higher concentrations. Therefore, it is advisable to conduct measurements in other cities of Ethiopia as well.

4.2 Temporal variation

We did not find a prominent pattern for days of the week in our study. In Addis Ababa lowest concentrations were witnessed on Sundays (Kumie, 2020). In Addis Ababa, while the contribution of traffic with respect to biomass burning is higher, traffic is lower on Sundays. However, biomass burning related to cooking may not necessarily be lower on Sundays. In Arba Minch, a relatively higher share of biomass burning might mask lower emissions of traffic. We did find a clear temporal pattern during the day, with highest concentrations during the morning hours. Minda (2014) found distinct peaks of black carbon (BC) concentrations during these hours as well. BC originates from combustion sources and is part of PM2.5. Traffic and household biomass burning are important sources for both PM2.5 and BC. BC concentrations during morning and evening hours reached up to 20 µg/m^3 while afternoon and nighttime concentrations were mostly below 5 µg/m^3. The morning and evening hours match with cooking times and traffic rush hours. With respect to roadside exposure, a higher number of people on the road during morning and evening hours is a double problem: exposure concentrations are high, but the number of people experiencing this exposure is also high.

Another temporal aspect is seasonal variation. Measurements in this study were all conducted in April/May, which are the wettest months within the bimodal rainfall pattern in Arba Minch (Mulugeta et al., 2017; Shalishe et al., 2022). In Addis Ababa, highest concentrations were reported during the wet season (Kumie, 2020; Tefera et al., 2020), but studies in other countries reported highest concentrations during dry seasons (Jinsart et al., 2012; Kim Oanh et al., 2013). Tefera et al. (2020) hypothesized that concentrations during the wet season in Addis Ababa were higher owing to heating-related emissions. Temperatures in Arba Minch are higher than those in Addis Ababa. Heating during the wet season is therefore not a common phenomenon. Data at a background location in Arba Minch show highest concentrations in November and December (dry season), and lowest concentrations in April/May (Dingemanse, 2022b). Compared to the findings of our study, concentrations are expected to be higher in other months that experience less rainfall. Based on this, we conclude that measurement results in our study were the bottom line for concentrations in Arba Minch, and yearly average concentrations are expected to be higher. Therefore, most likely WHO and Ethiopian yearly average guideline values of

respectively 5 and 15 µg/m^3 (Environmental Protection Authority, 2003; WHO, 2021a) are exceeded.

4.3 Spatial variation

The findings suggested that the bus station was a hotspot. Cheng et al. (2011) found average concentrations of 50-70 µg/m^3 PM2.5 at a bus terminal in Taiwan, approximately 1.5 times higher than inside the buses in the same area, and about 10 times higher than urban background. Likewise, Salama et al. (2017) found concentrations exceeding air quality standards at three different bus stations in Saudi Arabia. Like us, they found that concentrations were distinctly higher during the morning than during the afternoon. Bus travel is an important means of transport in Ethiopia. As bus stations are located at a central location, for other cities of Ethiopia it is also expected that a bus station is an important contributor to urban air pollution. At other locations in Arba Minch, concentrations also exceed guideline values. It was found that concentration differences at distinct locations were statistically significant. Although PM2.5 concentration differences within the same city have not been adequately researched, the findings of Kumie, 2020 and Tefera et al., 2020 suggested a significant difference as well. At a daily averaged level, this study found strong correlations between some of the locations. Measurements are needed at separate locations for insight in roadside exposure in cities of Ethiopia. The strong correlations suggest, however, that with a short period of measurements at multiple locations, measurements can be changed to a limited number of locations in combination with extrapolation of those concentrations to other locations. Spatial variation can also be mapped if mobile measurements are combined with GPS measurements.

4.4 Next to the road versus on-road

It was found that on-road concentrations had a higher variation and are higher than concentrations next to the road, especially in the afternoon (10:00-17:00). Kim Oahn et al. (2013) measured concentrations of 21-30 and 52-60 µg/m^3 next to the road during respectively wet and dry season, respectively, while inside a vehicle during those seasons concentrations of 35 and 47 µg/m^3, respectively, were measured. In their study, on-road concentrations were not continuously higher than concentrations next to the road. Still, other studies found high

concentrations for road users. Jinsart et al. (2012) compared exposure of different drivers in Bangkok: the highest exposure was recorded for tricycle drivers and vehicles with open windows. Similarly, in a city in Iraq Al-sareji et al. (2022) found that out of four transportation modes the car with open windows experienced the highest exposure, while motorcycles experienced the lowest exposure. Those studies found that PM2.5 concentrations were 86-350 $\mu g/m^3$ for these highest exposure modalities. The fact that tricycles and open-window vehicles experience the highest exposure suggests that for Arba Minch the Bajaj is the transport modality with highest exposure. Next to that, a common public transport mode in Arba Minch is a minibus, which drives with open windows as well. This suggests a similar high exposure.

4.5 Sources

High concentrations result from traffic and surrounding biomass burning. Concentrations getting higher on-road than next to the road suggested that traffic was a dominant source. Likewise, morning concentrations at bus stations came from buses waiting in the morning. If the dominant source was biomass, we would not see a distinction in morning and evening peak for that location. Whatever the source, there are ramifications for other cities. Other cities of Ethiopia have traffic and biomass burning as well. More than ten cities in Ethiopia have a higher population than Arba Minch. A higher population means an increase in both sources. The 2007 census reported that use of firewood was around 89% while electricity was only 0.2% in SNNPR and at country level (Population Census Commission, 2007). Since then, the use of electricity for cooking might have increased. However, there is no reason to expect that SNNPR will significantly differ from country average. The concentrations measured in Arba Minch are therefore not likely to be an overestimation relative to other cities.

4.6 Student science as method

The application of the student science method resulted in the limitation of sampling time to the course duration and a lower cooperation of location managers at the bus station. The measurements gave a good reflection of relative differences between locations. Insight in year-round and genuine 24-hour average concentrations was missing. Data collection during day and night at multiple locations and over different seasons requires a higher investment in supervision

and course load, or dedicated measurement stations. Sharing a measurement project across multiple courses may result in higher course load and more supervision. However, the application of student science in the current study brought about relevant insight into city concentrations. The findings of this study conformed with concentration patterns found in other studies, pointed to peaks in time and locations, and underlined the burden of exposure above guidelines. In a situation with limited resources for data collection, student science fills the gap in knowledge on PM2.5 exposure in Ethiopian cities.

5. CONCLUSIONS AND RECOMMENDATIONS

In an application of student science and low-cost sensors, students conducted measurements at four stationary and two mobile stations in Arba Minch for six weeks. Daily average roadside concentrations in Arba Minch ranged from 10-50 µg/m^3, with 5-minute averages up to 100 µg/m^3. Daily averages exceeded air quality standards. This study revealed a distinct morning- and evening concentration peak at all measurement locations. Concentrations during 6:00-10:00 were twice as high as those during daytime. The two mobile stations showed the highest variation in concentration while the measurement location at the bus station showed both highest average concentrations and high variations. Highest concentrations at the bus station were primarily due to high concentrations during morning hours (6:00-10:00). On a daily average level, strong correlations were found between some of the locations; however, this was not the case on an hourly level. Apart from the bus station, on-road concentrations on average were higher than concentrations next to the road primarily owing to higher afternoon concentrations.

Results for Arba Minch imply exposures exceeding air quality guidelines in multiple cities of Ethiopia. This underlines the need for increased data collection across Ethiopia. With limited resources, it is important to find ways to make research cheaper. We found that, on a daily level, it was possible to monitor at one location and extrapolate it to some other locations within the same city. Furthermore, this study showed that student science and low-cost sensors were useful for increasing the availability of data collection. Limitations originating from student science, such as locations not trusting the data collectors, can be resolved by more active involvement of staff. While this study was limited to the duration of one course, data collection across different

seasons becomes possible through student science if there is cooperation amongst different course instructors and universities.

Acknowledgements

We thank Meseret Tesfaye for constructing the SPSA set-ups. Thanks also go to Dagmawi Matewos for assisting the students in instrument installation. We especially thank the 2021/2022 G3 WSEE students, for selecting measurement locations, and conducting measurements.

Data availability

All data used and code created in this study is made available on the OSF repository, https://doi.org/10.17605/OSF.IO/WHU6A.

REFERENCES

Al-sareji, O. J., Grmasha, R. A., Hashim, K. S., Salman, J. M., & Al-Juboori, R. A. (2022). Personal exposure and inhalation doses to PM1 and PM2.5 pollution in Iraq: An examination of four transport modes. *Building and Environment, 212*, 108847. https://doi.org/10.1016/j.buildenv.2022.108847

Babatola, S. S. (2018). Global burden of diseases attributable to air pollution. *Journal of Public Health in Africa, 9*(3), 813. https://doi.org/10.4081/jphia.2018.813

Central Statistical Agency (Ethiopia). (2023). *Population projection: Population Size by Sex Zone and Wereda July 2023*. https://www.statsethiopia.gov.et/wp-content/uploads/2023/08/Population-of-Zones-and-Weredas-Projected-as-of-July-2023.pdf

Central Statistics Agency (Ethiopia). (2013). *Population Projection of Ethiopia from all Regions at Wereda Level for 2014-2017*. www.csa.gov.et

Cheng, Y.-H., Chang, H.-P., & Hsieh, C.-J. (2011). Short-term exposure to PM10, PM2.5, ultrafine particles and CO2 for passengers at an intercity bus terminal. *Atmospheric Environment, 45*(12), 2034–2042. https://doi.org/10.1016/j.atmosenv.2011.01.061

Dingemanse, J. D. (2022a). Evaluation of Three Low-Cost Particulate Matter (PM2.5) Sensors for Ambient and High Exposure Conditions in Arba Minch, Ethiopia. *Ethiopian Journal of Water Science and Technology*, *4*, 33–61. https://doi.org/10.59122/134080D

Dingemanse, J. D. (2022b). *Evaluation of three PM2.5 LCS (article)* [dataset]. OSF. https://doi.org/10.17605/OSF.IO/YTV79

Dingemanse, J. D., Abiyu, M. A., Tesfaye, K. G., & Roro, F. F. (2022). Using student science to identify research priority areas for air pollution in a university environment: An Ethiopian case study. *Clean Air Journal*, *32*(2), Article 2. https://doi.org/10.17159/caj/2022/32/2.13470

Dingemanse, J. D., & Dingemanse-de Wit, G. (2022). An evaluation of best practices in an air quality student science project in Ethiopia. *Aquademia*, *6*(1), ep22001. https://doi.org/10.21601/aquademia/11828

Environmental Protection Authority. (2003). *Guideline Ambient Environment Standards for Ethiopia*.

Gakidou, E., Afshin, A., Abajobir, A. A., Abate, K. H., Abbafati, C., Abbas, K. M., Abd-Allah, F., Abdulle, A. M., Abera, S. F., Aboyans, V., Abu-Raddad, L. J., Abu-Rmeileh, N. M. E., Abyu, G. Y., Adedeji, I. A., Adetokunboh, O., Afarideh, M., Agrawal, A., Agrawal, S., Ahmadieh, H., … Murray, C. J. L. (2017). Global, regional, and national comparative risk assessment of 84 behavioural, environmental and occupational, and metabolic risks or clusters of risks, 1990–2016: A systematic analysis for the Global Burden of Disease Study 2016. *The Lancet*, *390*(10100), 1345–1422. https://doi.org/10.1016/S0140-6736(17)32366-8

Institute for Health Metrics and Evaluation. (2020, October 15). *PM2.5 Exposure | State of Global Air*. State of Global Air. https://www.stateofglobalair.org/air/pm#uneven-progress

Isaxon, C., Eriksson, A., Abera, A., & Malmqvist, E. (2019). Assessment of outdoor air pollution in Adama, Ethiopia. *Environmental Epidemiology*, *3*, 176. https://doi.org/10.1097/01.EE9.0000607732.53692.f6

Jinsart, W., Kaewmanee, C., Inoue, M., Hara, K., Hasegawa, S., Karita, K., Tamura, K., & Yano, E. (2012). Driver exposure to particulate matter in Bangkok. *Journal of the Air & Waste Management Association*, *62*(1), 64–71. https://doi.org/10.1080/10473289.2011.622854

Kim Oanh, N. T., Kongpran, J., Hang, N. T., Parkpian, P., Hung, N. T. Q., Lee, S.-B., & Bae, G.-N. (2013). Characterization of gaseous pollutants and PM2.5 at fixed roadsides and along vehicle traveling routes in Bangkok Metropolitan Region. *Atmospheric Environment*, *77*, 674–685. https://doi.org/10.1016/j.atmosenv.2013.06.001

Kumie, A. (2020). The profile of fine particulate matter (PM2.5) using Beta Attenuator Monitor (BAM) in Addis Ababa, Ethiopia. *ISEE Conference Abstracts*. https://doi.org/10.1289/isee.2020.virtual.P-1019

Minda, T. T. (2014). *Measuring and Modelling Ambient Air Quality in Arba Minch, Ethiopia* [Wageningen University]. https://edepot.wur.nl/332396

Misker, D., Tunje, A., Mengistu, A., Abera, F., Yalelet, M., Gebrie, M., Yimam, M., & Anemaw, S. (2017). *Magnitude and Factors Associated with Road Traffic Accident among Traumatized Patients in Arba Minch General hospital, 2017*. *2*(3).

Mulugeta, M., Tolossa, D., & Abebe, G. (2017). Description of long-term climate data in Eastern and Southeastern Ethiopia. *Data in Brief*, *12*, 26–36. https://doi.org/10.1016/j.dib.2017.03.025

Population Census Commission. (2007). *The 2007 Population and Housing Census of Ethiopia: Statistical Report for Southern Nations, Nationalities and Peoples' Region.* Ethiopia.

Salama, K. F., Alhajri, R. F., & Al-Anazi, A. A. (2017). Assessment of air quality in bus terminal stations in Eastern province, Kingdom of Saudi Arabia. *Int. J. Community Med. Public Health*, *4*, 1413. http://dx.doi.org/10.18203/2394-6040.ijcmph20171748

Shaddick, G., Thomas, M. L., Amini, H., Broday, D., Cohen, A., Frostad, J., Green, A., Gumy, S., Liu, Y., Martin, R. V., Pruss-Ustun, A., Simpson, D., van Donkelaar, A., & Brauer, M. (2018). Data integration for the assessment of population exposure to ambient air pollution for Global Burden of Disease assessment. *Environmental Science & Technology*, *52*(16), 9069–9078. https://doi.org/10.1021/acs.est.8b02864

Shalishe, A., Bhowmick, A., & Elias, K. (2022). Meteorological Drought Monitoring Based on Satellite CHIRPS Product over Gamo Zone, Southern Ethiopia. *Advances in Meteorology*, *2022*, 9323263. https://doi.org/10.1155/2022/9323263

Sousan, S., Regmi, S., & Park, Y. M. (2021). Laboratory Evaluation of Low-Cost Optical Particle Counters for Environmental and Occupational Exposures. *Sensors*, *21*(12), Article 12. https://doi.org/10.3390/s21124146

Tefera, W., Kumie, A., Berhane, K., Gilliland, F., Lai, A., Sricharoenvech, P., Patz, J., Samet, J., & Schauer, J. J. (2021). Source Apportionment of Fine Organic Particulate Matter (PM2.5) in Central Addis Ababa, Ethiopia. *International Journal of Environmental Research and Public Health*, *18*(21), Article 21. https://doi.org/10.3390/ijerph182111608

Tefera, W., Kumie, A., Berhane, K., Gilliland, F., Lai, A., Sricharoenvech, P., Samet, J., Patz, J., & Schauer, J. J. (2020). Chemical Characterization and Seasonality of Ambient Particles (PM2.5) in the City Centre of Addis Ababa. *International Journal of Environmental Research and Public Health*, *17*(19), Article 19. https://doi.org/10.3390/ijerph17196998

Weiß, C. I., Gohm, A., Rotach, M. W., & Minda, T. T. (2022). Dynamics of gap winds in the Great Rift Valley, Ethiopia: Emphasis on strong winds at Lake Abaya. *Weather and Climate Dynamics*, *3*(3), 1003–1019. https://doi.org/10.5194/wcd-3-1003-2022

World Health Organization. (2021a). *WHO global air quality guidelines. Particulate matter (PM2.5 and PM10), ozone, nitrogen dioxide, sulfur dioxide and carbon monoxide*. World Health Organization. https://apps.who.int/iris/handle/10665/345329

World Health Organization. (2021b). *Ambient (outdoor) air pollution*. WHO Newsroom. https://www.who.int/news-room/fact-sheets/detail/ambient-(outdoor)-air-quality-and-health

Ethiopian Journal of Water Science and Technology (EJWST)

DOI: https://doi.org/10.59122/15519a9

Vol. 5 , 2022, pages: 74~101 ISSN(Print): 2220-7643

Implications of Uncontrolled Water Withdrawal and Climate Change on Water Supply and Demand Gap in Tana Lake Sub-basin

Mintamer Ferede[1], Assefa Gedle[1], Alemshet Kebede Yimer[1], Selamawit Damtew Amare[3], Alemseged Tamiru Haile[2], Meron Teferi Taye[2]

[1]Arba Minch Water Technology Institute, Faculty of Water Resource and Irrigation Engineering, Arba Minch University, Ethiopia. Email: Merader33@gmail.com
[2]International Water Management Institute, IWMI, Ethiopia.
[3]Bahir Dar Institute of Technology, Bahir Dar University, Ethiopia

ABSTRACT

Climatic variability, uncontrolled irrigation water abstraction, and other non-climatic factors create a great pressure on freshwater resources. This study focuses on the impact of three drivers (land use change, irrigation expansion, and climate change (CC)) on water resources of the Gumara Watershed of Lake Tana Sub-basin, Ethiopia. Land use land cover (LULC) and actual irrigated-area were mapped using the Random Forest (RF) machine learning classifier in the Google Earth Engine (GEE) platform. Climate data was obtained from the Climate Hazards Group InfraRed Precipitation (CHIRP), Ethiopian Meteorological Institute (EMI) and global climate models. Streamflow and crop water demand were estimated using the HBV model and Crop Wat software, respectively. The supply-demand gap was estimated for the current and future climate. The results revealed the increasing trend of cropland in the expanse of forest, grassland, waterbody, and shrubland. A widespread irrigation was observed near the lake shore and upstream parts of the catchmentwhich experienced an increasing trend of potential evapotranspiration because of the increase in temperature. The rising of potential evapotranspiration created high water demand for irrigation. The supply-demand relationship showed uneven distribution in the current and future periods. The increase in temperature and uncontrolled expansion of irrigated land area will increase the unmet water demand for irrigation in the future. This can cause conflict of interest between the users, and potentially affect available water for environmental demands. Therefore, there is strong need to promote sustainable water resource management practices and adaptive management of irrigation in the Gumara Catchment.

Keywords: Random Forest, Google Earth Engine, supply-demand, unmet demand, adaptive management

Received: 08 Oct 2022; accepted 06 December.2022

1. INTRODUCTION

The water resources of Lake Tana Sub-basin, which is the source of the Blue Nile River, is under pressure owing to multiple climatic and non-climatic factors. Climate variability is causing erratic rainfall distribution that produces large streamflow and lake level variations (Gebremicael et al., 2013, Tesemma et al., 2010). The sub-basin receives low rainfall amount in the northern part and highest rainfall amount in the southern part of the sub-basin (Birara et al. 2018; Haile et al. 2009). Most studies agree with the projected increasing rate of rainfall and temperature in the future. The annual rainfall is projected to increase by 202 mm and 255 mm by 2050s and 2080s, respectively (Setegn et al. 2009; Getachew & Manjunatha 2021; Enyew et al. 2014; and Desalegn et al. 2016).

Historically, the sub-basin had minimum and maximum temperature increase by 0.037°C and 0.15 °C per decade, respectively (Mengistu et al. 2014; Mohamed & Mahdy 2021; Fetene et al. 2018). Similarly, studies predicted the rise of maximum temperature from 1.38 °C to 3.59 °C under RCP 4.5 scenarios by 2080s, while minimum temperature increase by 5.92 °C under RCP 8.5 by the end of the 21st century in Tana Lake Sub-basin (Getachew & Manjunatha 2021). The increasing trends of temperature will lead to increased evapotranspiration by 4.7% to 12.2% (Chakilu et al. 2020; Teklay et al. 2020). Such increase in temperature and evaporation rates may result in less freshwater sources while increasing water demand for various purposes.

Literature shows significant land cover change in the sub-basin because of increasing rate of cultivated land that ranges from 29.95% to 48.02% over the last 40 years (Tewabe and Fentahun 2020; Woldesenbet et al., 2017; Tefaw et al. 2023). Some studies reported forestland, wetland, bush/shrublands, and grassland have continuously decreased over the recent decades (Asitatikie 2019; Elhamid et al. 2019). The changes in land use are primarily driven by population growth, agricultural expansion, urbanization, increasing energy and food demands, and changes in lifestyle and socio-economic conditions (Malede et al. 2023; Alemayehu 2006; Tewabe and Fentahun 2020).

Non-climatic aspects such as population and economic growth including urbanization have their own impact on water resources of the Lake Tana- Sub-basin. The sub-basin has undergone

developmental changes since the start of 2000s with the growth of irrigation and hydropower projects (Alemayehu et al., 2010; Mequanent and Mingist, 2019; Yenehun et al., 2021). One of the major developmental changes occurred in 2010 with inter-basin water transfer from Lake Tana to Beles Basin for hydropower production (Yenehun et al., 2021). It is expected that a total of 60,077 ha of the sub-basin will be categorized under medium size irrigation schemes when all the planned irrigation schemes are completed (e.g., Koga, Ribb, Megech, Gumara, and Gilgel Abay). The construction of Koga Irrigation was completed in 2010 (Asres 2016) with planned irrigation command area of about 7,000 ha and with a reservoir storage capacity of 78.5 Mm3. In the Koga Watershed, there was a plan to improve rainfed agriculture, forestry, livestock, soil conservation, water and sanitation on 22,000 ha (Birhanu et al. 2015). The second multi-purpose reservoir in the basin was constructed in Ribb River. The reservoir had a capacity of 234 Mm3. The irrigation project was expected to be constructed on 20,000 ha of land and benefit 40,000 farmers.

Taye et al. (2021) reported that irrigation water abstraction by smallholder farmers during the dry season in Lake Tana Sub- basin is causing water scarcity, conflicts, and environmental damage. The researchers evaluated the implication of uncontrolled rate of water abstraction and irrigated land expansion on the water availability in the sub-basin. However, this paper did not consider the impacts of climate change on water irrigation . It did not combine different data sources (e.g., remote sensing data) and neither used hydrological models to characterize the sub-basin's water availability for different periods. In short, limited studies showed the implication of combined drivers (land use change, climate change, and irrigated land expansion) in the hydrology of Lake Tana Sub-basin at sub-basin scale (Dile et al.2013; Asitatikie 2019; Taye 2021; Shaka 2008).

Therefore, this study addresses some of the mentioned research gaps. It evaluates the implication of the three drivers (land use change, irrigation expansion, and climate change) on the current and future water availability across the sub-basin. Hydropower water use, domestic water use, and industrial water use in the sub-basin were already reported by Taye et al. (2022). These water uses would not be repeated here. Environmental flow was not considered since the current water use in Gumara did not allocate water for the environment. This study used both observed and remote sensing data to map the actual irrigated area and evaluate the land cover change

within the sub-basin. Taye et al. (2021) studied land and water constraints in the eastern side of the Tana Sub-basin especially water shortages in the dry season flow. This study showed the gap between water demand and supply in Gumara catchment the current and future period of , as an experimental site including climate change impacts. The information generated on current quantified volume of abstracted water, and the projected available water in the river is important to minimize the negative impacts of climate change.

2. Study area

The Lake Tana Sub-basin extends from UTM coordinates of 260000 to 400000 m (36.8° to 38.2°) east and from 1210000 to 1420000m (11° to 12.8°) north. It is located at the headwater of the Blue Nile (Abbay) River Basin, in the North-western Ethiopia highlands (Figure 1). Elevation variation across the sub-basin ranges between 1779 and 4110 m. Most of the low land part of the sub-basin surrounds Lake Tana. The mean elevation of the basin is 2945 m. The sub-basin area under the highest elevation range (>4000 m) is in a small portion of northern, eastern and southern parts of the sub-basin.

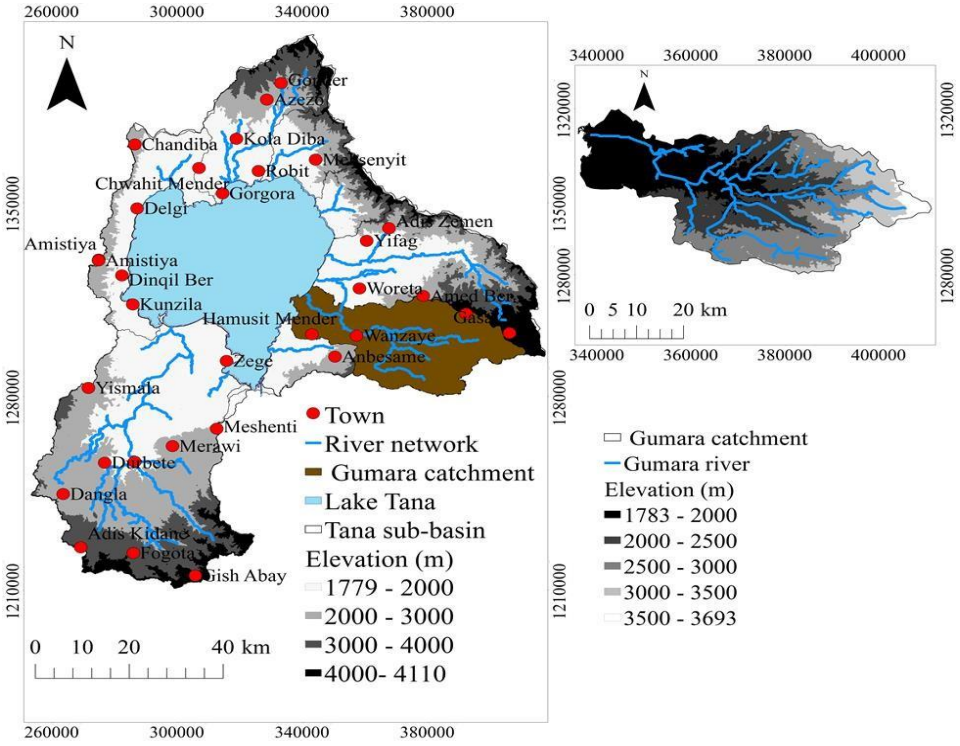

Figure 1: Elevation, drainage network and towns of Lake Tana sub-basin.

The length of the sub-basin from North-South and East-West is 203 km and 179 km., respectively. Based on various studies, the sub-basin covers a drainage area between 15,000 and 16,000 km2. (Rientjes et al.2011; Chebud and Melesse, 2009, Dessie et al., 2014) and the lake covers about 3,000 km2 which is 20% of the drainage area. The mean annual rainfall of the sub-basin is 1,280 mm (Setegn et al. 2008) but it varies from 815 to 2344 mm/year, and it shows large variation across the sub-basin. It has one main rainy season that extends from June to September, which accounts for more than 80% of the annual rainfall. The rest of the year is dry except for some rains from March to May. Rainfall variation in Lake Tana Sub-basin is large spatially and temporally. Rainfall magnitude shows an overall decreasing trend from south to north.

Unlike the rainfall, the temperature of the sub-basin is on average 20°C with small seasonal changes. The mean annual temperature of the area varies from 7.26-23.4 °C (Goshu and Aynalem 2017) with the highest temperature from March to May whereas, the lowest temperature from July to September (ADSWE: LUPESP, 2015). Average annual evaporation over the lake surface is approximately 1,675 mm (SMEC 2008).

There are four major rivers that feed Lake Tana; they account for 93% of the inflow (Kebede et al., 2006). These are Gilgel Abay, Gumara, Megech, and Ribb. Gilgel Abay is in the south, Gumara and Ribb are in the east, and Megech in the north. Studies reported that the mean annual rainfall of Ribb and Gumara falls in the range between 1278and1279 mm. As shown in Table 1, the Gilgel Abay receives the highest annual rainfall compared to others. The highest mean potential evapotranspiration (1633 mm/year) is reported in Megech, the north part of the sub-basin while the lowest (1193 mm/year) in Gilgel Abay. ,. The east part of the sub-basin has potential evapotranspiration ranging from 1223to 1247 mm/year in Gumara and Ribb. The Lake Tana gets the highest inflow from Gilgel Abay (Atanaw et al. 2018) and the minimum from Megech in the northern catchment.

Table 1. Characteristics of the main catchments of Lake Tana sub-basin

Sub-catchment	Area (% of sub-basin area)	Mean annual rainfall (mm)	Mean annual Evapotranspiration (PET) (mm)	% Contribution to Lake Tana's inflow
Gilgel Abay	11.62	1407	1193	28
Ribb	9.32	1278	1247	27
Gumara	8.42	1279	1223	27
Megech	3.4	1248	1633	11

Extensive wetlands surrounding the lake provide broad ecosystem services. In the sub-basin, an increasing rate of irrigation water use resulted in hydropower, domestic water supply, environmental flow, industrial water use, navigation, and tourism developments (de Fraiture et al., 2001). The challenges of water resources management in the Lake Tana Sub-basin are many and it is important to consider the trade-off between hydropower, irrigation, navigation, and fishing considering the changing climate.

3. Data Collection and Methodology

3.1 Dataset

Data for this study were obtained from various sources including global and national data sources, and field surveys. A Digital Elevation Model (DEM) of 30 m resolution was obtained from Shuttle Radar Topography Mission (https://doi.org/10.5066/F7K072R7). The DEM was used to delineate the catchment, its sub-catchments, and the drainage network.

To map the land use land cover (LULC) in the Tana Sub-basin, Landsat Surface Reflectance Tier 1 imagery of Landsat OLI/TIRS and TM sensors available in Google Earth Engine were used. At a decade interval, LULC was mapped for the years 1990, 2000, 2010, and 2021 during the dry season (January to March). Images acquired during the dry season were used to minimize the effects of seasonal land cover dynamics and the cloud cover. Ground Control Points (GCPs)

were collected between February 12 and 17, 2022 and served as reference data for training and validating the LULC classification algorithm. A Global Positioning System (GPS) device with positional error of ±3 meter was used to record the geographic coordinates of the 523 GCPs. SPOT images of 2006 and 2016 and Google earth map were used to generate GCPs for classifying LULC historical periods.

For remote sensing based irrigated area mapping, Sentinel-2 (S2) satellite images were used for the entire sub-basin. The mapping was using S2 images which were acquired in the main irrigation season that stretched from October-2021 to April-2022.

Meteorological data were obtained from Ethiopian Meteorology Institute (EMI). Only one station at Deber Tabor was a first-class station and hence provided data on maximum and minimum temperature (oC), relative humidity (%), wind speed (km/day) and sunshine hours to calculate evapotranspiration (ETo) for the period 1996–2019. Satellite daily rainfall data (CHRIP) was downloaded from climate SERV 2 web page (https://climateserv.servirglobal.net/) for the period 1981 – 2021. CHRIP data had 0.05 ◦ x 0.05 ◦ horizontal resolution.

Historical trends of rainfall and temperature were evaluated using Climate Hazards Group InfraRed Precipitation with Station data, CHIRPSv2 (C. Funk et al., 2015; C. C. Funk et al., 2014) and Climate Hazards Group InfraRed temperatures and stations (CHIRTS, Funk et al., 2019), respectively. The historical and projected daily precipitation and temperature (min and max) with a spatial resolution of 0.25 by 0.25 degrees were downloaded from NASA Global Daily Downscaled Projections (NASA NEX GDDP), (available at https://doi.org/10.7917/OFSG3345).

The period 1985–2014 indicated the historical climate while 2035-2064 showed the projected future scenarios for SSP45 and SSP85. . Data was obtained from 9 General Circulation Models (GCMs) to study the climate change impact. The data were statistically downscaled (using delta approach). The models' name and resolutions are summarized in Table 2.

Table 2:-Summary of the models used for climate change analysis

Model name	Modelling Center	Horizontal resolution (Atmosphere) (km)	Horizontal resolution (ocean) (km)	Vertical resolution (levels)
HadGEM3-GC31-MM		100	25	75
HadGEM3-GC31-HM		50	25	75
HadGEM3-GC31-HH		50	8	75
CNRM-CM6-1	CERFACS	100	100	91
CNRM-CM6-1-HR		50	25	91
EC-Earth3P	SMHI, KNMI, BSC, CNR, and 23other institutes	100	100	91
EC-Earth3P-HR		50	25	91
MPI-ESM1-2-XR	Max Planck institute for Meteorology	100	50	95
MPI-ESM1-2-HR		50	50	95

3.2 Methods

3.2.1 LULC Classification and Change detection

The major LULC classes in the sub-basin were identified through unsupervised classification and validated during field survey. There are nine major LULC classes in the Lake Tana sub- basin (bare land, built-up, cropland, grassland, natural forest, plantation, shrubland, water body, and wetland). Sampling points for GCPs were identified from unsupervised classification. Google earth images were selected for identifying locations of GCPs from each LULC class. Stratified and random sampling were used to identify the sampling points.

Although a minimum of 60 GCPs should be collected from each class through survey (Cochran, 1953 and Shetty, 2019), 523 field observation data were collected by random sampling criteria and 700 additional GCPs from high resolution SPOT and Google earth images. This study used SPOT and Google earth images to minimize the complexity of the environment. As a result, a total of 1223 GCPs were recently generated.

To work out historical period images, visual inspection of the Landsat image and prior knowledge about the region during the field survey were used as data sources. As a result, 700, 850, 950, and 1223 GCPs were collected for the years 1990, 2000, 2010, and 2021. Of the collected GCPs, about 75% of the data was used for training, whereas 25% was used for accuracy assessment of the LULC maps.

The LULC was classified using the random forest (RF) machine learning classifier available at the Google Earth Engine (GEE) platform. The classified LULC maps were analyzed to identify the gains and losses in each of the LULC classes. Changes in each LULC class were estimated for the periods 1990-2000, 2000-2010 and 2010-2021.

3.2.2 Mapping of actual irrigated area

Actual irrigated area was mapped using GEE following four steps: (1) generation of time series of Normalized Difference Vegetation Index (NDVI) from Sentinel-2 images over a crop growing season (12 images were acquired between October 2021 and April 2022).

The NDVI values range from +1.0 to -1.0; (2) training of a remote sensing algorithm for multi-crop irrigated area mapping using Sentinel-2 images; (3) validation of the irrigated area map using GCP data, and (4) post processing of the actual irrigated area map to exclude areas which were less likely to be irrigated. To map the irrigated area, we used a multi-temporal supervised random forest (RF) classification algorithm (Biggs et al. 2006; Velpuri et al. 2009). When compared to other traditional machine learning algorithms, the RF classifier produced high-quality classification mapping while requiring minimal computing time (Rodriguez-Galiano et al. 2012; Inglada et al. 2017). The number of trees increased gradually and set at 1000 until the classification accuracy converge reached the best classified range (Li et al. 2021). The RF classification algorithm was used to classify image pixels into two classes: non-irrigated and irrigated. To discriminate between irrigated and non-irrigated areas, multi-temporal data analysis was used. Supervised classification was applied in this study; GCPs were used to train the algorithm.

3.2.3 Classification accuracy assessment

The accuracy of the LULC and actual irrigated area maps was evaluated through visual inspection, a confusion matrix with appropriate accuracy indices (user accuracy, producer accuracy and overall accuracy) and nonparametric Kappa coefficient. The overall accuracy was calculated by summing the number of pixels correctly classified and dividing them by the total number of pixels. This was expressed in percentages, 100% accuracy being a perfect classification whereas accuracy of more than 85% was considered an acceptable level of accuracy (Gashaw et al. 2017). Kappa values between 0.70 and 0.85 were regarded as excellent predictors of the classified image's ability to represent ground truths (Monserud 1990).

3.2.4 Evaluation of historical climate change

Both datasets provided gridded data. Using CHIRPS and CHIRTS data over the Lake Tana Basin, linear trends were estimated at each grid cell with statistical significance of 95% and 90% for precipitation and temperature, respectively.. The p-value for testing statistically significance whose null hypothesis, the slope is zero, was tested using Wald Test.

The t- distribution of the test statistic was used to map the trends. During analysis, the durations 1981-2020 and 1981-2016 indicated precipitation and temperature, respectively.

3.2.5 Irrigation crop requirement

The crop water requirements for all existing crops in Gumara Watershed were computed using CROPWAT 8.0 software developed by FAO (Food and Agriculture Organization). The input data included climate data, crop evapotranspiration (ETo), monthly rainfall data, crop data, and soil physical properties. CROPWAT 8.0 uses Penman- Monteith method for ETo computation. The Gumara Catchment, upstream of its river gauging site, was discretized to 29 sub-catchments and the downstream of the gauging station was considered as a single watershed for the crop water requirement analysis. As a result, a total of 30 watersheds were considered during crop water requirement analysis for the entire Gumara Catchment.

Crop types and percentage of area coverage by the major three crop types were selected based on Taye et al. (2021). The crop calendar (planting and harvesting date of the crop) was obtained from agronomists in the respective districts of the sub-catchments. The soil texture information was obtained from FAO-UNESCO soil map of the world.

To calculate gross irrigation water requirement (GIR), the estimated net irrigation requirement (NIR) was divided by 45% of efficiency value to consider application and other losses. GIR was estimated for the current period (1994-2021) and future period (2035-2064).

3.6 Rainfall-runoff modeling

Surface water supply to irrigation sites in each of the 30 sub-catchment was estimated using the Hydrologiska Byråns Vattenbalansavdelning (HBV) rainfall-runoff model. The model was used to simulate the current and projected future water supply in Gumara River and in its tributaries. First, model calibration was conducted for six years (i.e.1994 -2000 G.C.), and validation was done for three years (i.e.2001-2003 G.C.). Rainfall input of HBV was obtained from CHRIP rainfall data corrected using the Power Bias Correction method. The LULC map generated was one of the data inputs for modeling the catchment using HBV model.

The classes of land cover were aggregated into two major classes (field and forest) for HBV purpose. In the forest category only one class, forest, was considered and the remaining eight classes (bareland, built-up, cropland, grassland, plantation, shrubland, water body, and wetland) were considered together as single land cover class in the field category. Then, streamflow of the 30 sub-catchments was simulated assuming that the model parameters remain the same across the Gumara Catchment. The simulation was run for all sub-catchments for the current (1994-2021) and future (2035-2064) periods. Delta change bias correction method was used to correct temperature data from the GCMs for the future period. The future rainfall data bias was corrected using the power bias correction method.

A subtraction method was applied for analyzing the supply-demand relationship. The analysis started from upstream part of the catchment. At each irrigation demand site, the estimated irrigation water requirement was subtracted from the estimated annual streamflow of the watersheds. . The surplus streamflow from upstream watershed was added to the next tributary river flow and was considered for the supply-demand analysis of the downstream irrigation site. This continued until the outlet of the catchment was estimated either as supply-demand gap or surplus.

4. Results and Discussion

4.1 LULC classification and change

The accuracy evaluation of the generated LULC maps indicated a good classification performance with at least 85% overall accuracy and Kappa values greater than 0.80. Also, the producer and user accuracies showed good agreement (>70%). However, for the year 2000, built up, plantation, and wetland areas were poorly classified with 68%, 66% and 68% user accuracies and 67%, 68%, and 67% producer accuracy, respectively. Similarly, in 1990, built up, plantation, and wetland were poorly classified with 69%, 65%, and 68% user accuracies and 68%, 64%, and 65% producer accuracy, respectively. The lower accuracies for the built up might have contributed to their spectral similarity with barelands and croplands. Similarly, the lower accuracy in plantation was due to plantations being confused with shrublands and natural forest whose spectral profiles were similar.

The relatively low user accuracy of wetlands could be related to the spectral similarity of wetland with grassland and water body. Classification of past LULC maps was constrained by lack of archived GCPs collected through field surveys.

Fig 2 depicts the LULC classification maps of Lake Tana Sub-basin. The LULC spatial distribution reveals that cropland is the dominant land cover in the basin. The next dominant land cover types are grassland and shrubland mostly concentrated in the North- Eastern and South-West of the sub-basin. Over the past few decades, the southern part of the sub-basin has experienced a decline in both grassland and shrubland. Moreover, bare lands and natural forest are scattered in few pocket areas of the sub-basin but dominantly exist in the East and South-West of the sub-basin. Plantations have been increasing in the southern and northern parts of the basin since 2010. Furthermore, wetland and cropland areas have increased in most parts of the sub basin, more particularly in the northern and eastern parts. Conversely, grassland has disappeared in the eastern part of the sub-basin.

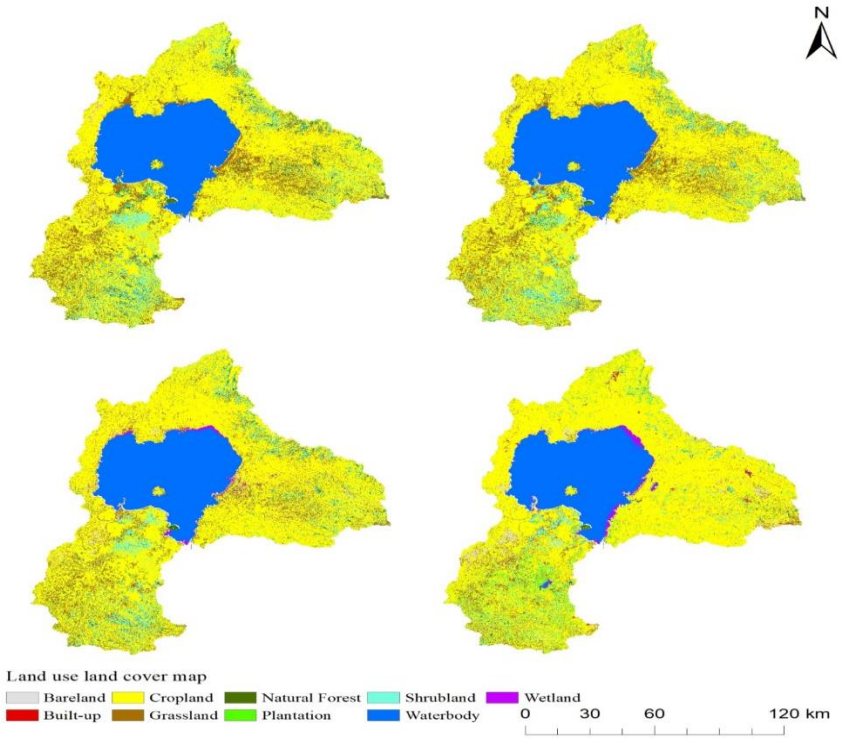

Figure 2: LULC maps of Lake Tana sub-basin in 1990 (top left), 2000 (top right), 2010 (bottom left) and 2021 (bottom right).

Fig 3 shows the coverage of the major LULC classes and the corresponding changes during 1990-2000, 1990-2010 and 1990-2021. In the base year (i.e., 1990), the dominant LULC types included cropland (covered about 53.49% of the total land area), waterbody (20.09%), grassland (11.83%), shrubland (9.29%), and forestland (4.44%). The remaining areas were covered by plantation, bare land, settlement, and wetlands.

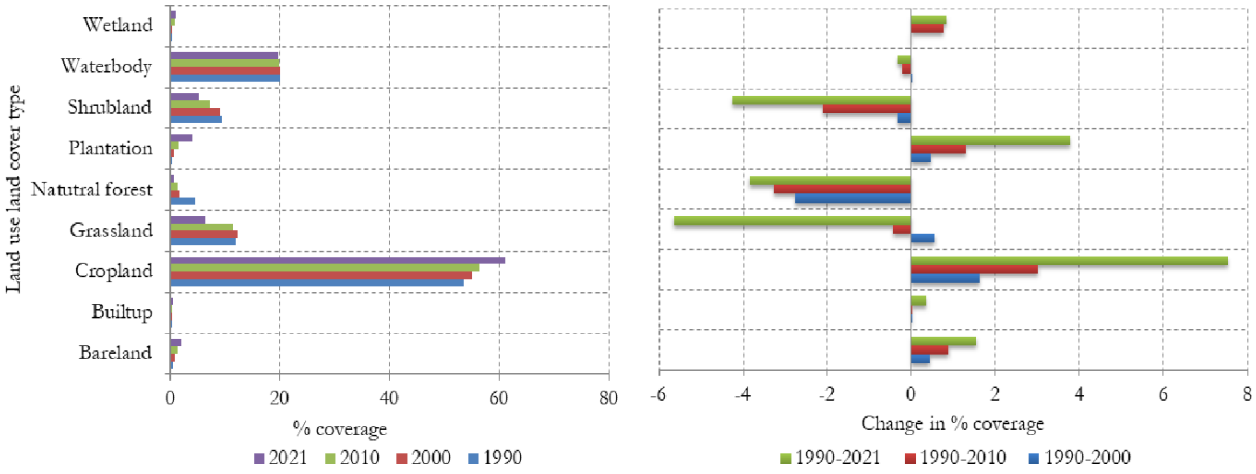

Figure 3: Coverage of LULC classes and changes in percent for three periods.

The results reveal that LULC of Tana Basin has changed significantly since 1990. Cropland, bare land, built-up, plantation, and wetland displayed positive changes over 30years while forest, grassland, waterbody, and shrubland showed negative changes. As a benchmark result, in 2021, 61% of the sub-basin was covered by cropland while nearly 20% was covered by grassland. The coverage of built-up area and shrubland was very small. As a result, cropland exhibited a larger net gain (8.65%) followed by bare land (2.71%) and plantation (1.5%). The expansion of cropland lands over the last 30 years was mainly due to the expense of forest land, grasslands, and shrubland. During this period, about 5.85% of grassland and 9.31% of shrubland have been converted to cropland. Tewabe (2020) showed the significant increasing rate of agricultural land and residential area for the last 32 years (1986-2018) by 13% and 9% respectively in the sub-basin. For the last 30 years (1989-2019), the farmland and built-up areas increased by 17.6% and 0.2%, respectively (Getachew and Manjunatha, 2022). The sub-basin experienced the largest changes in LULC in the most recent decade.

The increasing rate of crop land in the expenses of natural forest, shrub land, and grassland might have caused high soil erosion, runoff/flood, and lower rate of groundwater recharge or base flow. High percentage of rainfall amount was converted into runoff because of reduced time to infiltrate and enter into the ground.

4.2 Actual irrigated area

The actual irrigated area of the Lake Tana Sub-basin was mapped with high overall accuracy (i.e., 93%) and with Kappa coefficient value of 0.86. The classification algorithm result indicated that 94% of the irrigated area on the map was irrigated.,. It captured 95% of the irrigated lands, which indicated very good classification accuracy. In this study, the irrigated area of the Lake Tana Sub-basin covered 777.21 km2 (5.14%) of the total sub-basin. (Fig 4). The map shows that the irrigated land is clustered near to the lake, which agrees with our field observation. Farmers are also diverting river water to irrigate upstream areas. Irrigated areas cover 37.36, 23.10, 15.43 and 24.11 % of the eastern, southern, western and northern parts of the sub-basin.

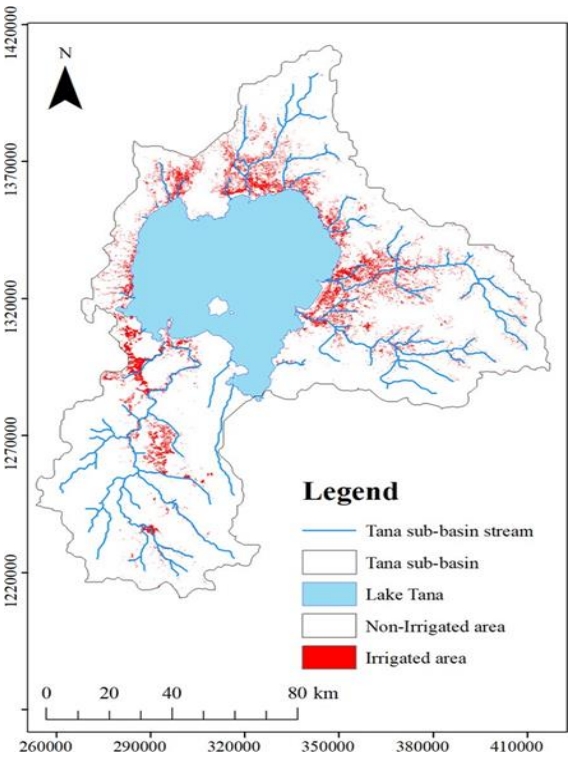

Figure 4- Spatial distribution of the actual irrigated area of Tana sub-basin based on the classification of multi-temporal Sentinel- 2 images

4.3 Historical climate analysis

According to the SSP scenarios, the temperature in Lake Tana Sub-basin showed a significant increase from 1983 to 2016 over the last three seasons (January–May, June–September, and October– December) (Fig 5). The largest increase in temperature occurred in the period from January to May (up to ~0.6 oC increment per decade). This might have contributed to increased potential evapotranspiration during the irrigation season. While maximum temperature was basin wide, minimum temperature was localized (not shown).

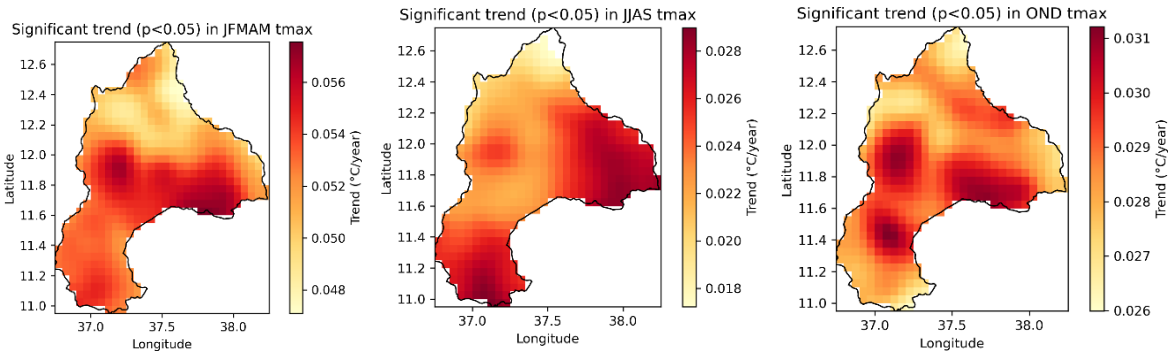

Figure 5: Trends of maximum temperature in the Lake Tana sub-basin from 1983 to 2016

The annual and dry season rainfall of Lake Tana Sub-basin had not changed significantly over the period 1981-2020. However, the rainfall amount showed a statistically significant increase (by up to ~5 mm/year) in JJAS (wet) season except for the southern part of the sub-basin (Fig 6). Moreover, the inter-quartile range (IQR) showed that most parts of the sub-basin experienced significant inter-annual change in rainfall variability during the wet season.

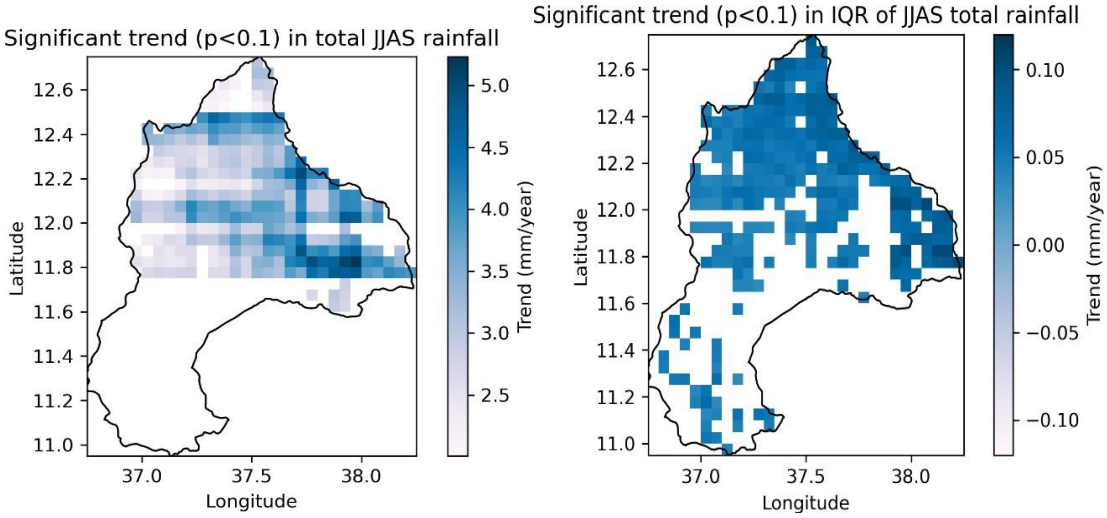

Figure 6: Historical trends in seasonal rainfall amount of the Lake Tana Sub-basin from 1981-2020

4.4 Supply-demand gap

Table 3 shows the calibrated values of HBV model parameters of Gumara Watershed. Default values indicated the parameters that were not used during model calibration.

Table 3: Summary for calibrated default and calculated parameters and values

Parameter	Value	Calibrated value	Default value	Calculated value
Alfa	0.2	*		
Beta	1.6	*		
Cflux	0.72	*		
Fc	330	*		
K4	0.02	*		
Khq	0.16	*		
Lp	0.87	*		
Perc	1.1	*		
Maxbaz	0.5	*		
Athorn	0		*	
Cevpfo	1.15		*	
Ecalt	0		*	
Ecorr	1		*	
Pcalt	0		*	
Pcorr	1		*	
Rfcf	1		*	
Hq	7.2			*

As shown in Fig 7, the simulated streamflow captures the overall patterns of observed streamflow in a good way except in 1996. The rising and falling limbs of the hydrograph were similar to simulated and observed ones. However, the simulated streamflow suggested some overestimation and underestimation of the peak flows. Baseflow was well captured except for minor overestimation in the first falling limb of 1995 and 1996.

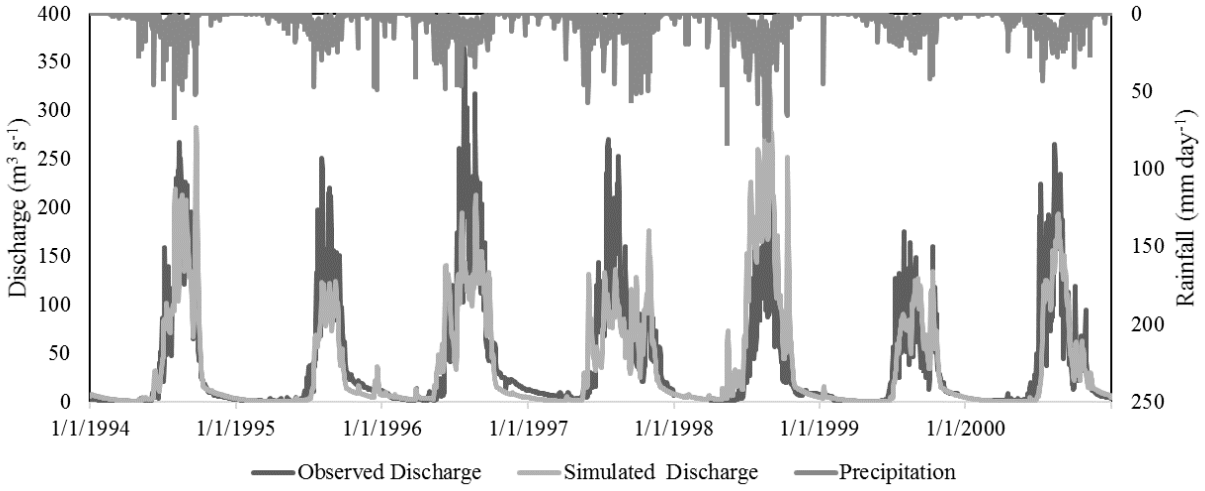

Figure 7: HBV Model Calibration result of Gumara Catchment from 1994-2000 G.C

The NS for calibration and validation indicated a relatively good performance of 0.61 and 0.62, respectively. NS values between 0.6 and 0.8 indicated fair to good performance (Nash and Sutcliffe, 1970). Based on the relative volumetric error analysis, the model performance was categorized under the well performance (+5% and −5%) during the calibration period with the estimated value of 0.11%. The relative volume error was -1.78 %.

The HBV model showed that the simulated streamflow of the Gumara Watershed was 178.64 Mm3 from 1994-2001. The streamflow at the gauged and ungauged part of Gumara was 160.57 Mm3 and 18.07 Mm3, respectively. For the future period (2035-2064), the streamflow may increase to 221.35 Mm3; specifically, the gauged and ungauged part of Gumara may have a streamflow of 196.5 Mm3 and 24.85 Mm3 , respectively. Similarly, Chakilu et al. (2020) reported the increasing rate of the annual average streamflow of Gumara Catchment because of climate change under RCP 2.6, RCP4.5, and RCP8.5 at a rate of 4.06%, 3.26%, and 3.67% increase, respectively for the period 2020-2080. Wubneh et al. (2022) showed impacts of climate change under RCP4.5 for the 2040s and 2070s in Gumara Catchment, with percentage increment of streamflow between 0.5% and 36.2% and 7.7% and 58.2 %, respectively. Fig 8 shows the gross irrigation requirement (GIR) of Gumara Catchment. GIR peaked twice during the irrigation season, the first was in December and January and the second in April, suggesting that farmers

grew crops twice during the irrigation season. For the current period, the GIR was estimated to be 29.7 Mm3 per irrigation season, comprising GIR values of 14.6 and 15.1 Mm3 for the gauged and ungauged parts of the Gumara Watershed. In the future, the GIR will be estimated to be 36.4 Mm3 per irrigation season, comprising GIR values of 15.61 and 20.77 Mm3 for the gauged and ungauged parts of the watershed.

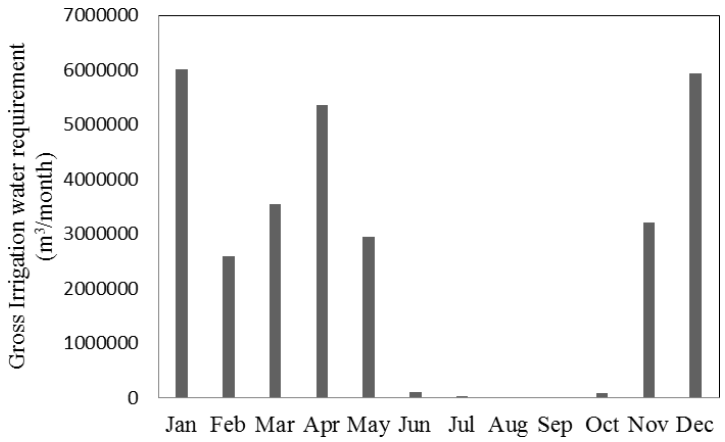

Figure 8. Monthly variation of the total Gross irrigation water requirement of Gumara Catchment

In current and future scenarios, there will be uneven distribution of water in the Gumara Watershed. This may lead to conflict betwe farmers having more water and those experiencing water shortage.. According to the supply-demand relationship analysis, most farmers demanded nodes in the middle of the watershed might have a positive relationship. This indicated the availability of sufficient irrigation water supply to meet the required water demand. However, unmet irrigation water demand existed at some demand nodes that diverted water from tributaries. Despite the surplus water in the middle of the watershed, farmers in this part of the watershed will still face water shortages in the future due to climate change. Similarly, climate change will worsen the water shortage problem for farmers who are receiving less water than they demand. In Gumara, many irrigation schemes were concentrated in small tributaries because farmers could more easily divert small streams than large ones. This could also relate to land suitability for irrigation. Furthermore, most negative supply-demand relationships (irrigation water scarcity) were observed downstream of the watershed. Fig 9 shows that the future period scenario will have more water stress compared to the current one because of the increase of

temperature that causes the rising of evapotranspiration in the catchment. Again, the rise in evapotranspiration can cause increase in irrigation crop water demand. If evapotranspiration increases in dry season, the water demand in various sectors also will increase. The other cause of water stress in Gumara Catchment was uncontrolled water withdrawal for irrigation. Farmers withdrew excess amount of water without any controlling and monitoring infrastructures. Owing to lack of awareness and organized rule and regulation, farmers in this area diverted unlimited amount of water day and night without considering the current and future water sectors' demand (environmental, domestic etc.). As a result, the supply-demand relationship of the catchment showed irrigation water abstraction was unbalanced with the supply for the entire watershed in both periods. When uncontrolled water withdrawal and climate change impact come together, the water stress will significantly increase for all water sectors and the unmet demand of irrigation land will expand widely in the catchment in the future.

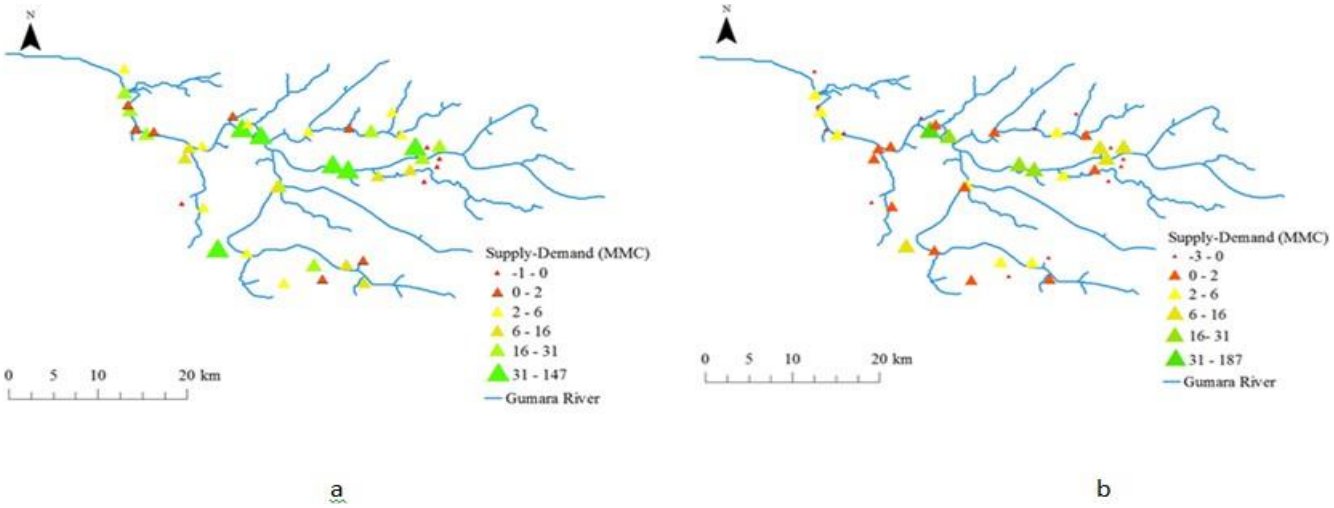

Figure 9 :- The current Supply-demand relationship (a) and future supply-demand relationship (b) of Gumara Catchment (MMC:- million meter cube)

5. Conclusion

In this study, we evaluated how climate change, irrigation, and LULC in the Lake Tana Subbasin are impacting the gap between water supply and demand. Our findings indicated that the Gumara Catchment experienced significant conversion of forest, bushland, and grassland into agricultural and residential areas.

There was a widespread irrigation near the lake shore and it was rapidly expanding to the upstream parts of the watersheds. Change in climate was manifested in the sub-basin through historical increasing temperatures with evidence of possible warming in the future. These changes had a potential impact on water availability and demand in the sub-basin.

In the study area, the increasing rate of evapotranspiration owing to rising of temperature was causing water shortages in the dry season, and it will likely exacerbate in the future. Besides, the significant increasing rate of rainfall in the wet season might cause floods in the sub-basin. Therefore, there was a strong need to investigate the role of various water storage mechanisms (small ponds, weir/dam. etc.) to store the excess rainfall in the wet season and supply to smallholder farmers in the dry season. Research should address the role of land management practices (soil and water conservation), and adaptive management of irrigation (monitoring, learning and continuously revising the irrigation management accordingly) to prevent the occurrence of conflict over water. Hence, we need to raise awareness from farm to basin administration office level.

Acknowledgements

This research is funded by the Future Leader – African Independent Research (FLAIR) fellowship programme (FLR\R1\201160 FLAIR Fellowships 2020). The FLAIR Fellowship Programme is a partnership between the African Academy of Sciences and the Royal Society funded by the UK Government's Global Challenges. The research was partially funded by Land and Water Solutions for Sustainable Intensification (LWS) of the CGIAR Research Program on Water, Land and Ecosystems (WLE). The authors acknowledge the Ministry of Water, Irrigation, and Energy and the Ethiopian Meteorological Institute (EMI) of Ethiopia for the provision of hydrological and climatic data. We also acknowledge the Abbay Basin Development Office for supporting the data collection of this study.

REFERENCES

1 ADSWE: LUPESP, 2015. Tana Sub-Basin Land Use Planning and Environmental Study Projects: Fisheries and Wetlands Resource Assessment. Bahir Dar, Ethiopia

2 Afera H., Ermias S., Tesfa W., Deepak K., Mihret D., Kannan N. 2018. Precipitation and Runoff Modelling in Megech Watershed, Tana Basin, Amhara Region of Ethiopia, American Journal of Environmental Engineering, Vol. 8 No. 3, pp. 45-53. doi: 10.5923/j.ajee.20180803.01.

3 Alemayehu, M. McCartney, S. Kebede.2010.The water resource implications of planned development in the Lake Tana catchment, Ethiopia.Ecohydrol. Hydrobiol., 10 , pp. 211-221

4 Alemayhu 2006 GIS Applications in Suitability Modelling for Livestock Production in Tana Subbasin-Blue Nile River Basin, Ethiopia. Master's Thesis, Addis Ababa, Ethiopia.

5 An M, Fan L, Huang J, Yang W, Wu H, Wang X, et al. (2021) The gap of water supply—Demand and its driving factors: From water footprint view in Huaihe River Basin. PLoS ONE 16(3): e0247604. https://doi.org/10.1371/journal.pone.0247604

6 Anteneh.M. 2017.Demographic Characteristics of the Lake Tana Basin. Social and Ecological System Dynamics.Springer,pp. 283-29

7 Asitatikie A. N. 2019. Land Use/Land Cover Dynamics in Upper Ribb Watershed, Lake Tana Sub Basin, Ethiopia. Research & Reviews: Journal of Ecology and Environmental Sciences. Volume 7 | Issue 3

8 Asres S.B. 2016. Evaluating and enhancing irrigation water management in the upper Blue Nile basin, Ethiopia: The case of Koga large scale irrigation scheme, Agricultural Water Management, Volume 170, Pages 26-35, ISSN 0378-3774,

9 Atanaw, Fasikaw M., Mamaru A. , Essayas D., Solomon T., Seifu & S., Tammo. 2018. Budgeting suspended sediment fluxes in tropical monsoonal watersheds with limited data: The Lake Tana basin. Journal of Hydrology and Hydromechanics. 66. 65-78. 10.1515/johh-2017-

0039.

10 Awulachew, S.B., Yilma, A.D., Loulseged, M., Loiskandl, W. , Ayana, M. , Alamirew, T. , 2007. Water Resources and Irrigation Development in Ethiopia. Colombo, Sri Lanka: International Water Management Institute. 78p. (Working Paper 123).

11 Biggs T.W., Thenkabail P.S., Gumma M.K., Scott C.A., Parthasaradhi G.R., Turral H.N. 2006. Irrigated area mapping in heterogeneous landscapes with MODIS time series ground truth and census data Krishna Basin India. Int. J. Remote Sens, 27, 4245–4266

12 Birara, H., Pandey, R. P., & Mishra, S. K. 2018. Trend and variability analysis of rainfall and temperature in the Tana basin region, Ethiopia. 555–569. https://doi.org/10.2166/wcc.2018.080

13 Birhanu K.T., Alamirew T., Olumana M.D., Ayalew S., Aklog D. 2015. Optimizing Cropping Pattern Using Chance Constraint Linear Programming for Koga Irrigation Dam, Ethiopia. Irrigat Drainage Sys Eng 4: 134. doi:10.4172/2168-9768.1000134

14 Breiman L. 2001. Random Forests Mach. Learn, 45, 5–32

15 Chakilu.G.G, Sándor.S., and Zoltán T. 2020.Change in stream flow of gumara watershed, upper blue nile basin, ethiopia under representative concentration pathway climate change scenarios.Water (Switz.), 12 (11) , pp. 1-14, 10.3390/w12113046

16 Chebud, Y.A. and Melesse, A.M. 2009. Modelling Lake Stage and Water Balance of Lake Tana, Ethiopia. Hydrological Processes, 23, 3534-3544.http://dx.doi.org/10.1002/hyp.7416

17 Cochran, W. G. 1953. *Sampling techniques.* John Wiley

18 Cohen J. 1960. A Coefficient of Agreement for Nominal Scales. Educational and Psychological Measurement. 20(1):37-46. doi:10.1177/001316446002000104

19 CSA. 2008. The 2007 population and housing census of Ethiopia for Amhara Region. Central Statistics Authority, Addis Ababa

20 de Fraiture, C., Molden, D., Amarasinghe, U., Makin, I., 2001. PODIUM: projecting water supply and demand for food production in 2025. Phys. Chem. Earth - Part B Hydrol. Oceans Atmos. 26, 869–876.

21 Desalegn, A., Demissie, S., & Admassu, S. 2016. Extreme Weather and Flood Forecasting and Modelling for Eastern Tana Sub Basin, Upper Blue Nile Basin, Ethiopia. Journal of Waste Water Treatment & Analysis, 7(3). https://doi.org/10.4172/2157-7587.1000257

22 Desta H, Lemma B. 2017.SWAT based hydrological assessment and characterization of Lake Ziway sub-watersheds. Ethiopia J Hydrol Reg Stud 13:122–137. https://doi.org/10.1016/j.ejrh.2017.08.002

23 Dile Y.T, Berndtsson R., Setegn S.G. 2013. Hydrological Response to Climate Change for Gilgel Abay River, in the Lake Tana Basin - Upper BlueNile Basin of Ethiopia. PLoS ONE 8(10): e79296. doi:10.1371/journal.pone.0079296

24 Elhamid A. M. I. Abd, Rasha H. A. Monem & M. M. Aly. 2019. Evaluation of Agriculture Development Projects status in Lake Tana Sub-basin applying Remote Sensing Technique, Water Science, 33:1, 128-141, DOI: 10.1080/11104929.2019.1688067

25 Enyew, B., van Lanen, H., & van Loon, A. 2014. Assessment of the Impact of Climate Change on Hydrological Drought in Lake Tana Catchment, Blue Nile Basin, Ethiopia. J Geol Geosc. https://doi.org/10.4172/2329-6755.1000174

26 Fetene, Z. A., Weldegerima, T. M., Zeleke, T. T., & Nigussie, M. 2018. Harmonic Analysis of Precipitation Time Series in Lake Tana Basin, Ethiopia. Advances in Meteorology, 2018. https://doi.org/10.1155/2018/1598195

27 Funk, C. C., A. Verdin, J. Michaelsen, P. Peterson, D. Pedreros, andG. Husak. 2015. "A global satellite-assisted rainfall climatology."Earth Syst. Sci. Data 7 (2): 275–287. https://doi.org/10.5194/essd-7-275-2015

28 Funk, C. C., P. J. Peterson, M. F. Landsfeld, D. H. Pedreros, J. P. Verdin,J. D. Rowland, B. E. Romero, G. J. Husak, J. C. Michaelsen, andA. P. Verdin. 2014. A quasi-global rainfall time

series for droughtmonitoring. Washington, DC: USGS.

29 Funk, C., P. Peterson, S. Peterson, S. Shukla, F. Davenport, J. Michaelsen, K.R. Knapp, M. Landsfeld, G. Husak, L. Harrison, J. Rowland, M. Budde, A. Meiburg, T. Dinku, D. Pedreros, and N. Mata, 2019: A High-Resolution 1983–2016 Tmax Climate Data Record Based on Infrared Temperatures and Stations by the Climate Hazard Center. J. Climate, 32, 5639–5658, https://journals.ametsoc.org/doi/pdf/10.1175/JCLI-D-18-0698.1

30 Gashaw T., Tulu T., Argaw M., Abeyou W. 2017. Evaluation and prediction of land use/land cover changes in the Andassa watershed Blue Nile Basin Ethiopia. Environ Syst Res 6 17

31 Gashaw, Temesgen T., Taffa A., Mekuria W., and Abeyou. 2017. Evaluation and prediction of land use/land cover changes in the Andassa watershed, Blue Nile Basin, Ethiopia. Environmental Systems Research. 6. 10.1186/s40068-017-0094-5.

32 Gebremicael. T.G. , Mohamed Y.A. , Betrie G.D. Van der Zaag, P. , Teferi, E. 2013. Trend analysis of runoff and sediment fluxes in the Upper Blue Nile basin: A combined analysis of statistical tests, physically-based models and landuse maps.J. Hydrol., 482, pp. 57-68

33 Getachew, B., & Manjunatha, B. R. 2021. Climate change projections and trends simulated from the CMIP5 models for the Lake Tana sub-basin, the Upper Blue Nile (Abay) River Basin, Ethiopia. Environmental Challenges, 5(November). https://doi.org/10.1016/j.envc.2021.100385

34 Goshu, G., Aynalem, S. 2017. Problem Overview of the Lake Tana Basin. In: Stave, K., Goshu, G., Aynalem, S. (eds) Social and Ecological System Dynamics. AESS Interdisciplinary Environmental Studies and Sciences Series. Springer, Cham. https://doi.org/10.1007/978-3-319-45755-0_2

35 Haile, A. T., Rientjes, T., Gieske, A., & Gebremichael, M. 2009. Rainfall variability over mountainous and adjacent . https://doi.org/10.32388/EOKAWN 14/16 lake areas: The case of Lake Tana basin at the source of the Blue Nile River. Journal of Applied Meteorology and Climatology, 48(8), 1696–1717. https://doi.org/10.1175/2009JAMC2092.1

36 Inglada J, Vincent A, Arias M, Tardy B, Morin D, Rodes I. 2017. Operational High Resolution Land Cover Map Production at the Country Scale Using Satellite Image Time Series. Remote Sens. 9 95

37 Kebede, Travi, Y., Alemayehu, T., & Marc, V., 2006. Water balance of Lake Tana and its sensitivity to fluctuations in rainfall, Blue Nile basin, Ethiopia. Journal of Hydrology, 316(1-4), 233-247. http://dx.doi.org/10.1016/j.jhydrol.2005.05.011

38 Li R., Xu M., Chen Z., Gao B., Cai J., Shen F., He X., Zhuang Y., Chen D. 2021.Phenology-based classification of crop species and rotation types using fused MODIS and Landsat data: The comparison of a random-forest-based model and a decision-rule-based model. Soil and Tillage Research, 206(October 2020), 104838. https://doi.org/10.1016/j.still.2020.104838

39 Malede, Demelash .A, Tena .K, Job A.,and Tesfa. 2022. Analysis of land use/land cover change trends over Birr River Watershed, Abbay Basin, Ethiopia. Environmental and Sustainability Indicators. 17. 100222. 10.1016/j.indic.2022.100222

40 Mengistu, D., Bewket, W., & Lal, R. 2014. Recent spatiotemporal temperature and rainfall variability and trends over the Upper Blue Nile River Basin, Ethiopia. International Journal of Climatology, 34(7), 2278–2292. https://doi.org/10.1002/JOC.3837

41 Mequanent.D,and Mingist.M. 2019.Potential impact and mitigation measures of pump irrigation projects on Lake Tana and its environs, Ethiopia.Heliyon, 5, Article e03052

42 Mohamed, M. A.-H., & Mahdy, M. E.-S. 2021. Evaluation of climate change impact on extreme temperature variability in the Blue Nile Basin, Ethiopia. Geoscientific Instrumentation, Methods and Data Systems, 10(1), 45–54. https://doi.org/10.5194/gi-10-45-2021

43 Monserud R.A. 1990. Methods for comparing global vegetation maps, Report WP-90-40. IIASA, Laxenburg

44 Rientjes T.H, Perera B.U, Haile A.T, Reggiani P., Muthuwatta L.P.2011. Regionalisation for lake level simulation–the case of Lake Tana in the Upper Blue Nile, Ethiopia. Hydrol Earth

Syst Sci. ;15(4):1167-1183.

45 Rodriguez-Galiano V.F., Ghimire B., Rogan J., Chica-Olmo M., Rigol-Sanchez J.P. 2012. An assessment of the effectiveness of a random forest classifier for land-cover classification. ISPRS J. Photogramm. Remote Sens. 67 93–104

46 Setegn, S. G., Srinivasan, R., Dargahi, B., & Melesse, A. M. 2009. Spatial delineation of soil erosion vulnerability in the Lake Tana Basin, Ethiopia. Hydrological Processes, 23(26), 3738–3750. https://doi.org/10.1002/HYP.7476

47 Sewnet A., Kameswara K.R. 2011. Hydrological dynamics and human impact on ecosystems of Lake Tana, Northwestern, Ethiopia doi:10.4314/ejesm.v4i1.7

48 Shaka A. K. 2008. Assessment of climate change impacts on the hydrology of gilgel Abbay catchment in Lake Tana basin, Ethiopia. ITC. PhD Thesis. https://webapps.itc.utwente.nl/librarywww/papers_2008/msc/wrem/abdo.pdf

49 Shetty, V. K. 2019. Impact of Supply Chain Management Practices on Performance of Companies. Journal of Supply Chain Management Systems, 8, 3.

50 SMEC. 2008. Hydrological Study of the Tana-Beles sub-basins, main report. Ministry of Water Resource, Ethiopia

51 Taye M.A. 2021. Agro–ecosystem sensitivity to climate change over the Ethiopian highlands in a watershed of Lake Tana sub–basin, Heliyon,Volume 7, Issue 7,e07454,ISSN 2405-8440,https://doi.org/10.1016/j.heliyon.2021.e07454.

52 Taye, M., & Haile, A. 2022. Consequences of uncontrolled irrigation water withdrawals in Lake Tana sub-basin Water Science Policy, 3(5). doi: https://dx.doi.org/10.53014/FBYI9408

53 Teklay A., Dile Y.T., Asfaw D.H., Bayabil H.K., Sisay K. 2021.Impacts of climate and land use change on hydrological response in Gumara Watershed, Ethiopia. Ecohydrol Hydrobiol. 21(2):315-332

54 Tesemma Z.K. , Mohamed Y.A. , Steenhuis T.S. 2010).Trends in rainfall and runoff in the

Blue Nile Basin: 1964–2003Hydrol. Process., 24 (25) , pp. 3747-3758

55 Tesfaw.B.A., Dzwairo.B.,and Sahlu.D. 2023. Assessments of the impacts of land use/land cover change on water resources: Tana Sub-Basin, Ethiopia. Journal of Water and Climate Change 14 (2): 421–441.https://doi.org/10.2166/wcc.2023.303

56 Tewabe D. & Fentahun T. 2020 Assessing land use and land cover change detection using remote sensing in the Lake Tana Basin, Northwest Ethiopia. Cogent Environmental Science 6 (1), 1778998. https://doi.org/10.1080/23311843.2020.1778998.

57 Uhlenbrook S, Mohamed Y, Gragne A.S 2010. Analyzing catchment behavior through catchmentmodeling in the Gilgel Abay, Upper Blue Nile River Basin, Ethiopia. Hydrol Earth Syst Sci14:2153–2165

58 Ulsido, Mihret A., Ermias. (2014). Irrigation Water Management in Small Scale Irrigation Schemes: the Case of the Ethiopian Rift Valley Lake Basin. Environmental Research, Engineering and Management. 67. 10.5755/j01.erem.67.1.6240.

59 Velpuri, M., Thenkabail, P. S., Gumma, M. K., Biradar, C. B., Dheeravath, V., Noojipady, P. and Yuanjie, L. 2009. "Influence of resolution or scale in irrigated area mapping and area estimations.". In *Photogrammetric Engineering and Remote Sensing* accepted, in press

60 Woldesenbet T. A., Elagib N. A., Ribbe L. & Heinrich J. 2017 Hydrological responses to land use/cover changes in the source region of the Upper Blue Nile Basin, Ethiopia. Science of the Total Environment 575, 724–741. https://doi.org/10.1016/j.scitotenv.2016.09.124.

61 Yenehun.A, Dessie.M, Azeze.M, Nigate.F, Belay.A.S, Nyssen.J, Adgo.E, Van Griensven.A, Van Camp.M, Walraevens. K 2021.Water resources studies in headwaters of the blue nile basin: a review with emphasis on lake water balance and hydrogeological characterization.Water, 13, p. 1469

Ethiopian Journal of Water Science and Technology (EJWST)

DOI: https://doi.org/10.59122/1551910

Vol. 5 , 2022, pages: 102~141 ISSN(Print): 2220-7643

Evaluation of Hydrometeorological Characteristics in Northern Ethiopia, Gerado Catchment

[1]Amare Gebre Medhin Nigusse . [1]AbdulAziz Hussien, [2] Destalem Niguse, [3]Equbay Gebre Medhin, [1]Gebrerufael Hailu , [4]Tesfalem Gebre, [5]Desta Leuel, [2]Abrhaley Teklay

[1]Institute of Geo-information and Earth Observation Sciences, Department of Geo-information and Earth Observation Sciences for Natural Resource Management, [2]School of Computing Science, EiTM, [3]Tigray Bureau of Agriculture, [4]Institute of Water and Environment, [5]Institute of Pedagogical Science (IPS)
Mekelle University, P.O. Box 231, Mekelle, Ethiopia
**Corresponding Email Address: gerenigusse@gmail.com*

ABSTRACT

In the northern Ethiopia, land degradation together with population pressure have resulted in high surface runoff, low groundwater recharge and high evapotranspiration. All together combined become very serious challenge to agricultural production and economic growth in the region. Understanding the characteristics and dynamics of hydro-meteorological variables is important in water resources development projects that have direct impact on agricultural production. The present study was carried out to evaluate hydro-meteorological characteristics in northern Ethiopia, Gerado catchment. Long term meteorological data such as precipitation, temperature, sunshine, and other climatic factors were collected from existing meteorological stations. Thornthwaite Empirical Equation and Thornthwaite Soil Water Balance models were employed to estimate potential and actual evapotranspiration. The approach used air temperature as an index of energy available for evapotranspiration. Similarly, groundwater recharge of the area catchment was computed as a difference between outflow and change in water storage. The runoff of the area was estimated based on the rainfall coefficient, annual precipitation and aerial coverage. On the other hand, groundwater potential (GWP) of the area was mapped based on selected spatial factors. The result indicated that the annual potential and actual evapotranspiration of the catchment were was found to be 755 mm/year and 723 mm/year, respectively. The actual evapotranspiration was evaluated and weighted based on the dominant soil textures, depth root soil, and the respective land uses. As result, high evapotranspiration was observed in moderate deep rooted cereal crops and sandy loam soil texture which accounted for 48.5% of influence. But, cereal crops with moderate deep rooted and clay loam type had lower AET (42.2%). Because of the absence of gauging stations in the catchment, the volume runoff was computed using the runoff coefficient method. Accordingly, surface runoff from the catchment was calculated to be 120,581,841 cubic meter (m^3) or 326 mm. per year. However, the groundwater recharge of the area was found to be 52,208,159.5 cubic meter (141.5mm/year). Thus, out of the given mean annual precipitation, 27.6%, 12% , and 60.4% of the mean annual

rainfall lost because of runoff, groundwater recharge, and evapotranspiration, respectively. Regarding GWP, the most determinant factors affecting groundwater mapping potential were suitability mapping, lithology, liniment density, and geomorphology. . The suitable GWP areas were located within lithology and geomorphology classes. Moreover, areas with flat slope and low lineament density lay in most rich groundwater areas. In general, although the study area had high amount of annual rainfall, most of it was lost in the form of evapotranspiration and thus little amount of water was recharged. Eventually, installation of metrological stations in appropriate sites was recommended for all-inclusive and consistent data availability.

Keywords: Hydro-meteorological, Gerdo Catchment, groundwater recharge, runoff, evapotranspiration, GWP

Received: 08 Oct 2022; accepted 06 December.2022

1. INTRODUCTION

Land degradation in the form of soil erosion increases runoff, evapotranspiration, and low groundwater recharge which are serious environmental problems having negative impact on agricultural productivity and economic growth in Ethiopia. High population pressures densities, climatic change impact variability, and improper utilization of land resource are the major causes of such problems (Nyssen, 2005 and Nyssen, 2011). These, in turn, have resulted in declining of agricultural productivity, water scarcity, and persistent food insecurity. On the other hand, water resources demand grows up in order to enhance agricultural and industrial developments, create incomes, and reduce poverty of rural people. This problem is more conspicuous in least developed countries whose livelihood depends on rainfall agriculture. In these regions, most of the rain goes in the form of runoff which causes low groundwater recharge. Runoff is part of the rainfall not interrupted by vegetation but reaches on the surface of earth and flows overland into streams, lakes or and oceans (Horton, 2003). And this has a direct impact on agricultural production. Updated reliable information on the spatio-temporal variation of runoff / the aforementioned parameters are at a watershed level essential to understand its impact on watershed hydrology and monitoring of water resources. Thus, estimating surface runoff, evapotranspiration, and groundwater recharge are essential for water resources development projects (Rolland and Rangarajan, 2012; Fan et al., 2013). There are conventional techniques for runoff measurements but in most situations such techniques are very costly, time consuming, and difficult in areas of inaccessible terrains. Thus, the use of rainfall runoff model is the most commonly used approach in hydrological modeling.

In most arid and semi-arid regions where there is limited hydro-climatological data, runoff estimation modeling approach is given due emphasis (Ai-Ahmadi, 2005). It is used to estimate how much rainfall changes transform to runoffs (Jenicek, 2007). Understanding and modeling rainfall transformation into runoff is difficult and dynamic since it exhibits temporal and spatial variabilities. It has a comprehensive range of applications that include modeling of gauged catchments like flood forecasting and evaluation of water resource management. Runoff estimation of un-gauged catchments and estimation soil erosion are essential input components for water resource development projects (Džubáková, 2010). It is known that rainfall is the main sources of surface runoff although it is rare and uncommon practice to find documented rainfall particularly in developing countries like Ethiopia (Gedefaw, 2020). Studies have shown that there is a direct relationship between rainfall and surface runoff. Hydrological parameters such as rainfall, groundwater recharge, evapotranspiration, and runoff vary in space and time (Suryawanshi, et al., 2012) because of different factors. The rainfall-runoff relationship is one of the most complex hydrological spectacles to apprehend because of the tremendous spatial and temporal variability (Josh and Patel, 2011). Scholars have developed several equations to make this prediction. Of these, rational method is the simplest one. In other words, evapotranspiration process if other key factor in relation to runoff. When it rains, most of the rain water goes back to the atmosphere through evaporation and transpiration. It can be affected by different biological and physical factors. The actual and potential evapotranspiration are the most important terms used in hydrology and those can be estimated calculated using different techniques.

The other variable of hydro-metrological in relation to runoff is groundwater recharge, which is mainly controlled by land use land cover, soil texture type, and geological features. Understanding the groundwater recharge variability at a given watershed level has its own impacts on monitoring and efficiently using water resources for sustainable development. Nowadays, Geographic Information System (GIS) based hydrological modeling plays a great role in exploring, identifying, and managing groundwater resources in areas where there is scarcity of water. Hence, estimating and mapping groundwater recharge at a catchment or basin level is very essential for wise utilization of the resource. Groundwater recharge is the vertical

movement of water into saturated zone of the earth surface; it percolates through the pores of the land surface. On the other hand, precipitation is the most important driving parameter in groundwater recharge process. It is also the most significant factor driving force in hydrological cycle and it can percolate into the groundwater through groundwater recharge system. But, when it rains, it changes into runoff and whose intensity and amount are affected by different features as stated above. And this has direct impact on groundwater recharge and occurrence. Groundwater recharge can be appraised by using a number of methods which depend on the availability of data and level of accuracy.

Groundwater delineation investigation and mapping is another essential hydrological variable. The existing conventional methods of mapping groundwater potential sites using in situ approaches are expensive and time consuming. Recently, the introduction of geospatial technologies to delineate groundwater make the task speedy, easy and cost effective. It has the capability to capture, merge, and integrate the remote sensing satellite data together with the in-situ field data. brings to one system of modeling. These methods significantly reduce the failure of drilling groundwater projects and thus areadopted by many users. Nowadays, Remote Sensing and Geographic Information Systems (RS and GIS) has emerged as an effective tool methods for handling huge spatial data and decision making in several field of studies. Geospatial technologies (GIS and Remote Sensing) are very important tools which have invaluable importance to map, identify, delineate, and evaluate groundwater potential by considering significant factors such as geology and topography (Syed & Satapathy, 2015; Liu et al., 2015). Moreover, Khan, et al., (2017) noted that, these methods as compare to conventional methods have the competency to accurately map the controlling parameters, integrate and model the potential suitable sites of groundwater. Therefore, assessing, investigating, and delineating groundwater potential zones through these techniques has immeasurable advantage over conventional methods.

All the aforementioned hydrometrological elements have a great impact on hydrology and agriculture in particular and economy of a given region in general. The nature, distribution, and variabilities (i.e. spatial and temporal) of these environmental and climatic factors are not well understood. This was due to lack of ground based supported stations and incompleteness of

data. However, all these environmental factors are caused by land degradation. and this that are more pragmatic in northern Ethiopia. According to Derege (2012) & Abdulaziz et al. (2016) because of land degradation, most of the rainfall was lost as runoff and evapotranspiration which resulted in poor groundwater recharge in the northern Ethiopia particularly in Gerado Catchment. In general, such environmental elements have a direct impact on food security, drought, and flood in the study area. However, studies have not been carried out so far on this topic. Therefore, the present study was carried out with the aim of evaluating and understanding the different hydrometeorological characteristics (runoff, evapotranspiration, groundwater recharge and groundwater potential) in Northern Ethiopia, Gerado Catchment.

1.1 Description of the Study Area

The study area, Gerado catchment is located in the North East of Ethiopia that covers a total area of 372 km^2. The average elevation of the catchment ranges from 1965m to 3552m above mean sea level and bounded within 552428 to 572576 E and 1210451 to 1243825 N (UTM/ADINDAN) respectively. Figure 1 is the map of the study area derived from digital elevation model (DEM) with spatial resolution 30m*30m. The general topography of the catchment is characterized by undulating hills, plane, and valley. It gradually decreases its elevation to the north and north-west directions. Numerous narrow and shallow river valleys originate from the mountains, and merge to form Gerado Perennial River. Intermittent rivers like Kelina, Yito and Negeweli are among the main tributaries of Gerado River which flows to Beshlo River, the main tributary of the Blue Nile River (Abdulaziz et al., 2016).

Table 1 Agro-climatic zone of the study area

Altitude (m)	Temperature	Classification	Local name
Below 500	25 and above	Hot	Bereha
500-1500	20-25	Hot temperature	Kola
1500-2300	15-20	Temperate	Woina dega
2300-3300	10-15	Cool temperate	Dega
3300 and above	10 or less	Cool	Kur

Source: Ethiopian Metrological Institute (EMI, 20008)

The characteristics, types, and distribution of soil for a certain area depends on geomorphology (landscape), geology, and the type of land use activity. The dominant soil type of the study area is classified into clay, sandy cay, and rocky. Clay soil covers 43.2 km^2 which is approximately 11.68% of the catchment. It is highly exposed to the left side of the river along the flat and gentle to flat. Such type of soil is mostly covered with cereal crops. . Sandy clay is the other type of soil that covers 50.1 km^2 which accounts for 13.54% of the catchment. More than 74% of the study area is covered by rocky soil type that covers 276.7km^2 of the catchment. Such soil coverage is highly vulnerable along the steeper part of the catchment. This rocky soil is especially available at the steeper part of the catchment covered with shrubs and plantations like eucalyptus and cereal crops. In line with FAO's soil classification, the dominant soil type in the study area include: cambisols, lithosols, and rock surface (Abdul Aziz et al., 2016).

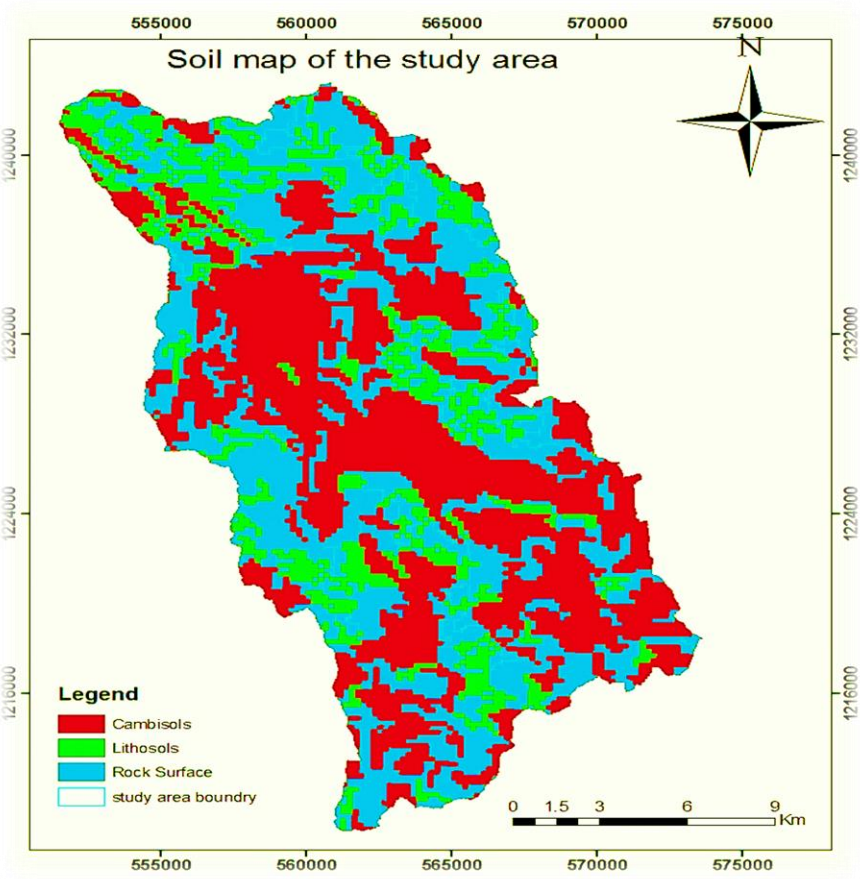

Figure 1 Soil map of the study area

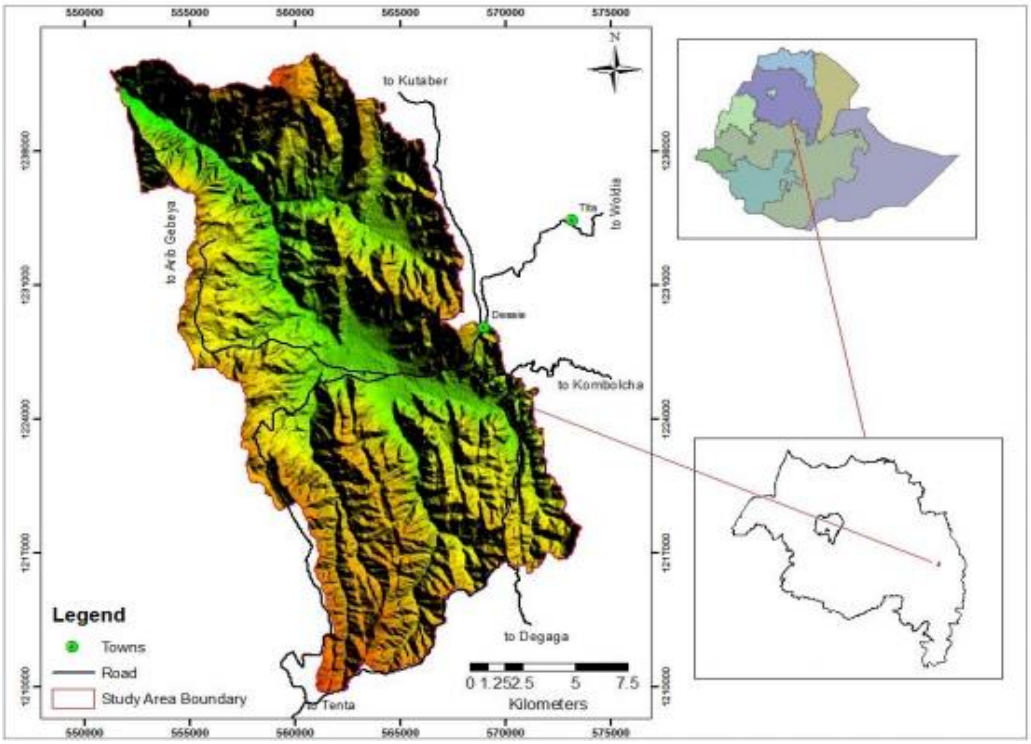

Figure 2 Location of the study area

Volcanic rocks and alluvial deposits form the main geological units of the study area. . The volcanic rocks having tertiary age covered 78.8% of the area ranging from lower basalt to Aiba basalt. On the other hand, alluvial deposits of quaternary covered 21.2% of the study area. Major and inferred faults, fractures, and lineament having an alignment of N-S, NNW-SSE, NW-SE, NNE-SSW, and NE-SW were observed. Moreover, two hydro-stratigraphic units were noticed during the hydro-geological investigations. Alluvial deposits having inter granular porosity and permeability could be found along the flat and gentle slope consisting of clay and silt. Similarly, volcanic unit also comprised highly fractured, unweather basalt, and ignimbrite. Though the fracturing and weathering rate of these formations was prominent due to topographic locations, the volcanic units were characterized by negligible groundwater potential. Gerado River Catchment is situated in the Ethiopian highland plateau adjoining the western escarpment of the Rift Valley and the Abay River Basin (Abdul Aziz etal, 2016).

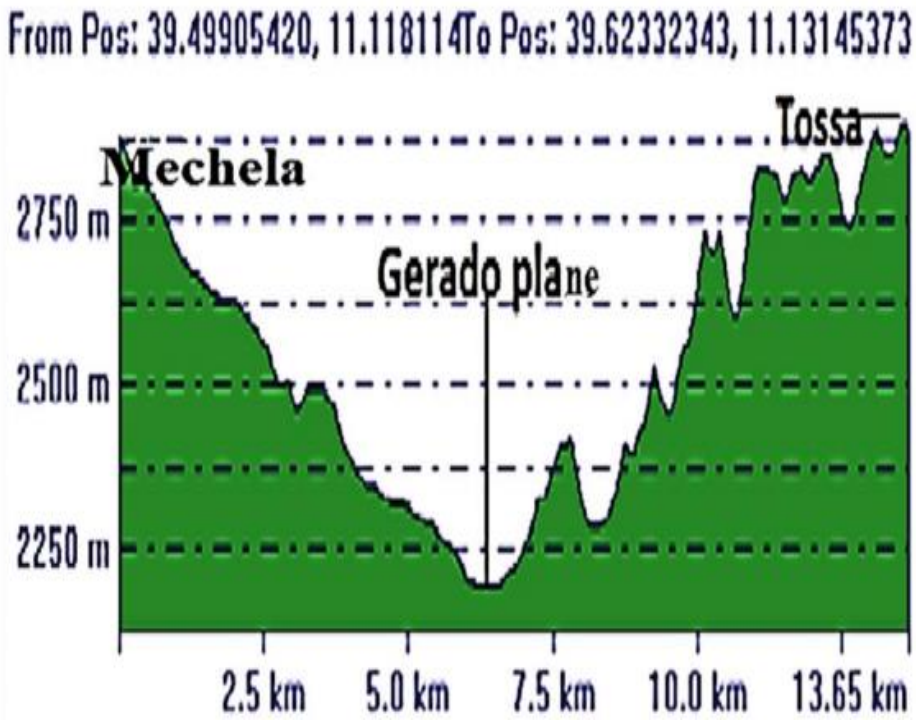

Figure 3 Cross-section of the study area (E-W) (Derege, 2012)

2. RESEARCH METHODOLOGY

Long term meteorological data such as precipitation, temperature, relative humidity, and sunshine hours were the most essential input data employed for this study. Those data were collected from Ethiopian Meteorological Institute (EMI) branch office (Kombolcha and Dessie) as presented in table 2. Once the data were collected, data completeness and quality were checked up. Determination of water balance in a certain catchment is based on hydro-meteorological data so as to use the resource effectively in water resource management. To determine the water balance of the study area, important long term meteorological data were collected from Kombolcha Meteorological Station. The meteorological stations within and around the study area were presented in table 2 below. These data were taken from the stations based on their availability.

Table 2 Meteorological stations of the study area

No.	Stations	Location (UTM)/ADINDAN			Recording periods(years)	
		Easting	*Northing*	*Elevation*		
1	Dessie	569342	1231348	2400	1990-2010	*
2	Guguftu	553039	1203569	3450	1990-2010	**
3	Albuko	569855	1194487	2482	2006-2010	*
4	Kutaber	558212	1245405	2600	1990-2010	*
5	Kombolcha	576448	1227015	1825	1985-2007	**
6	Tita	573693	1233807	2480	2001-2006	**

* Records of rainfall only ** Records of rainfall and temperature

Since rainfall measurement is a point observation, it may not provide a representative value for the area under consideration. To get more reliable and representative result, it is essential to obtain an effective uniform depth of rainfall of the catchment. Hence, the rainfall of the catchment was computed using different interpolation techniques such as arithmetic mean, isohyetal, and thiessen polygon interpolation. . Hence, data were collected from six meteorological stations around the study area. The rainfall coefficient method was used to compute the monthly distribution of rainfall and discriminate between rainy and dry months. The rainfall coefficient method becomes complicated while calculating the rainfall of each month. Usually, it should be the ratio between the mean monthly rainfall and one-twelfth of the annual mean rainfall. However, the thornthwaite empirical formula was adopted to calculate the potential evapotranspiration for the study area as in equation (1). This method uses air temperature as an index of energy available for evapotranspiration, assuming that air temperature is correlated with net radiation and evapotranspiration. Thus, the available energy is shared in fixed proportion between heating the atmosphere and evapotranspiration (Dunne and Leopold, 1978). For this purpose, we adopted the thornthwaite empirical equation as shown below: -

$$PETm = 16Nm\,(10TI\,m)a \qquad 1$$

Where PET is potential evapotranspiration in mm/month,

m is the months 1, 2, 3…….12

Nm is the monthly adjustment factor related to hours of daylight

It is found from standard table by dividing possible sunshine hours for the appropriate latitude (100 N) of the study area (Gerado river catchment) by twelve months. Tm, is the monthly mean temperature in ^{0}C, I is the heat index for the year.

To calculate the actual evapotranspiration, the thornthwaite soil water balance model was used. The required parameters to determine actual evapotranspiration are mean monthly precipitation and potential evapotranspiration. Moreover, water holding capacity of the dominant soil texture and monthly soil moisture storage are also determinant factors. Furthermore, to evaluate and check for the shortage or addition of moisture to the soil, the difference between precipitation and potential evapotranspiration was calculated and presented as in equation (1) below. Hence, positive values indicate the addition of moisture to the soil whereas negative values imply monthly demand of moisture by vegetation not satisfied by the monthly rainfall. The accumulated potential water loss that was calculated by cumulating the negative values of the differences between monthly precipitation and evapotranspiration and used to estimate calculate the soil moisture for the dry months.

$$SM = W * exp(-APWLW) \quad 2$$

Where, SM, is the Soil moisture during the month m (mm),

APWL, is the accumulated potential water loss and

W, is the available water capacity of the root zone (mm).

The soil moisture surplus which is in excess of soil moisture values (Sm) especially in wet season is calculated using the equation (3) as follow

$$\mathrm{Sm} = \mathrm{P} - \mathrm{AET} + \Delta\mathrm{Sm} \quad 3$$

The actual evapotranspiration (AET) for the dominant soil types and the respective land use is weighted according to the proportion of the area it represents. The actual evapotranspiration, AET, for the dominant soil types and the respective land use in the area was weighted according to the proportion of the area it represented as given here:

$$AWTw = \frac{\sum(AETi)ai}{iAt} \quad 4$$

Where $AET_{w,}$ is weighted actual evapotranspiration

AETi, is actual evapotranspiration of the dominant soil

ai, is area of each soil

At, is total area of soil coverage

Runoff takes place when the rainfall not fully infiltrated forms a flow as a thin sheet across the land surface. (Tenalem and Tamiru, 2001). In the study area, there was no river with gauged hydro-meteaorological stations; so, it was difficult to determine the runoff generation of the catchment. The volume of runoff from the catchment was also computed using the runoff coefficient method as given in equation (5) below:

$$Q = K.P.A \quad 5$$

Where: Q, is run off in m^3

K, is a constant also called runoff coefficient;

P, is precipitation (mm): and

A, is area of the catchment (m^2)

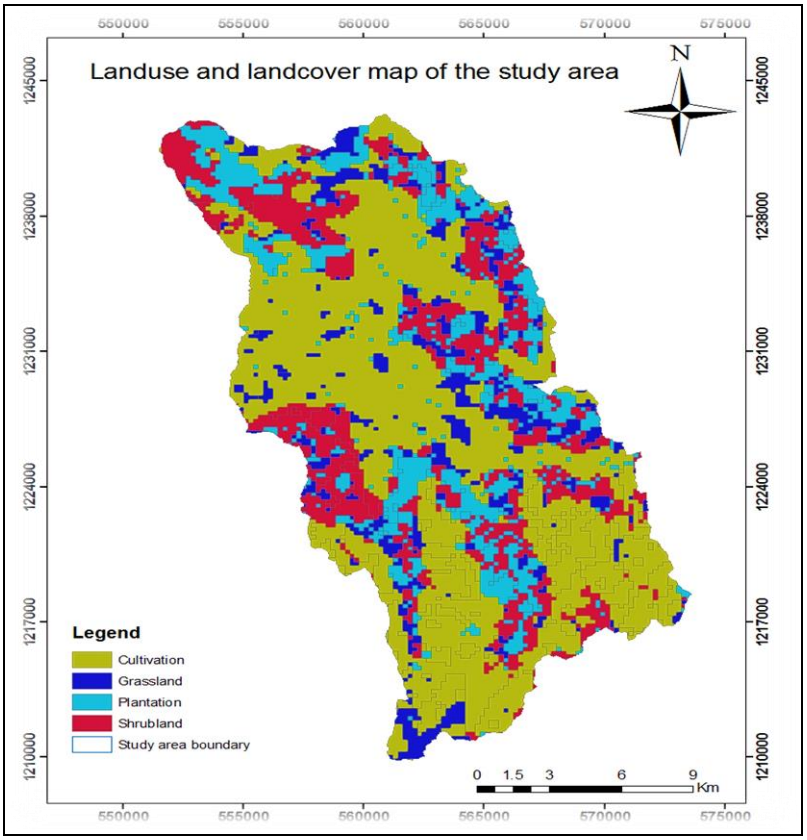

Figure 4 Soil map of the area

On the other hand, groundwater recharge flows to saturated zone as a precipitation that infiltrates into soil to a depth below the root zoned of surface vegetation where it cannot be removed by evaporation (Tesfaye, 2015). It is the downward flow of water reaching the water table, forming an addition to the groundwater reservoir (Lerner et al., 1990). Different techniques of recharge estimation have been widely applied under various climatic and hydrogeological conditions all over the world. Groundwater recharge estimation using hydrograph separation, isotopic tracers (stable isotopes of oxygen and hydrogen), lysimeters, soil moisture technique, mixing-cell models (compartment models, lumped models and black box models) and tracer techniques have been extensively experimented and used by many workers in different parts of the world. Three independent methods were used for comparative evaluation of recharge methods in the small watersheds in the rain forest belt of Nigeria. The methods included recharge estimation using water level and porosity, base flow recession analysis, and water balance method. The results showed that groundwater recharge obtained from water balance method was constantly higher than values from other methods. So, , groundwater recharge estimation of the study area was computed using water balance method formula as in equation 6:

$$Inflow = outflow \pm change\ storage \quad 6$$

$$P + Gi = AET + SRQ + R + Go \pm \Delta S$$

Where, P – annual precipitation

AET- actual evapotranspiration

ΔS - Change in water storage

Go - Groundwater out flow

Gi - Groundwater inflow

SRO – annual surface runoff

Investigation of groundwater potential site is complicated because of the lack of common understanding of the several environmental, climatic, and topographical factors (Lentswe & Molwalefhe, 2020; Makonyo & Msabi, 2022). Moreover, demarcation of potential areas demanded evaluating many spatial factors based on scientific methods (Malczewski & Rinner,

2015). Most previous groundwater investigations had applied conventional techniques based on geophysics, geology, and hydrogeology. However, the recent introduction of geospatial technologies to water resource ^ makes it very effective and constant. For the present study, groundwater potential map of the area was developed by integrating geology, geomorphology, LULC, slope, soil, drainage, lineament density, and rainfall raster layers to one system modeling. Each layer was given a rank and weight based on their importance for groundwater occurrence. The procedure followed was based on multiplication of each factor's raster map with given factors weight which is generated in multi criteria decision analysis based analytical hieratical process and spatial analysis.

3. RESULT AND DISCUSSION

3.1 Annual Rainfall Estimation:

Good understanding of the nature and characteristics of rainfall helps to conceptualize and predict its effects on runoff generation and evapotranspiration. Knowing the nature, amount, and aerial distribution of rainfall characteristics is also essential for hydrological modeling analysis. It is a significant hydrological factor and its duration and magnitude are the main cause of groundwater recharge (Champak and Dinesh, 2018). According to Tesfaye (2015), we can hypothesize and estimate its effects on runoff, infiltration, and evapotranspiration. Therefore, for better rainfall analysis, it is important to know its areal distribution and coverage. Since rainfall measurement is a point observation, it might not represent the area under consideration. In such situations, it is essential to obtain a more reliable and representative rainfall of the catchment. In the current study, simple arithmetic mean, isohyetal, and thiessen polygon interpolation methods were used to estimate the rainfall.. However, the selection of appropriate interpolation methods depends normally on the density of gauging stations, the nature of the area, the objective of the study, and the availability of time (FAO, 1997).

Arithmetic mean interpolation: This method was used to determine the mean monthly rainfall of the study area. In the study site, there were five meteorological stations: Dessie, Albuko,

Guguftu, Kombolcha, and Kutaber. Arithmetic mean rainfall was computed using the interpolation technique as given below:

$$P = P^1 + P^2 + P^3 \pm \quad +Pn/n \qquad 7$$

Where --P is the average depth of precipitation of the area, P1, P2, P3

Pn are the rainfall records at the stations 1, 2, 3 etc.

and n is the number of meteorological stations.

Hence, the mean annual rainfall of the catchment was 1251.37 mm. (table 3). Similarly, other studies in Abay Basin indicated that the annual depth rainfall was 1373.3 mm (Tesfa, et al, 2021). The highest mean monthly rainfall of the area was recorded in July, August, and September. However, the lowest mean monthly precipitation was recorded from November to January. According to Daniel (1977), the study area had two rainfall regimes (a bimodal rainfall characteristics). From March to April (Belg Season), the area got a small rainfall of 11%. While the area had annual rainfall of 70% in July, August, and September. and the rainfall in the rest of the months amounted to 18% (table 3).

Thiessen polygon interpolation: This interpolation method determines areal depth of precipitation assuming any point in the area under consideration and the rainfall the same as the nearest gauge. So, the depth recorded at a given gauge is applied to a distance halfway to the next station in any direction. The relative weights for each gauge were determined by the corresponding areas created in a thiessen polygon network. The boundaries of the polygons are formed by the perpendicular bisectors of the lines joining adjacent gauges (Chow, 1988). This interpolation provides non-uniform distribution of raingauge by determining a weighted factor for each gauge and it is generally more accurate than the arithmetic mean method. According to this interpolation, the annual mean rainfall of Gerado Catchment was computed and found to be 1180.31 mm. as in figure (3) and table (4). According to Tesfa, et al., (2021), the annual rainfall in Abay Basin was estimated to be 1399.8 mm using thiessen polygon interpolation. A similar study by Yibralem (2013) stated that this method requires a less simple division of the area than the arithmetic mean method because not all rain gauges have the same weight.

Table 3: long term mean monthly precipitation (mm.)

Stations	Long term mean monthly precipitation (mm.)												
	Jan	Feb	Mar	Apr	May	Jun	Jul	Aug	Sep	Oct	Nov	Dec	Total PCP
Dessie	18.26	31.02	61.0	84.25	57.1	36.6	339.6	34 2.2	14 0.3	58.2	19.36	20.85	1208.74
Albuko	25.54	53.18	42.1	113.8	79.3	37.2	461.4	43 9.4	12 9.7	59.3	59.12	46.62	1546.66
Gguftu	23.22	24	64.6	59.05	55.9	59.1	439.7	40 5.8	10 1.1	33.4	16.06	17.9	1299.83
Kombolcha	24.5	31.6	74	95.55	59.1	29.5	264.5	24 7	11 2.6	43.4	21	18.1	1020.8
Kutaber	10.87	12.83	51.1	51.04	52.4	38.6	342.4	35 0.8	11 3.4	45.3	17.27	6.261	1092.27
Mean	21.64	28.09	63.3	79.62	58.9	41.9	373.4	36 8.3	12 0.8	47.7	2 5.1	22.57	***1251.3***

Table 4: Thiessen polygon annual rainfall interpolation

Stations	Mean rain fall (mm)	Area of influence (km^2)	Area Wtd (km^2)	Weighted Area (%)	Weighted rainfall (mm.)
Dessie	1208.74	218	0.5860215	58.60215	720.1603
Albuko	1546.66	26	0.0698924	6.98924	67.9234189
Kombolcha	1020.80	48	0.1290322	12.90322	123.323676
Kutaber	1092.27	80	0.2150537	21.50537	223.440086
Total	4868.47	372	1	100	***1180.31***

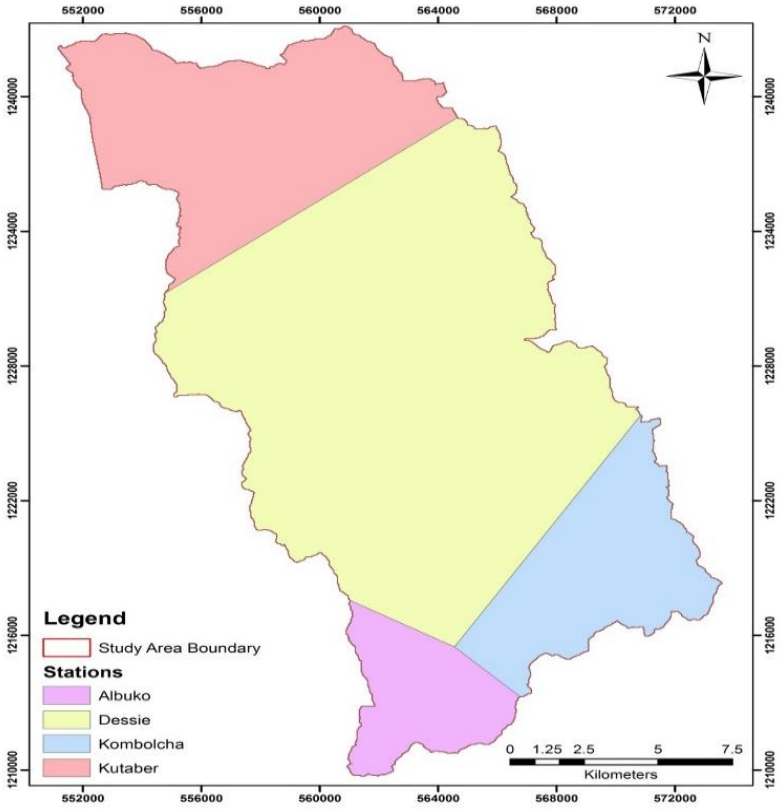

Figure 5 Thiessen polygon annual rainfall interpolation

Isohyetal interpolation: This type of interpolation takes into account the impact of physiographic parameters which include elevation, slope, distance from the coast, and exposure to rain bearing winds (Shaw, 1988). It accounts for local effects like prevailing wind and uneven topography (Wilson, 1990). It is done by drawing contours of equal areal depth of precipitation and measuring their inter-isohyetal area. For this study, the mean annual rainfall of Gerado River was found to be 1307.76 mm. (table 5). Rainfall is not evenly distributed over the study area because of topographic variations of the basin and the extreme dry and rainy seasons. In this case, the isohyetal polygon interpolation technique is the most preferable approach to estimate the areal depth rainfall over the entire catchment (Stefan and Gerd 2004). Of the three methods of interpolations to determinate mean annual rain fall, isohyetal method

is the most important and preferable. This interpolation resolves actual evapotranspiration areal depth as it considers different physiography effects.

On the other hand, quantitative seasonal category of rainfall distribution can be explained by using the rainfall coefficient (R.C), which is the ratio between mean monthly rainfall and one twelfth of the annual mean of the total rainfalls (Daniel, 1977), i.e. $R.C = \frac{12\text{Pm}}{\text{Pa}}$, where R.C= rainfall coefficient,

Pa =Annual total rainfall of the area, which is 1307.76 mm, Pm = mean monthly rainfall. Runoff coefficient shows the percentage of rainfall that is converted into runoff. The runoff coefficient varies from season to season and is strongly influenced by land cover of the catchment. The rainfall coefficient of the area was found to be < 0.6 for dry months and >0.6 for rainy months respectively as shown in table 4.

Table 5: Isohyetal annual rainfall interpolation

No.	Isohyetal range (mm)	Average Isohyets (mm)	Enclosed Area (km^2)	Weighted area (km^2)	Weighted RF (mm)
1	<1050	1037.5	7	0.02	21.68
2	1050-1100	1075	44	0.13	141.19
3	1100-1150	1125	41	0.12	137.69
4	1150-1175	1162.5	57	0.17	197.80
5	1175-1200	1187.5	123	0.37	436.01
6	1200-1225	1212.5	40	0.12	144.78
7	1225-1275	1250	36	0.11	134.33
8	1275-1325	1300	17	0.05	65.97
9	1325-1375	1350	6	0.02	24.18
10	>1375	1387.5	1	0.00	4.14
	Total	12087.5	372	1.11	**1307.76**

	Months												
Parameter	Jan	Feb	Mar	Apr	May	Jun	Jul	Aug	Sep	Oct	Nov	Dec	Total
Arithmetic	21.64	28.09	63.3	79.62	58.9	41.98	373.4	368.3	12	47.67	25.10	22.57	1251.37
Isohyet	20.47	30.5	58.6	80.72	60.8	40.2	369.5	357.0	11	47.92	26.56	21.94	1233.61
R.C	0.2	0.3	0.6	0.81	0.54	0.4	3.72	3.6	1.2	0.48	0.26	0.17	12.28

Table 4: Monthly rainfalls and rainfall coefficient (R.C)

Using rainfall coefficient (R.C) values, the following precipitation category can be made for dry months (October, November, December, January and February, May, June) which had R.C < 0.6 in Gerdo River Catchment. :. In contrast, R.C was found greater than or equal to 0.6 (R.C >= 0.6) for rainy seasons (March, April, July, August and September). From the six meteorological stations, only three stations Kombolcha, Guguftu, and Tita had records of monthly maximum and minimum temperatures. Since temperature is greatly influenced by altitude, only Tita Station was used for determining the mean monthly temperature.

The result showed that the study area was found at lower elevation than Tita Meteorological Station. So, the temperature data from Tita Meteorological Station was extrapolated to the study area by allowing an increment of 0.6 ºC for 100 m (Nata, 2006). The mean minimum (min) monthly, the mean maximum (max) monthly, and the mean annual temperature was presented below in table 6. Similarly, the extrapolated mean monthly max. and mean monthly min. result was given in table 7 and therewas a slight differnce between the two approaches.

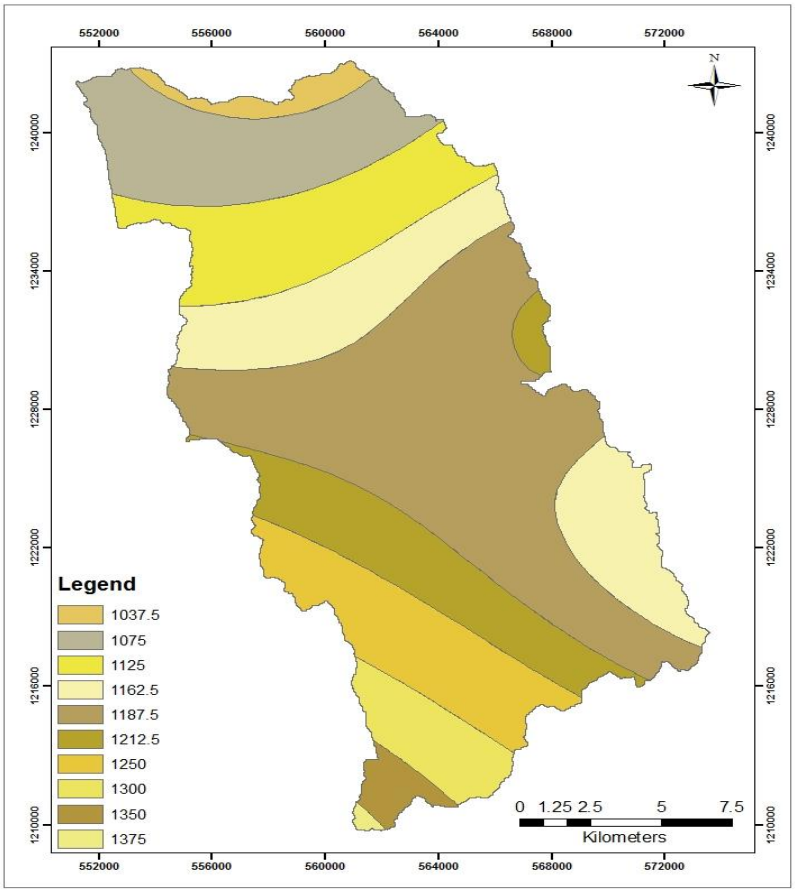

Figure 6: Isohyetal annual rainfall interpolation

Table 6: mean monthly temperature variability of Tita station

Month	Jan.	Feb.	Mar.	Apr	May	Jun	Jul	Aug	Sep	Oct	Nov	Dec
Max.	16.5	17.9	18.2	21.9	23.7	24.9	23.1	21.9	18.03	21.2	20.8	19.4
Min	8.4	9.2	10.3	10.8	10.6	11.5	11.9	11.8	10.7	8.1	7	7.5
Mean	12.45	13.55	14.25	16.35	17.15	18.23	17.5	16.85	14.36	14.65	13.90	13.45

Table 7 Extrapolated mean monthly temperature variability of Tita station

Month	Jan.	Feb.	Mar.	Apr	May	Jun	Jul	Aug	Sep	Oct	Nov	Dec
Max.	17.66	19.16	19.35	23.05	24.86	26.16	24.3	23.06	19.23	22.38	22.02	20.6
Min.	9.6	10.4	11.5	12	11.8	12.7	13.1	13	11.9	9.3	8.2	8.7
Mean	13.63	14.78	15.42	17.52	18.33	19.43	18.7	18.03	15.56	15.84	15.10	14.65

Extrapolated mean annual temperature T=16.42°c
Mean max. monthly T = 21.819 ℃
Mean min. monthly T = 11.01 ^{o}C

3.2 Evapotranspiration: The result indicated that the potential evapotranspiration of the study area (catchment) was found to be 755 mm/year. Nevertheless, the actual evapotranspiration of the catchment was 723 mm per year (table 8 and table 9). The value of actual evapotranspiration (AET) over a basin or a catchment is often estimated by calculating the potential evapotranspiration (PET) and then modifying the value based on the actual soil moisture content (Shaw, 1988). Similar studies in Abay Basinreported that 1300 mm. of the annual rainfall (96%) was lost due to evapotranspiration. Besides, the findings suggested that 63% of the total rainfall was lost because of environmental factor. Although these areas had similar physiographic and climatic setting, the variation in result was due to different methods employed. Similarly, a study conducted in Tigray Region showed that of the total rainfall recharge accounted for 12% while the rest 81% and 7% were due to evapotranspiration and surface runoff, respectively (Tekelebrhan, 2011). So, in general it can be concluded that very high potential evapotranspiration can result in low groundwater recharge (Portela et al., 2019).

Table 8: Calculated potenial evapotranspiration (PET) in mm.

Parameter	Month												Annual
	Jan	Feb	Mar	Apr	May	June	July	Aug	Sep	Oct	Nov	Dec	
N(Hrs)	11.6	11.8	12	12.3	12.6	12.7	12.6	12.4	12.4	11.8	11.6	11.5	12.1
N_m	0.97	0.98	1	1.02	1.05	1.05	1.05	1.03	1.03	0.98	0.96	0.95	1.01
T_m(0c)	13.3	14.8	15.2	17.5	18.33	19.4	18.7	18.03	15.56	15.8	15.1	14.7	16.37
i_m		5.08	5.3	6.56	7	7.6	7.2	6.8	5.4	5.6	5.24	5.01	5.94
ta =1.62													
I=71.26							4.5						
PETm	43.92	51.12	55.87	70.7	77.62	85.31	80.1	74.16	58.39	57.2	51.89	48.9	752.2

The essential factors to determine actual evapotranspiration (AET) of a given catchment are mean monthly precipitation, mean monthly potential evapotranspiration (PET), and water holding capacity of the dominant soil (Dunne & Leopold, 1978). To calculate the actual evapotranspiration (AET) of the area, the soils should be classified into two major groups with their vegetation cover and the proportion of different types of soil and vegetation cover of the catchment. Based on the long term (20-25) years meteorological data with the exception of Tita Station, the actual evapotranspiration (AET) and potential evapotranspiration (PET) of the specific land use was estimated and summarized in table 11. The difference between monthly precipitation (Pm) and PET yielded positive value during summer and spring season and negative during winter time (table 11). This was due to very low rainfall throughout the winter season as opposed to summer and spring seasons.

To evaluate and check for shortage or addition of moisture of to the soil, the difference between PET and rainfall is very important. Accordingly, positive and negative values indicate an addition of moisture to soil and monthly demand moisture by vegetation. High amount of PET and AET values were recorded during summer and spring periods. In contrast, low AET and PET values were observed through the dry season (winter) (table 9). Relatively, high

amount of AET and PET recorded during the spring season (April – June) months as compare to summer season (July – September). This could be attributed to high sun radiation energy and less cloud coverage during spring season as compare to summer season. The AET is equivalent to PET if the mean monthly rainfall is greater than respective month's evapotranspiration. The change in soil moisture showed negative values during the dry season (winter) and 0 (zero) during spring and summer rainy months (table 9). Table 10 and table 11 presented AET using soil water balance method for clayloam (200mm and 0.80m) and clayloam (250mm and 1m) with unlikely results. AET depends on climatic condition of the environment, soil moisture content, soil texture, and vegetative factors (Abebe, 2013).

Accordingly, all hydrometerological factors values were similar except for soil moisture of clayloam. Soil moisture deficency showed an increament within 250mm and 1m as compare to 200mm and 0.80m (table 10 and 11). Based on soil water balance method for clayloam (200mm and 0.80m), AET and PET values were estimated 723mm. and 755 mm., respectively. For similar soil type and cereal crops with 250mm water holding capacity root zone and 1meter (m) depth, AET and PET were estimated 728 mm/year and 755 mm/year, respectively. The annual PET values in all circumstances yielded similar values i.e 755 mm/year. But, the actual evapotranspiration results slightly deviated from each as other as it considered certain correlated environmental elements affecting it as given in table 9, 10, 11 and 12. Therefore, the real annual AET value was found 722 mm/year since it showed impacts of land use, land cover, soil texture, and depth root (table12).

The actual evapotranspiration for the dominant soil types and the respective land uses of the area was computed based on the proportion of the area and the weighted actual evapotranspiration. Besides, more AET resulted from sand loam and clay loam with root depth 1m and o.8m with 357 mm/year and 302 mm/year, respectively. But, deep rooted grasses with similar soil texture and 1m soil depth was estimated to be 64 mm/year as the aerial covergae was very small in comparison to the others. Sandy loam (49%) and clay loam (42.2%) had an impact on actual evapotranspiration (AEP) process. Based on table 12, weighted AET, high evapotranspiration (48.5%) was observed in moderate deep rooted cereal crops with sandy loam. . In other words, cereal crops with moderate deep root and clay loam have low AET

relatively with 42.2% percentage influence. However, deep rooted grasses are found to have the least weighted impact on AET as compare to moderate cereal crops. Cereal crops under sandy soils are more vulnerable to evapotranspiration as radiation energy easily penetrates them. At the same time, deep rooted grasses in clay loam soil texture are less likely exposed because of less sun radiation penetration. So, taking all these essential elements into account, AET was estimated to be 722 mm/year. However, PET theoretically hardly takes all aforementioned factors into consideration..

Accordingly, the annual actual evapotranspiration of the catchment was estimated to be 722.27 mm. Table 9 and 10 presented AET (in mm) using Soil Water Balance Method for sandy and clay covered with cereal crops having rooting depth of 1m and available water capacity of the root zone 150 mm. Yibralem (2013) reported that the water inflow into the catchment area was coming only from rainfall and the water leaving the catchment area were only surface runoff (R) and actual evapotranspiration ^ (ETa). The difference between them constitutes the change both in groundwater and soil moisture storage (ΔS). The actual evapotranspiration of the catchment can easily be obtained by satellite technologies., the progressive reduction in the cost of images and the development of computer technology and associated software's and models. Hence, this opened the opportunity to extract fundamental hydrological parameters like actual evapotranspiration and others on pixel basis.

Generally, this study showed that the potential and actual evapotranspiration of the area was estimated statistically to be 755 mm/year and 722 mm/year, respectively. Simultaneously, the runoff and groundwater recharge of the area was 120,581,841m3 (326 mm) and 52,208,159.5 meter cubic (m3) or 141.5 mm., respectively. Hence, 27.6% and 12% of the mean annual rainfall was lost because of surface runoff and groundwater recharge and the rest 67% was due to evapotranspiration. The high amount of evapotranspiration was mainly due to the bimodal rainfall pattern. Moreover, the study further disclosed that rainfall coefficient was greater than 0.6 (>0.6) but less than 0.6 (< 0.6) during rainy and dry seasons (table 4).

Table 9 : Calculated potenail evapotraspiration in m

Parameters	Months												
	Jan	Feb	Mar	Apr	May	June	July	Aug	Sep	Oct	Nov	Dec	Total
P	20.47	30.52	58.57	80.72	60.76	40.2	369.5	357.0	119.4	48.4	26.56	21.94	1234.04
PET	43.9	51.12	55.87	70.77	77.62	85.31	80.18	74.16	58.39	57.19	51.89	48.85	755.25
P-PET	-23.5	-20.6	2.7	9.95	-16.9	-45.1	289.3	282.9	61.03	-8.79	-25.3	-26.9	478.79
APWl	-84.5	-105	0	0	-16.9	-62	0	0	0	-8.79	-34.1	-61.0	-372.3
Sm	85.48	74.45	150	150	134.1	99.24	150	150	150	141.5	119.5	99.86	1504.1
AET	34.9	41.48	55.87	70.77	76.71	75.02	80.18	74.16	58.39	56.93	48.54	41.56	714.5
ΔSm	-14.4	-10.9	75.55	0	-15.9	-34.8	50.76	0	0	-8.53	-21.9	-19.6	0.23
SMD	-8.99	-9.64	0	0	-0.91	-10.3	0	0	0	-0.25	-3.34	-7.28	-37.71
S	0	0	78.25	9.95	0	0	340.1	282.9	61.03	0	0	0	772.1

Table 10 : AET (in mm.) Using soil water balance method for clayloam (200mm and 0.80m)

Param.	Months												
	Jan	Feb	Mar	Apr	May	June	July	Aug	Sep	Oct	Nov	Dec	Total
P	20.47	30.52	58.5	80.7	60.76	40.2	369.5	357.0	119.4	48.4	26.56	21.94	1233.95
PET	43.92	51.12	55.8	70.7	77.62	85.3	80.18	74.16	58.39	57.19	51.89	48.85	755.12
P-PET	-23.4	-20.6	2.7	9.95	-16.86	-45.1	289.3	282.9	61.03	-8.79	-25.3	-26.9	478.93
APWl	-84.5	-105	0	0	-16.86	-62	0	0	0	-8.79	-34.1	-61.0	-372.25
Sm	131.1	118.3	200	200	183.8	146.7	200	200	200	191.4	168.6	147.4	2087.3
AET	36.77	43.35	55.8	70.7	76.92	77.3	80.18	74.16	58.39	57.00	49.33	43.17	723.07
ΔSm	-16.3	-12.8	81.74	0	-16.17	-37.1	53.28	0	0	-8.59	-22.8	-21.2	0.06
SMD	-7.14	-7.77	0	0	-0.69	-7.99	0	0	0	-0.19	-2.56	-5.68	-32.02
S	0	0	84.4	9.95	0	0	342.6	282.9	61.03	0	0	0	780.88

** for clay loam soil covered with cereal crops having root depth 0.8m and available water capacitym 200mm*

Table 11: AET (in mm) using soil water balance method. for clayloam (250mm and 1m)

Para-meter	Months												
	Jan	Feb	Mar	Apr	May	June	July	Aug	Sep	Oct	Nov	Dec	Total
P	20.47	30.52	58.57	80.72	60.76	40.2	369.52	357.03	119.42	48.4	26.56	21.94	1234.11
PET	43.92	51.12	55.87	70.77	77.62	85.31	80.18	74.16	58.39	57.19	51.89	48.85	755.27
P-PET	-23.45	-20.6	2.7	9.95	-16.86	-45.1	289.34	282.9	61.03	-8.79	-25.33	-26.91	478.88
APWL	-84.48	-105	0	0	-16.86	-62	0	0		-8.79	34.12	-61.03	-372.28
Sm	178.31	164.2	250	250	233.69	195.1	250	250	250	241.3	218.1	195.85	2676.55
AET	38.005	44.62	55.87	70.77	77.06	78.78	80.18	74.16	58.39	57.03	49.81	44.198	728.87
ΔSm	-17.54	-14.1	85.7	0	-6.304	-38.6	54.88	0	0	-8.63	-23.25	-22.2	10.03
SMD	-5.915	-6.49	0	0	-0.556	-6.53	0	0	0	-0.15	-2.07	-4.654	-26.37
S	0	0	88.4	9.95	0	0	344.2	282.9	61.03	0	0	0	786.6

** the root depth of 1m and available water capacity of the root zone 250 mm.*

Table 12: Weighted AET calculated for each soil texture and land use

Soil texture	Land use/land cover	Root Depth (m)	W (mm)	Coverage (km^2)	Wtd	%	AET	Wtd. AET
Sandy loam	Moderately deep rooted (cereal crops)	1	150	50.1	0.4895	48.95	728.8	356.75
Clay loam	Moderately deep rooted (cereal crops)	0.8	200	43.2	0.422	42.2	714.5	301.58
Clay loam	Deep rooted (grass)	1	250	9.05	0.0884	8.84	723.2	63.947
	Total	2.8	600	102.4	1	100	2166.5	722.27

3.3 Surface Runoff Estimation: -

Runoff results from rainfall that does not infiltrate but forms flows as thin sheet of across the land surface. (Tenalem & Tamiru, 2001). In this study area, the absence of gauged hydro-meteorological stations posed difficulty to work out a model for the runoff generation of the catchment. The volume runoff of the study area was computed using the runoff coefficient model as given in Equation (6). Based on the model, the study revealed that the volume of runoff was projected to be 120,581,841 m^3 which is 326 mm. (table 11). Of the total rainfall, 27.62% of the mean annual rainfall of the catchment was lost through surface runoff. A study at Illala Catchment in North Ethopia identified that about 93% of the surface runoff occured during the wet months while the remaining 7% happened during the dry seasons (Tekelebrhan, et al., 2011). He added that groundwater recharge accounted for 12% of the precipitation while the rest 81% and 7% were converted into evapotranspiration and surface runoff, respectively. Runoff generation is significantly affected by various factors such as land use, land cover (LULC), topography (slope and elevation), and soil textures. Furthermore, Table 11 clearly disclosed that the type of land use, land cover, soil type, and slope type were very essential environmental agents that directly controlled runoff formation. The amount of rainfall, runoff coefficient factor, and depth of soil were also found to be significant factors in affecting surface runoff formation.

In hydrological cycle, natural vegetation regulates influence on runoff and it protects from erosion (Abebe, 2013). Among the land uses, grazing and cultivated lands are more prominent in surface runoff generation. On the other hand, cultivation, plantation, and shrubs played less role in surface runoff creation. In terms of topography, flat and gentle sites are less vulnerable to runoff as compare to steepy areas. Soil texture is also other determinant element controlling runoff generation. In this study, clay and sandy clay soils were less likely exposed as compare to rocky and silty soils. The highest amount of runoff was generated from shrubs, plantation, and cultivation because of large area coverage but with slight difference in K values. In other words, grazing and cultivating lands have less impact on surface runoff generation. The highest and lowest runoff were 120,581,841 m^3 ; 43,959,708 m^3 and 11,913,780 m^3 ; 11,913,780 m^3 respectively (table 11). Runoff has a direct relationship with area and runoff

coefficient. Hence, the total amount of runoff genearted from the study area was 1189mm. (1.189 m) as in table 11. The modeling of surface runoff in arid and semi-arid area is hardly possible as the mean annual rainfall and evapotranspiration are very difficult to determine (Yongxin & Beekman, 2003).

In this study, aerial coverage and runoff coefficient were found the most influential in estimating surface runoff creation. However, this method of estimation had some drawbacks as it hardly represented the space and time vulnerability. The mean annual rainfall was taken as constant but precipitation greatly varied during winter and summer season. In arid and semi-arid areas, in situ measurement of surface runoff is considered to be more accurate and explanatory. But, this cannot happen anytime and anywhere as it requires labor, material, and other constraints. It is more expensive and demanded more time and resources (Ybralem, 2013). Nowadays, satellite remote sensing technologies provide spatial and temporal hydro-meteorological data such as precipitation and evapotranspiration.

Table 13: Runoff values using the runoff coefficient method

S.N	Land use	Soil	Slope	Area(m^2)	PPT(m)	K	Runoff (m^3)
1	Grazing	Clay	Flat	9,050,000	1.189	0.16	1,721,672
2	Cultivation	Clay	Gentle to flat	65,210,000	1.189	0.25	19,383,673
3	Cultivation	Sandy clay	Gentle-Gentle to flat	50,100,000	1.189	0.2	11,913,780
4	Shrubs	Rocky*	Steep	123,240,000	1.189	0.3	43,959,708
5	Plantation	Rocky*	Steep	122,240,000	1.189	0.3	43,603,008
	Total			370,000,000	1.189		120,581,841

3.4 Groundwater Recharge:

Groundwater recharge areas are mostly located at higher topography of a given basin. In this study area, recharge areas had negligible groundwater potential zone. A hydro Geological map in fig. 7 , it was indicated that the main recharge sites were in the upper, left, and right side of Gerado Catchment. These areas were valleys and ridges on the way to Kombolcha, Albuko, Mekaneselam, and Kedijo and they covered a relatively large part of study area in comparison

to the discharge area (figure 7). The lower elevated land of the study area got recharge not only from precipitation but also from groundwater flow from the upstream. However, the left and right side of the catchments had high recharge because of fractures and faults. . These areas were mostly located in the lower topography of the basin. The discharge areas in the study were low lands of Gerado well fields. They covered a relatively small area than the recharge area, which made the Gerado well field to have high groundwater potential. Identifying the recharge and discharge area of a certain basin is important for identifying potential sites and utilizing water resource management.. In the study area, recharge areas had a negligible groundwater potential zone.

There are various methods of estimating groundwater recharge; for example, water level and porosity, base flow recession analysis and water balance method. Different studies suggested that recharge values obtained from water balance method were constantly higher than values from other methods. However, these methods complemented each other and thus can be used depending on the availability of data (Simmers, 1988). The CMB (chloride mass balance) approach has been extensively used in estimating low recharge rates mainly because of the lack of other suitable methods. Low water fluxes ranging from 0.05 to 0.1 mm/ year have been estimated in arid regions in Australia and in the USA. The storage concept method using water table fluctuation has been used in various climatic conditions (Scanlon et al., 2003). Recharge rates estimated by this technique range from 5 mm/year in the Tabalah Basin of Saudi Arabia (Abdulrazzak et al. 1989) to 247 mm/ year in a small basin in a humid region of the eastern USA (Rasmussen & Andreasen, 1959). Identifying the recharge and discharge area of a certain basin is important for identifying potential sites and for water resource management and utilization. The amount of water extracted from an aquifer without causing depletion is primarily dependent upon groundwater recharge. Quantification of the rate of natural ground water recharge is basic for efficient groundwater resource development and management. It is particularly important in areas with large demand for groundwater supplies. Such resources are the key to economic development. The main purpose of this computation is to make a quantitative evaluation of the amount of water that infiltrates into the ground to recharge the ground water circulation occurring in the study area. The most important terms of the factors

in water balance are precipitation, evapotranspiration, and discharge (Claudia, 2007). As the result, the change in water storage on water balance depends on the period over which the water balance was computed. The important method to determine water that recharges the ground water is water balance method, which is based on the law of conservation of energy.

The finding of this study showed that the volume of water that recharged the groundwater of the catchment was found to be 52,208,159.5m^3(141.5 mm) per year. Table 14 showed that 60. 4% of precipitation was lost as evapotranspiration; 27.6 % as surface runoff and the amount of water that recharges the groundwater was only 12% of the annual precipitation. Recharge areas were mostly found at higher topography of the basin. The finding of the current study conformed with a study done in north Ethiopia and it was found that 12% of the annual rainfall was lost in the form of ground recharge (Tekelebrhan, et al., 2012). Similarly, Tesfa et al., (2021) found that the annual groundwater recharge was found to be 197.23 mm/year. Again within the basin, two watersheds (Ribb and Gumara) had recharge of 204.76 mm and 184.83 mm., respectively. This difference was due to physiographic and climate settings. A similar study in the semi-arid of North Ethiopia by Esayas, et al., (2019) showed that more than 83% of the total annual rainfall was converted into evapotranspiration and the rest 7.4 % and 7.1% were lost as recharge and runoff. This result deviated from the current finding because of the method employed and climate settings. The current study had a bimodal rainfall while that site was in semiarid zone.

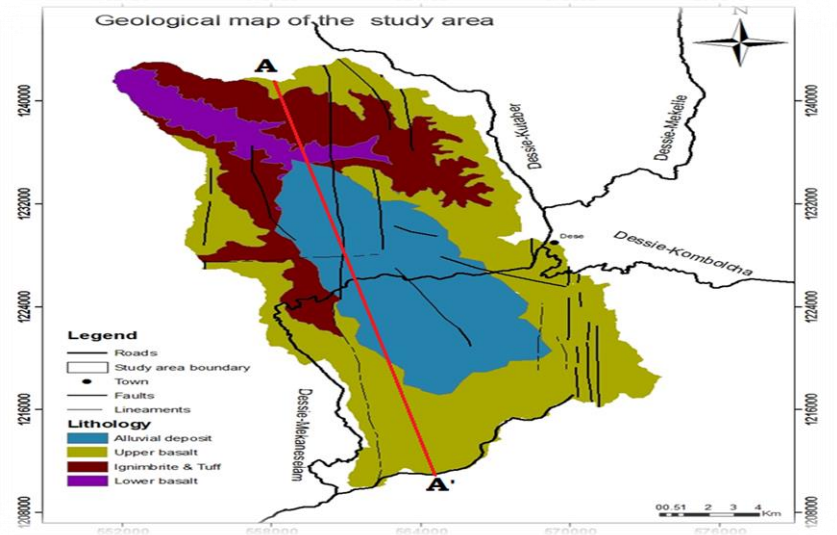

Figure 7: Geology map of Gerado Catchment

Table 14: Summary of water balance components

PPT (MM)	AET (MM)	RUNOFF (MM)	RECHARGE (MM)
1307.76	722.3	327	145.5

3.5 Groundwater Potential Mapping

For this research, the groundwater prospect map of the area was prepared by integrating eight thematic layers using spatial model analysis. Based on the multi-criteria evaluation technique, each layer and field value were assigned a rank and weighting (Arivalagan, et al., 2015**)** as all variables hardly had the same impact in determining groundwater occurrence and movement (Satty, 1980). Table 15 showed that the three factors affecting groundwater occurrence were lithology (34.5%), lineament (23.4%), and geomorphology (15.5%). On the other hand, the five least influencing factors were slope, soil, drainage density, rainfall, and land use/cover. The pair wise comparison (table 15) of groundwater potential mapping (GWP) and controlling weighted factors were shown in table 15.

The groundwater potential (GWP) of the area was computed using mathematical equation given below:

$$GP = \sum_{i=1}^{n} WiXi \qquad 8$$

Where GP = Groundwater potential, WI = weight for each thematic layer and

Xi = Rates for the classes with in the thematic layer.

*GWP=0.3456*LT+0.2339*LD+0.1548*GM+0.1033*SL+0.0689*SOL+0.0449*DD+0.0286* RF+0.0203*LULC*

Were GWP = Groundwater potential, LT = lithology, LD = lineament density, GM = geomorphology, SL = slope, SOL= soil, DD = drainage density, RF = rainfall, and LULC = Land Use Land Cover.

Table 15: Pairwise Comparison Matrix among GWP Thematic Layers (CR = 0.0805)

	LT	LD	GM	SL	SDL	DD	RF	L	WEIGHT	%
LT	1	2	4	5	6	7	8	9	0.3453	34.53
LD	½	1	2	4	5	6	7	8	0.2339	23.39
GM	¼	½	1	2	4	5	6	7	0.1548	15.48
SL	1/5	¼	½	1	2	4	5	6	0.1033	10.33
SOL	1/6	1/5	¼	½	1	2	4	5	0.0689	6.89
DD	1/7	1/6	1/5	¼	½	1	2	4	0.0449	4.49
RF	1/8	1/7	1/6	1/5	¼	1/2	1	2	0.0286	2.86
LULC	1/9	1/8	1/7	1/6	1/5	1/4	½	1	0.0203	2.03

The potential groundwater areas lay within lithology class of alluvia deposits and geomorphology class of alluvia plain (figure 5 &6). Moreover, areas with flat slope and low lineament density were found in most potential areas of groundwater. If we observe the spatial distribution of the groundwater suitability map, the least potential areas are located in the western, northern, and southern parts of the study area. And these are characterized by steep slope and high drainage density which facilitate high run off creation and hence result in low groundwater potential. Thus, areas with good classes of groundwater map account for small areal coverage. Hence, it can be generalized that the study area had little groundwater potential suitability as compared to its total areal coverage. Furthermore, geospatial techniques with the help of multi-criteria decision analysis (MCDA) were good to investigate the relationship between different geomorphological and environmental factors. Therefore, those tools were very effective and indispensable for planning and managing groundwater in watershed areas.

The groundwater prospect map of the area was classified into four zones: very good, good, moderate, and poor. The very good groundwater prospect zones were mostly found within alluvial plains/valleys with smooth and irregular plain geomorphological classes. Moreover, it overlaps with flat to moderate slope classes. Groundwater zones were compared with borehole yield data to check the validity of the result. Similar studies by Olutoyin, (2013), Singh et al, (2014), and Soumen (2014) stated that validation of the groundwater potential zones should be done using existing data (dung wells and bores). Thus, out of the collected and reviewed 60

water points, 57 were measured and estimated actual yield data. In general, the data indicated high yield (≥30 l/s) in the very good potential areas while very low yield (<5 l/s) in the very poor potential areas. Intermediate values appeared in the zones between these extremes. Water points with yield 5-<12 l/s occurred in the poor, 12-17 l/s in the moderate, and 18.5-20 l/s in the good zones of groundwater potential. As shown in figure 6, 5, most of the suitable groundwater areas were found in the central and eastern part of the study area. In contrast, the northern and western part of the Gerado Catchment had less potential groundwater.

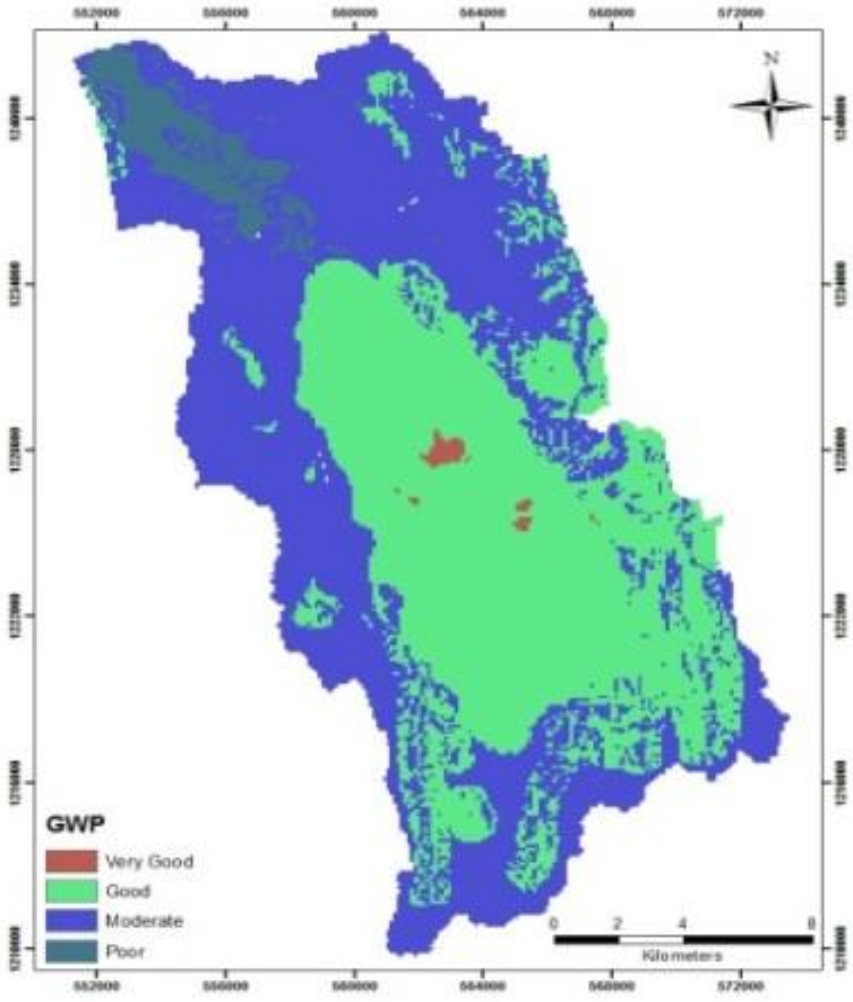

Figure 8: Groundwater potential map

4 CONCLUSIONS AND RECOMMENDATIONS

In the Northern Ethiopia owing to the absence of gauged metrological stations and continuous land degradation, understanding hydro-metrological nature and characteristics was difficult. And this had a direct impact on agriculture in particular and the economy of the region in general. However, in such circumstances understanding, evaluating, and analyzing the hydro-metrological characteristics of these factors using the existing traditional conventional methods was very essential. This was more appropriate in remote areas which hardly had ground based installed stations data. The present study was carried out in the Gerado Catchment, in the Northern Ethiopia to investigate and understand the hydro-meteorological characteristics (runoff, evapotranspiration, groundwater recharge, and mapping groundwater potential). Meteorological data were collected from existing metrological station (Dessie, Guguftu, Albuko, Kutaber, Kombolcha, and Tita). since some of the data were missing, an appropriate technique was used to fill the gaps. Once the data quality was checked, spatial interpolation methods were applied to create surface map climatic data. Thornthwaite Empirical Modeling was used to calculate the potential evapotranspiration of the catchment. This method used air temperature as an index of energy available for evapotranspiration. On the other hand, the volume of runoff from the catchment was also computed using the runoff coefficient scheme. Mapping the groundwater sites were done through the application of geographic information sciences. The finding of the study indicated high potential groundwater areas were found in the central part of the study area with alluvial geological unit. The central and eastern of the area lay within good groundwater prospect areas. In contrast, the western, northern, and southern parts were located under moderate and poor water potential zones. The result further disclosed that the potential and actual evapotranspiration of the area had about 755 mm/year and 722 mm/year. This suggested that the actual evapotranspiration result was less than the potential evapotranspiration because it considered various factors like soil and land use cover. At the same time, the runoff and groundwater recharge of the area were estimated to be 120,581,841m^3 (326 mm.) and 52,208,159.5 m^3 (141.5 mm.), respectively. Hence, out of the total rainfall, 27.6% of the mean annual rainfall was lost because of runoff. Nevertheless, the remaining 40% was wasted owing to evapotranspiration and only 12% was recharged to the ground. Therefore, having updated information on hydro-meteorological ^ of the catchment

would be significant in water resource development projects such as dams and reservoirs. However, this study didn't show the spatial and temporal dynamics and trend of the aforementioned hydrological variables. So, further studies should be carried out using Remote Sensing and Geographic Information System (Geo-Spatial Technologies) as it covered large area but less costly. But, they have to consider using updated and high quality data for better outcome and findings. Moreover, such studies have to be supported through extensive ground field survey for better and accurate outputs. Installation of hydrological stations in the study area should be undertaken for better understanding of hydrological conditions.

Conflict of Interest: on the behalf the corresponding author, I can assure you that there is no conflict of interest among the authors of this research work.

REFERENCES

Abeba Adugna (2013). Impact of Land Cover Change on Runoff Generation using Continuous Rainfall-Runoff Modeling: the case of Upper Gilgel Abbay Catchment, Ethiopia. MSc thesis submitted to Institute of Geo-information and Earth Observation Sciences, Mekelle University, Ethiopia.

Abebe Debele (2021) Groundwater potential mapping using geospatial techniques: a case study of Dhungeta- Ramis sub-basin, Ethiopia, Geology, Ecology, and Landscapes, 5:1, 65-80, DOI: 10.1080/24749508.2020.1728

Addulrazzak MJ, Sorman Au, Alhames AS. (1989). Water balance approach under extreme arid conditions- a case study of Tabalah basin, Saudi Arabia. Hydrol Proc 3.107-122.

Al-Ahmacli, M. E. (2005). Groundwater investigation in Hadat Ash Sham area, Western Saudi Arabia.

Allison, G. B., Gee, G. W., & Tyler, S. W. (1994). Vadose-zone techniques for estimating groundwater recharge in arid and semiarid regions. *Soil Science Society of America Journal*, *58*(1), 6-14.

Arivalagan J, Sleight VA, Thorne MA, Peck LS, Berland S, Marie A, Clark MS (2015) Characterisation of the mantle transcriptome and biomineralisation genes in the blunt-gaper clam, Mya truncata. Mar Genom 27:47–55. doi:10.1016/j.margen.2016.01.003.

Beven K. J., Kirkby M.J., Schofield N. & Tagg A. (1984) Testing a physically based flood forecasting model (TOPMODEL) for three UK catchments. *Journal of hydrology. 69*, 119- 143.

Champak and Dinesh (2018). Review on practices and state of the art methods on delineation of ground water potential using GIS and remote sensing. Bulletin Department of Geology Tribhuvan University Kathmandu Nepal Vol. 20-21 Pp. 7-20.

Claudia, 2007. Water balance study and rainfall-runoff modeling. The issel catchment.

Daniel Gemechu, 1977. Aspect of climate and water balance in Ethiopia. Addis Ababa University press, Addis Ababa, 79pp.

Dereje, G. (2012) Groundwater potential assessment and water quality investigation. Gerado Dessie, M.Sc., thesis, Mekelle University, Ethiopia

Dunne, T., & Leopold, L. B. (1978). *Water in environmental planning*. Macmillan.

Džubáková, K. (2010). Rainfall-Runoff Modelling: Its development, classification and possible applications. *ACTA Geographica universitatis comenianae*, *54*(2), 173-181.

Engman ET, Gurney RJ (1991). Remote Sensing in Hydrology. Chapman and Hall, London, 225pp

Espinosa, L. A., Portela, M. M., & Rodrigues, R. (2019). Spatio-temporal variability of droughts over past 80 years in Madeira Island. *Journal of Hydrology: Regional Studies*, *25*, 100623.

Ethiopian water well drilling enterprise, 2004. Dessie town water supply project Well completion report, Addis Ababa.

FAO (1997) 'The digital soil and terrain database of east africa (sea) notes on the arc/info files', pp. 1–30.

Farnsworth RK, Barret EC, DhanjuMS(1984). Application of Remote Sensing to Hydrology including Ground Water. IHP-II Project A. 1.5, UNESCO, Paris.

Faust N, Anderson WH, Star JL (1991). Geographic information systems and remote sensing future computing environment. Photogrammetric Engineering and Remote Sensing 57(6):655–668.

Fetter, C.W. (1994). Applied hydrogeology. Third edition, Prentice-Hall, New Jersy, 691 - 695PP.

Foster S (1998) Groundwater: assessing vulnerability and promoting protection of a threatened resource. Proceedings of the 8th Stockholm Water Symposium, 10–13 August, Sweden, pp. 79–90.

Freeze, R. A. and Cherry J. A. (1979). Groundwater. Prentice-Hall, New Jersy, 604-616.

Ganapuram, S., Kumar, G., Krishna, I., Kahya, E., Demirel, M., 2008.Mapping of groundwater potential zones in the Musi basin using remote sensing and GIS. Advances in Engineering Software 40, 506-518.

Gedefaw B, (2020). Spatial Analysis of Groundwater Potential Investigation in the Northern East Ethiopia Using Remote Sensing and GIS. M, Sc. thesis, Institute of Geo-Information and Earth Observation Sciences, Mekelle University, Ethiopia.

Gintamo, T. T. (2015). *Ground Water Potential Evaluation Based on Integrated GIS and Remote Sensing Techniques , in Bilate River Catchment : South Rift Valley of Ethiopia*.

Gogu RC, Carabin G, Hallet V, Peters V, Dassargues A (2001). GIS-based hydrogeological databases and groundwater modeling. Hydrogeology Journal 9:555–569

Horton, T. (2003). *Turning the tide: saving the Chesapeake Bay*. Island Press.

Hurni, H. (1993). Land Degradation, famine and resource scenarios in Ethiopia. In World Soil Erosion and Conservation. D. Pimentel. Cambridge University press, Cambridge.

Jenicek, M. (2007). Effects of land cover on runoff process using SCS CN method in the upper Chomutovka catchment. *Integrated catchment management for hazard mitigation*, *42*.

Justin-Visentin, E., Nicoletti, M., Tolomeo, L. and Zanettin, B. (1974). Miocene and Pliocene volcanic rocks of Addis Abba-Debrebirhan area (Ethiopia): geo-petrographic and radiometric study. Francesco Giannina and Pegli Napoli, Italy, 17pp.

Kazmin,V. (1979). Stratigraphy and correlation of volcanic rocks in Ethiopia. Ethiopian institute of geological survey, Addis Ababa, 26pp, 82pp.

Kebede.S., (2013). Groundwater Occurrence in Regions and Basins. *Springer Hydrogeology*, http://doi.org/10.1007/978-3-642-30391-3.

Keller, F., Meugniot, C. (2004). Flood and shield basalt from Ethiopia: Magmas from the African suppers well. Journal of petrology, volume-45, page 793-834.

Ketata Mouna R.,Gueddari M. and Bouhlila R. (2011). Use of Geographical Information System and Water Quality Index to Assess Groundwater Quality in El Khairat Deep Aquifer (Enfidha, Tunisian Sahel), Iranica Journal of Energy & Environment, 2 (2), pp. 133-144.

Khan, A., Khan, H. H., & Umar, R. (2017). Impact of land-use on groundwater quality: GIS-based study from an alluvial aquifer in the western Ganges basin. *Applied Water Science*, *7*, 4593-4603.

Khan, H., Patil, K. A., & GECA. (2017). Development of Groundwater Potential Zones Using Gis& Remote Sensing. *5*(3).

Khan, H., Patil, K. A., & GECA. (2017). Development of Groundwater Potential Zones Using Gis& Remote Sensing. *5*(3).

Kieffer, B., Arndt, N., Lapierre, H., Bastien, F., Bosch, D., Pecher, A., Gezahegn Yirgu, Dereje Ayalew, Weis, D., Jeram, D.A., and

Lentswe, G. B., & Molwalefhe, L. (2020). Delineation of potential groundwater recharge zones using analytic hierarchy process-guided GIS in the semi-arid Motloutse watershed, eastern Botswana. *Journal of Hydrology: Regional Studies*, *28*, 100674.

Lerner, D.N, Issar, A.S. & Simmers.I. (1990). Ground water recharge: A guide to understanding and estimating natural recharge. International Contributions to Hydrogeology, 8, Heise, Germany.

Liu, T., Yan, H., & Zhai, L. (2015). Extract relevant features from DEM for groundwater potential mapping. *The International Archives of the Photogrammetry, Remote Sensing and Spatial Information Sciences*, *40*, 113-119.

Loague K, Corwin DL (1998). Regional-scale assessment of non-point source groundwater contamination. Hydrological Processes 12(6):957–966.

Makonyo, M., & Msabi, M. M. (2022). Potential landfill sites selection using GIS-based multi-criteria decision analysis in Dodoma capital city, central Tanzania. *GeoJournal*, *87*(4), 2903-2933.

Malczewski, J., & Rinner, C. (2015). *Multicriteria decision analysis in geographic information science* (Vol. 1, pp. 55-77). New York: Springer.

Meijerink AMJ (2000). Groundwater. In: Schultz GA, Engman ET (eds), Remote Sensing in Hydrology and Water Management. Springer, Berlin, pp. 305–325.

Meresa, E., & Taye, G. (2019). Estimation of groundwater recharge using GIS-based WetSpass model for Birki watershed, the eastern zone of Tigray, Northern Ethiopia. *Sustainable Water Resources Management*, *5*(4), 1555-1566.

Mohr, P.A. (1962). The geology of Ethiopia. University college of Addis Ababa press, Addis Ababa, 268pp.

Myers VI, Moore DG (1972). Remote sensing for defining aquifers in glacial drift. Proceedings of the 8th International Symposium on Remote Sensing of the Environment, Environmental Research Institute of Michigan, Ann Arbor, MI, pp. 715–728.

Nata Tadesse, 2006. Surface Waters Potential of the Hantebet Basin, Tigray, Northern Ethiopia.

Nyssen, J. (2011). Erosion processes and soil conservation in tropical mountain catchment under threat of anthropogenic desertification-a case study from Northern Ethiopia. PhDthesis, Leuven, Belgium, KU.

Nyssen, J., Vandenreyken, H., Poesen, J., Moeyersons, J., Deckers, J., Haile, M., Salles, C., and Govers, G. (2005). Rainfall erosivity and variability in the Northern Ethiopian Highlands. Journal of Hydrology 311.

Nyssen, J., Vandenreyken, H., Poesen, J., Moeyersons, J., Deckers, J., Haile, M., & Govers, G. (2005). Rainfall erosivity and variability in the Northern Ethiopian Highlands. *Journal of Hydrology*, *311*(1-4), 172-187.

Olutoyin A, Fashae MN, Tijani AO, Talabi OI (2014) Delineation of groundwater potential zones in the crystalline basement terrain of SW-Nigeria: an integrated GIS and remote sensing approach. Appl Water Sci 4:19–38. doi:10.1007/s13201-013-0127-9.

Olutoyin AF, Tijani MN, Talabi AO, Oluwatola IA (2014) Delineation of groundwater potential zones in the crystalline basement terrain of SW-Nigeria: an integrated GIS and remote sensing approach. Appl Water Sci 4:19–38.

Rangarajan, R., & Andrade, R. (2012). Understanding Shallow Basaltic Aquifer System Near West Coast of Maharashtra, India. Journal of Geoscience Research 8, 49-57.

Rasmussen WC, Andreasen GE. 1959. Hydrologic budget of the Beaverdam Creek basin, Maryland. US Geol Surv water-supply pap 1472:106.

Rose RS, Krishnan N (2009) Spatial analysis of groundwater potential using remote sensing and GIS in the Kanyakumari and Nambiyar basins, India. J Indian Soc Remote Sens 37(4):681–692.

Saaty TL (1980) The analytic hierarchy process. McGraw-Hill, New York, p 278.

Saaty, T. L. (1980). The analytic hierarchy process: planning, priority setting, resource allocation.

Santosh Kumar Garg, 1987. Irrigation Engineering and Hydraulic structures.

Satapathy, I., & Syed, T. H. (2015). Characterization of groundwater potential and artificial recharge sites in Bokaro District, Jharkhand (India), using remote sensing and GIS-based techniques. *Environmental Earth Sciences*, *74*, 4215-4232.

Scanlon, B. R., Mace, R. E., Barrett, M. E., & Smith, B. (2003). Can we simulate regional groundwater flow in a karst system using equivalent porous media models? Case study, Barton Springs Edwards aquifer, USA. *Journal of hydrology*, *276*(1-4), 137-158.

Scanlon, B.R., Healy, R.W. & Cook, P.G. 2002. Choosing appropriate techniques for quantifying ground water storage changes in the Mississippi River basin (USA) using GRACE. Hydrology Journal 15 (1).

Shaw, E.M. (1988). Hydrology in practice. 2nd edition, Chapman and Hall, New York, 539pp

Singh A (2014) Groundwater resources management through the applications of simulation modeling: a review. Sci Total Environ 499:414–423.

Sisay L (2007) Application of remote sensing and GIS for groundwater potential zone mapping in Northern Ada'a plain (Modjo catchment) University/Publisher Addis Ababa University. http:// etd.aau.edu.et/dspace/handle/123456789/386.

Soumen D (2014) Delineation of ground water prospect zones using remote sensing, GIS techniques—a case study of Baghmundi development block of Puruliya district, West Bengal. Int J Geol Earth Environ Sci. ISSN: 2277-2081 (online). An open access, online international journal available at http://www.cibtech.org/ jgee.htm (2014) 4(2):62–72/Dey.

Stefan, T. and Gerd, F. , 2004, Water resources assessment in the Bilate River catchment – precipitation Variability, Lake Abaya Research Symposium, Research Institute for Water and Environment, University of Siegen,Paul-Bonatz-Str.9-11.57076 Siegen, Germany.

Suryawanshi, R. K., Gedam, S. S., & Sankhua, R. N. (2012). Inflow forecasting for lakes using Artificial Neural Networks. *WIT Transactions on Ecology and the Environment*, *159*, 143-151.

Syed, Q., Ali, W., Lal, D., & Ahsan, J. (2015). Assessment of groundwater potential zones in Allahabad district by using remote sensing & GIS techniques. *International Journal of Applied Research*, 1(13), 586–591.

Tenalem Ayenew and Tamiru Alemayehu (2001). Principle of hydrogeology. Department of geology and geophysics, Addis Ababa University, 125pp.

Tesfaye T (2010) Ground water potential evaluation based on integrated GIS and RS techniques in Bilate river catchment, South rift valley of Ethiopia. Am. Sci. Res. J. Eng. Technol Sci (ASRJETS). ISSN (Print) 2313-4410, ISSN (Online) 2313-4402Global Society of Scientific Research and Researchers. http://asrjetsjournal.org.

Tesfaye T. (2015). Ground Water Potential Evaluation Based on Integrated GIS and Remote Sensing Techniques, in Bilate River Catchment: South Rift Valley of Ethiopia. American Scientific Research Journal for Engineering, Technology, and Sciences (ASRJETS) (2015) Volume 10, pp 85-120.

Waikar ML, Nilawar AP (2014) Identification of groundwater potential zone using remote sensing and GIS technique. Int J Innov Res Sci Eng Tech 3. (ISSN: 2319-8753).

Wilson, E. M. (1990). Meteorological Data. In *Engineering Hydrology* (pp. 5-41). Red Globe Press, London.

Yibralem T., (2013). Surface Runoff Estimation Using Remote Sensing and GIS in Aynalem Catchment, Northern Ethiopia. Msc thesis submitted in Partial Fulfillment of the Requirements for the Master of Science Degree in- Integrated Water Resource Management.

Yongxin, X., & Beekman, H. E. 2003. Groundwater recharge estimation in southern Africa. Paris: United Nations Educational Scientific and Cultural Organization (UNESCO).